

**ADVANCED CONVEX RELAXATIONS FOR NONCONVEX STOCHASTIC
PROGRAMS AND AC OPTIMAL POWER FLOW**

A Dissertation
Presented to
The Academic Faculty

By

Yuanxun Shao

In Partial Fulfillment
of the Requirements for the Degree
Doctor of Philosophy in the
School of Chemical and Biomolecular Engineering

Georgia Institute of Technology

December 2020

© Yuanxun Shao 2020

**ADVANCED CONVEX RELAXATIONS FOR NONCONVEX STOCHASTIC
PROGRAMS AND AC OPTIMAL POWER FLOW**

Thesis committee:

Professor Joseph K. Scott, Advisor
School of Chemical and Biomolecular
Engineering
Georgia Institute of Technology

Professor Martha A. Grover
School of Chemical and Biomolecular
Engineering
Georgia Institute of Technology

Professor Fani Boukouvala
School of Chemical and Biomolecular
Engineering
Georgia Institute of Technology

Professor Andrew J. Medford
School of Chemical and Biomolecular
Engineering
Georgia Institute of Technology

Professor Santanu S. Dey
H. Milton Stewart School of Industrial and
Systems Engineering
Georgia Institute of Technology

Date approved: October 27 , 2020

If you're afraid to fail, then you're probably going to fail.

Kobe Bryant

FOR MY PARENTS AND GRANDPARENTS

ACKNOWLEDGMENTS

I have always stood firmly on the idea that the most precious treasure from a PhD journey is not the degree, but the fortune of being surrounded by a group of impossibly talented and warm people. I am deeply indebted to my family, mentors, colleagues and friends who have paved paths for me to grow technically and behaviorally. The only reason I can chase a dream without hesitation is I know you will always be there no matter what.

It is a truly incredible journey to work with my advisor Prof. Joseph K. Scott. The amount of efforts he has put into me is unbelievable, and this thesis represents his intellectual support over the period of my PhD. On a day-to-day basis, he has been easy to reach for discussions and always provided insightful feedback to my rough thoughts. The best thing about working with Prof. Scott is he equipped me with a mathematical thinking habit of only counting facts, not advertising numbers, which I will benefit from in the long run.

I am also grateful to my collaborators Prof. Carl D. Laird, Dr. Anya Castillo and Dr. Michael Bynum at the Sandia National Lab. Their insights and advice effectively helped us get into a new field and sorted out a workable plan. In addition, I would like to thank all my committee members Prof. Fani Boukouvala, Prof. Santanu S. Dey, Prof. Martha A. Grover and Prof. Andrew J. Medford for their help and advice. Moreover, I would like to express my appreciations to lab members Alphonse Hakizimana, Kai Shen, Xuejiao Yang, Dillard Robertson, Taehun Kim, Dylan Weber, Jason Ye, Pengfei Cheng and Bowen Mu. They made the research group more like a family.

It cannot be enough to thank many of the teachers and mentors I have met throughout my life, including Zuxiang Zhang, Ke Xu, Xiaoyang Yang, Fabai Jiang, Ruchun Pan, James C. Earthman, Shane Ardo, Yuyuan Ouyang, Taufiqar Khan, Brian Malloy, Shuangshuang Liu (to only name a few due to the limited space). They shed light on me, believed in me, and asked nothing in return. They have had a great impact on the major I chose, the career I will pursue, and have made me a better person all round.

I have always felt fortunate to have good friends around me. My confidence and toughness were cultivated from them. Especially, I owe a lot to Tianrong, Jiaqin and Pengzhi, who energized me to study abroad when I was weighting on several future directions as an undergrad in China, which opened up this new chapter in my life. Moreover, special thanks to Yutong, Mangmang and Jiwei. It has been super enjoyable to share tears and smiles, nuts and bolts in our lives.

Finally, what can I say to my parents and grandparents? I am who I am today because of you! I just want to become a parent and grandparent like you in the future!

TABLE OF CONTENTS

Acknowledgments	v
List of Tables	xi
List of Figures	xii
Summary	xiv
Chapter 1: Introduction and Background	1
1.1 Overview	1
1.2 Global Optimization	4
1.2.1 The Spatial Branch-and-Bound Algorithm	5
1.2.2 Convex Relaxations for Factorable Functions	6
1.3 Nonconvex Stochastic Optimization	7
1.3.1 Motivation and Existing Methods	9
1.3.2 Contribution	10
1.4 Nonconvex Stochastic Optimal Control Problems	11
1.4.1 Motivation and Existing Methods	12
1.4.2 Contribution	13
1.5 AC Optimal Power Flow Problems	13

1.5.1	Motivation and Existing Methods	14
1.5.2	Contribution	16
Chapter 2: Convex Relaxations for Global Optimization Under Uncertainty De-		
scribed by Continuous Random Variables		17
2.1	Introduction	17
2.2	Preliminaries	21
2.3	Problem Statement	23
2.4	Relaxing Expected-Value Functions	24
2.5	Convergence	30
2.6	Non-Uniform Random Variables	33
2.6.1	Primitive Random Variables	34
2.6.2	Factorable Random Variables	37
2.6.3	The Inverse Transform Method	39
2.6.4	Other Transformations	41
2.6.5	Dependent Random Variables	43
2.7	Conclusions	45
Chapter 3: Guaranteed Global Optimization of Expected-Value Minimization		
Problems with Continuous Random Variables		49
3.1	Introduction	49
3.2	Preliminaries	53
3.3	Problem Statement	54
3.4	A Novel Spatial Branch-and-Bound Algorithm	56
3.4.1	Upper and Lower Bounding Problems	56

3.4.2	Uncertainty Set $\bar{\Omega}$ Partition Rule	59
3.4.3	The Overall Spatial Branch-and-Bound Scheme	62
3.5	Convergence	63
3.5.1	Finite Termination of the Uncertainty Set Partition Rule	64
3.5.2	Convergence of the Relaxation Scheme	68
3.6	Numerical Results	70
3.6.1	A Chemical Reactor Design Problem	70
3.7	Conclusion	75
Chapter 4: Convex Relaxations for Nonlinear Stochastic Optimal Control Problems		76
4.1	Introduction	76
4.2	Problem Statement	79
4.3	Relaxing the Dynamics on $P \times \Omega$	80
4.4	Relaxing the Expected Value on P	83
4.5	Rigorous Bounds on Stochastic Optimal Control Problems	86
4.6	Numerical Example	88
4.7	Conclusions	89
Chapter 5: Efficient Bounds Tightening Based on Strengthened SOCP Relaxations for AC Optimal Power Flow		92
5.1	Introduction	92
5.2	AC Optimal Power Flow	95
5.3	Strengthened SOCP Relaxation	98
5.3.1	Equivalent Reformulation of ACOPF	99

5.3.2	Cycle-Based Relaxation	104
5.3.3	Reverse Cone Cuts	107
5.4	Bounds Tightening	108
5.4.1	Optimization-Based Bounds Tightening	108
5.4.2	Selecting a Subset of Variables for OBBT	109
5.4.3	OBBT Scheme	110
5.5	Numerical Results	110
5.6	Conclusion	112
Chapter 6: Conclusion		115
6.1	Summary of Contributions	115
6.2	Future Work	118
References		132

LIST OF TABLES

2.1	Primitive one-dimensional distributions on $\overline{W} = [\overline{\omega}^L, \overline{\omega}^U]$ with formulas for the CDFs $P(\omega)$ and the conditional expectations $\mathbb{E}[\omega W]$ with $\omega \in W = [\omega^L, \omega^U] \in \mathbb{I}\overline{W}$. Normal and Gamma distributions are truncated to \overline{W} [92]. Formulas for the Beta distribution are for $\overline{W} = [0, 1]$, but arbitrary \overline{W} can be achieved by linear transformation of the random variable (see §2.6.2).	36
2.2	Some common random variables ω that are factorable in the sense of Definition 17 with γ uniformly distributed on $\overline{\Gamma} = [0, 1]$ and factorable transformations $\psi(\gamma) = P^{-1}(\gamma)$ given by inverse CDFs. All random variables ω are truncated on the interval $\overline{W} = [\overline{\omega}^L, \overline{\omega}^U]$. $P_\eta^{-1}(\gamma)$ is the inverse CDF of the corresponding untruncated random variable, so that $P^{-1}(\gamma) = P_\eta^{-1} [P_\eta(\overline{\omega}^L) + (P_\eta(\overline{\omega}^U) - P_\eta(\overline{\omega}^L))\gamma]$	42
3.1	Computational times for solving the reactor design problem using our novel B&B algorithm with two different uncertainty set partitioning rules and using sample-average approximation (SAA).	72
5.1	Root node bounds tightening results for NESTA up to 300 buses. Columns 2–4 are the tightest optimality gaps achieved by existing OBBT methods using SDP, SOCP, and QC relaxations. Columns 5–8 show optimality gaps (%), number iterations, number of violated cones $ \mathcal{V} $, and wall-clock time (s) for our proposed OBBT scheme. Columns 9–10 show speed-up of our scheme relative to the methods in Columns 3–4.	114

LIST OF FIGURES

1.1	An illustration of global versus local optima.	5
1.2	Computational graph of $J(x, y) = xy(e^x + y^2)$ showing its decomposition into elementary operations (upper) and a convex underestimator for J on $[-1, 1] \times [-1, 1]$ using McCormick relaxations (lower).	8
2.1	Jensen-McCormick convex relaxations of F in Example 1 (shaded surfaces) with partitions of $\bar{\Omega}$ into 1 (top), 16 (middle), and 64 (bottom) uniform subintervals, along with simulated values of $f(\mathbf{x}, \boldsymbol{\omega})$ at sampled $\boldsymbol{\omega}$ values (\circ) and a sample-average approximation of F with 100 samples (black mesh).	28
2.2	Second-order pointwise convergence of Jensen-McCormick relaxations with respect to $\frac{1}{2}\text{diam}(X_\epsilon) = \epsilon$ for Example 2 under a uniform $\bar{\Omega}$ partitioning rule satisfying Equation (2.19) with $K = 100$. Plotted values are for $x = \text{mid}(X_\epsilon) = 25$	34
2.3	Jensen-McCormick convex relaxations of the objective function F in Example 3 (shaded surfaces) with partitions of $\bar{\Gamma}$ into 1 (top), 16 (middle), and 64 (bottom) uniform subintervals, along with simulated values of $f(\mathbf{x}, \boldsymbol{\omega})$ at sampled $\boldsymbol{\omega}$ values (\circ) and a sample average approximation of F with 100 samples (black mesh).	46
2.4	Second-order pointwise convergence of Jensen-McCormick relaxations with respect to $\frac{1}{2}\text{diam}(X_\epsilon) = \epsilon$ for Example 3 under a uniform $\bar{\Gamma}$ partitioning rule satisfying Equation (2.52) with $K = 10^8$. Plotted values are for $\mathbf{x} = \text{mid}(X_\epsilon) = (5, 6)$	47
3.1	Upper: Nodes X_k visited by the B&B algorithm using the uncertainty set partitioning rule in Algorithm 1 with $\alpha = 0.7$ for the reactor design problem, color coded by the size of the partition of $\bar{\Omega}$ when each node was fathomed (color bar). Lower: Close-up view near an ϵ -optimal solution (red diamond).	73

4.1	Convex and concave relaxations of $\mathcal{G}(\mathbf{p}) = \mathbb{E}[x_1(t_f, \mathbf{p}, \boldsymbol{\omega})]$ on $P = [0.1, 0.3] \times [0.1, 0.3]$ (shaded surfaces) using partitions of $\bar{\Omega}$ into 1 (top), 16 (middle), and 64 (bottom) uniform subintervals, along with simulated values of $x_1(t_f, \mathbf{p}, \boldsymbol{\omega})$ at sampled $\boldsymbol{\omega}$ values (\circ) and a sample-average approximation of $\mathcal{G}(\mathbf{p})$ using 200 samples (black mesh).	90
5.1	Convex (gold dashed) and concave (red dashed) relaxations of $\arctan(x)$ (black solid) for $x \in [0, 8]$ (left) and $x \in [-8, 8]$ (right). The gold star indicates x_*^L and the red star indicates x_*^U	105

SUMMARY

The work in this thesis has addressed two distinct problems of broad interest involving efficient guaranteed global optimization algorithms for complex engineering problems. First, global optimization of nonconvex stochastic programs with uncertainties described by continuous random variables was considered. Such problems are almost everywhere in practice, e.g., in chemical process design, water resource management, and robotics, all of which involve nonconvex models and various uncertainties including future investment returns, the availability of natural resources, process yields, reaction rates, etc. Addressing this class of problem is significant because taking uncertainty into consideration is essential for avoiding decisions that may lead to high costs in some future scenarios. To address this class of problems, we developed the first relaxation technique that can provide rigorous upper and lower bounds for these problems. Moreover, a theoretical analysis of the convex relaxation method was presented that provides a mathematical certificate of the convergence rate. Based on this relaxation technique, a novel branch-and-bound algorithm was designed that, for the first time, guarantees finding global solution in a finite time. This algorithm was further improved by an efficient uncertainty set partitioning rule that produces a coarse partition for the majority of searching space, and only requires a dense partition when close to the global solution.

Second, global optimization of large-scale AC optimal power flow (ACOPF) problems was considered. ACOPF is critical to power grid operations at all scales, including short-term power generation and dispatching, day-ahead unit commitment, and long-term network expansion planning. The Energy Information Agency estimates that local methods and heuristics might lead to a loss of 6 billion dollars annually for the US electricity markets. Practical ACOPF instances are too large to be solved by conventional global optimization algorithms. However, optimization-based bounds tightening (OBBT) techniques using advanced convex relaxations have been shown to achieve tight optimality gaps for

many test cases. Unfortunately, standard OBBT methods are still too costly because they require solving two convex subproblems per nonlinear decision variable in each iteration. To tackle these challenges, we first developed an equivalent ACOPF reformulation that is suitable for constructing tight and concise convex relaxations. Second, we developed a strengthened SOCP relaxation based on this reformulation. Third, we presented a new OBBT scheme that only performs bounds tightening on a selected subset of the decision variables. The algorithm significantly outperforms existing OBBT algorithms in terms of both optimality gap and efficiency for the NESTA benchmark problems up to 300 buses.

The new algorithms developed in this thesis enable more efficient solutions of nonconvex stochastic optimization problems, stochastic optimal control problems, and AC optimal power flow problems than previously possible. Moreover, this work contributes fundamental advances to global optimization theory that may lead to efficient solutions of larger and more complex optimization problems in other areas as well. Higher quality decision-making in such systems could possibly save energy and provide affordable products to impoverished areas.

CHAPTER 1

INTRODUCTION AND BACKGROUND

1.1 Overview

Mathematical optimization problems arise in nearly all areas of engineering design, operations, and control. However, for systems such as power networks, chemical processes, and robotics, the optimization models of interest are often nonconvex, large-scale, and uncertain. All of these factors severely complicate the solution of these problems and make it much more difficult to locate true global solutions rather than inferior local solutions. However, the ability to find global solutions of such systems can lead to tremendous gains in efficiency and profitability compared to local solutions. For example, according to a report from Energy Information Agency, using local solution methods for optimal power flow problems may lead to as much as 6 billion dollars of annual losses in US electricity markets alone [1], while locating global solutions would save energy and provide more affordable products to customers. Unfortunately, due to the scale and level of complexity of the models used in many applications, as well as the limited time budget available, existing algorithms for guaranteed global optimization often cannot address these problems in a feasible time frame or at all. Therefore, there is a critical need for efficient algorithms of locating guaranteed global solutions of complex engineering optimization problems. Toward this end, this thesis contributes novel theory and algorithms for two distinct problems in global optimization: nonconvex stochastic programs and large-scale AC optimal power flow (ACOPF) problems.

The first problem, nonconvex stochastic optimization, focuses on making reliable decisions under uncertainty. Such problems arise in, e.g., chemical process design, water resource management, and robotics, where the uncertainties may include future investment

returns, the availability of natural resources, process yields, reaction rates, etc. Taking such uncertainties into consideration is essential for avoiding decisions that may lead to high costs in some future scenarios. For example, considering uncertainty during the optimization of an antibody manufacturing plant design was shown to save 30 million £/yr in [2]. However, existing algorithms cannot solve many practical stochastic optimization problems to guaranteed global optimality without significant simplifications (e.g., considering linearized models or very few uncertain scenarios). In this thesis, we focus specifically on nonconvex, single-stage stochastic programs with uncertainties described by continuous random variables. At present, the most common approach for solving this class of problem is sample-average approximation (SAA). However, SAA is too expensive for many problems of interest either because it requires a prohibitive number of samples or because the required number of samples is unknown and must be determined through trial-and-error procedures. Moreover, SAA can result in highly suboptimal or even infeasible solutions when too few samples are used. An alternative approach is the stochastic branch-and-bound algorithm in [3], which applies spatial-B&B using probabilistic upper and lower bounds in each node based on a finite number of sampled scenarios. However, since the computed bounds are probabilistic rather than deterministic, stochastic B&B is not guaranteed to find a global solution. Solving nonconvex stochastic programs is even more challenging for dynamic systems, which leads to nonconvex stochastic optimal control problems. In this case, SAA is even more prohibitive because a complete copy of the system dynamics (e.g., ODEs) must be added to the optimization model for every sample of the uncertain variables. Thus, there is a critical need for a rigorous global optimization algorithm that can more efficiently solve nonconvex stochastic optimization and optimal control problems.

The second problem, the alternating current optimal power flow (ACOPF) problem, is to determine the real and reactive power outputs of all generators in a power network that minimizes cost while meeting all demands, satisfying all operating constraints, and obeying the nonconvex steady-state AC power flow equations. This problem and its various

extensions are critical to power grid operations at all scales, including short-term generator dispatching, day-ahead unit commitment, and long-term network design and expansion planning [1, 4, 5, 6]. Unfortunately, due to the size and complexity of the ACOPF problem for realistic power networks, grid operations today are much more commonly based on linear approximations of the ACOPF model [7], resulting in solutions that might be infeasible or potentially highly suboptimal. Indeed, the Energy Information Agency estimates that the ability to find the global solution of ACOPF could save the US 6 billion dollars annually in electricity markets [1]. Thus, finding global solutions of ACOPF is crucial for saving energy and providing affordable power to undeveloped areas.

To address these challenges, this thesis develops guaranteed global optimization algorithms capable of efficiently solving (i) nonconvex single-stage stochastic programs; (ii) nonconvex optimal control problems; and (iii) large-scale ACOPF problems. For (i)–(ii), existing approaches need to represent uncertainty using many scenarios, which leads to large global optimization problems and requires solving many repeats to test the solution quality. More importantly, it is difficult to determine a sufficient sample size in practice. In contrast, we develop novel branch-and-bound algorithms based on advanced convex relaxations and an adaptive uncertainty set partitioning rule to efficiently locate a global solution in a single run. For (iii), practical ACOPF instances are too large to be solved by conventional global optimization algorithms based on extensive search-space partitioning. We develop a new optimization-based bounds tightening (OBBT) algorithm, based on a new strengthened convex relaxation, that achieves tight optimality gaps while being more than one order of magnitude faster than existing methods. The algorithm significantly outperforms existing OBBT algorithms in terms of both optimality gap and efficiency on NESTA benchmarks.

The new algorithms developed in this thesis enable more efficient solutions of nonconvex stochastic optimization problems, stochastic optimal control problems, and AC optimal power flow problems than previously possible. Moreover, this work contributes fundamen-

tal advances in global optimization theory that may lead to an efficient solution of larger and more complex optimization problems in other areas as well. Such problems are likely to include other problems in power generation and distribution, chemical and pharmaceutical process design, and problems in robotics. Higher quality decision-making in such systems could possibly save energy and provide affordable products to impoverished areas.

1.2 Global Optimization

Optimization is a field of applied mathematics that finds the optimal value of a function in the domain of interests, subject to various constraints. Global optimization specifically aims to locate globally optimal solution for problems that may have multiple suboptimal local minima, such as nonconvex continuous, mixed-integer, dynamic, bilevel, and stochastic problems. Although many strategies have been devised to increase the likelihood of finding a global solution (i.e., stochastic global optimization algorithms), this thesis is concerned with *deterministic* global optimization algorithms. Deterministic algorithms provide a mathematical guarantee that they will terminate in finite time with an epsilon-global solution (i.e., a feasible solution whose objective value is within a specified tolerance epsilon of the true global minimum).

Global optimization has found an increasing number of applications in all branches of engineering and applied sciences, including refinery pooling, azeotropic distillation, power systems, phase and chemical equilibrium, and parameter estimation in nonlinear algebraic models, to name only a few. Figure 1.1 shows a simple two-dimensional nonconvex function with many local optima (red dots). For such functions, it can be challenging to find the global optimum (red star) using local optimization methods. Moreover, local optimization with multistart is time consuming and might still not be able to locate the global solution. For a nonconvex dynamic optimization problem in [8], the vast majority of multistart runs found a solution whose cost exceeded the global minimum by 5 orders of magnitude. Similarly, in [9], multistart found the global solution in only 4 out of 1000 runs. In addition, in

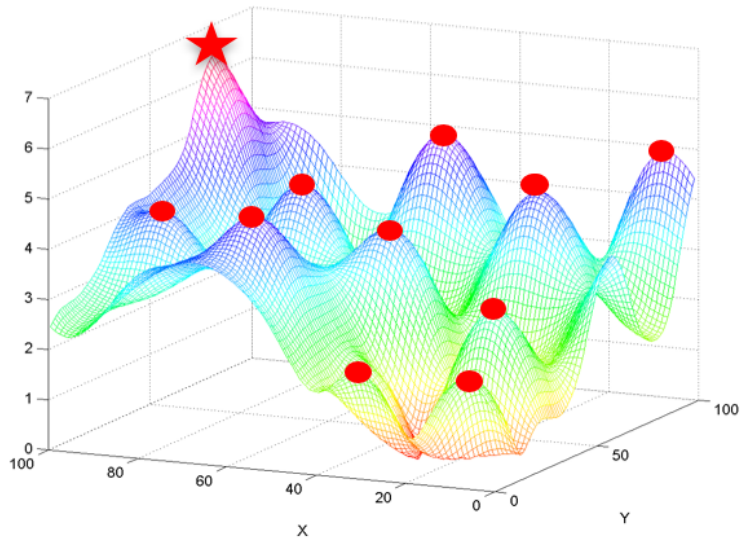


Figure 1.1: An illustration of global versus local optima.

some applications only global solutions are meaningful. For example, in [10], the authors concluded that a proposed reaction mechanism did not fit experimental data based on locally optimal parameter estimates, only to find later that the global solution fit the data well [9]. Thus, global optimization is critical for avoiding suboptimal solutions that are both frequent and potentially very costly in practical applications.

1.2.1 The Spatial Branch-and-Bound Algorithm

Most deterministic global optimization methods use some variant of the basic spatial branch-and-bound (B&B) algorithm, which searches for a global solution using a tree. Each node in the tree corresponds to part of the search space. The initial ‘root’ node contains the whole feasible space, and the successive child nodes are formed from their parent node by bisection so that an exhaustive cover of the feasible space is always maintained. For each node visited by the algorithm, the algorithm calculates a lower and an upper bound on the objective function obtainable on that node. The upper bound is obtained by evaluating the objective at a feasible point, while the lower bound is typically obtained by solving a convex relaxation. These bounds are then checked against the current best-known solution. If the node has a higher lower bound than the current best upper bound, which means that

a global solution cannot exist in this node, the node will be *fathomed* (i.e., removed from further consideration). Otherwise, the global lower and upper bounds will be updated to the lowest lower and upper bounds over all nodes in the search tree. Then, the node is partitioned into two or more child nodes (i.e., *branched*), and the child nodes are added to the search tree. This procedure is repeated until the global upper and lower bounds converge to a specified tolerance [11].

The spatial branch-and-bound (B&B) algorithm is guaranteed to find an epsilon-global solution in finite time, but the worst-case run-time scales exponentially in the number of decision variables due to the exhaustive partitioning of the search space. However, this worst-case performance is avoided for many problems in practice, and the tightness and convergence of the lower bounding method is a critical factor determining the practical performance. State-of-the-art B&B solvers can solve many problems with hundreds or thousands of decision variables, and are highly dependent on special problem structures for reducing computational time.

1.2.2 Convex Relaxations for Factorable Functions

The lower bounds needed in each node of the spatial-B&B algorithm are typically computed by solving a *convex relaxation*. For any given optimization problem, a convex relaxation is a related optimization problem that is convex, and hence easy to solve to global optimality, and whose optimal objective value is guaranteed to underestimate that of the original problem. Therefore, the solution of a convex relaxation provides global information (a lower bound) for the original program and is the core of global optimization. General-purpose convex relaxation methods rely on the ability to decompose the objective and constraints into ordered sequences of elementary operations (e.g., $+$, \times , x^n , e^x , etc.), which can be represented by a computational graph as shown in Fig. 1.2. Such functions are called *factorable functions* and include nearly all functions that can be written explicitly in computer code. Given any factorable function, one way to construct valid relaxations

is recursively applying known rules for relaxing each elementary operation, which can be done, e.g., using interval arithmetic [12], McCormick relaxations [13, 14], polyhedral outer approximation [15], or the reformulation-linearization technique [16]. For example, the McCormick relaxation of a nonconvex factorable function is shown in Fig. 1.2. Alternatively, the α BB relaxation method exploits factorability of the Hessian matrix for twice continuously differentiable functions, rather than factorability of the function itself, to compute a quadratic function that is guaranteed to convexify the original function when added to it [17].

These general convex relaxation approaches work for a wide variety of nonconvex functions, but often lead to weak relaxations and slow B&B performance for many problems. This has led to the development of more sophisticated methods, custom convex relaxations for specific problem structures, and domain reduction techniques to help convergence. Moreover, many functions of interest are not factorable, such as the solutions of implicit algebraic or dynamic models, which limits the use of conventional convex relaxation methods.

1.3 Nonconvex Stochastic Optimization

This section introduces the nonconvex stochastic optimization problem considered in this thesis in more detail. Consider minimizing a function of the form $F(\mathbf{x}) \equiv \mathbb{E}[f(\mathbf{x}, \boldsymbol{\omega})]$, where $\mathbf{x} \in \bar{X} \subset \mathbb{R}^{n_x}$, \mathbb{E} denotes the expected value over continuous random variables $\boldsymbol{\omega} \in \bar{\Omega} \subset \mathbb{R}^{n_\omega}$, the domains \bar{X} and $\bar{\Omega}$ are compact n_x and n_ω -dimensional intervals, and f may be nonconvex in both arguments. This leads to the following global optimization problem under uncertainty, where C is a compact feasible set contained in \bar{X} :

$$\min_{\mathbf{x} \in C} \mathbb{E}[f(\mathbf{x}, \boldsymbol{\omega})]. \quad (1.1)$$

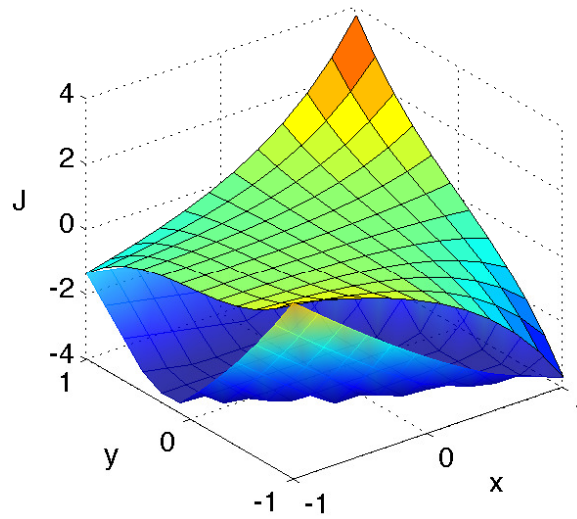
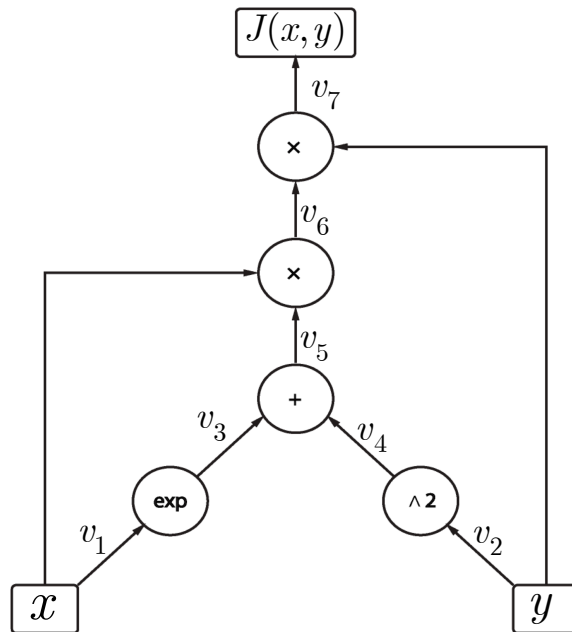


Figure 1.2: Computational graph of $J(x, y) = xy(e^x + y^2)$ showing its decomposition into elementary operations (upper) and a convex underestimator for J on $[-1, 1] \times [-1, 1]$ using McCormick relaxations (lower).

The objective is to develop a new technique for automatically constructing convex and concave relaxations of (1.1) and establish a novel branch-and-bound algorithm to solve it to guaranteed ϵ -global optimality without sampling errors.

1.3.1 Motivation and Existing Methods

Stochastic programming is a powerful framework for determining optimal design and operational decisions under uncertainty. Optimization problems involving nonconvex and stochastic models occur in almost all areas of science and engineering in practice. For example, nonconvexity is ubiquitous in oil, gas, and water networks [18, 19, 20], and uncertainty is naturally associated with future investment returns, availabilities of natural resources, process yields, and variations of reaction rates. Thus, nonconvex stochastic programming is critical in many applications. More importantly, explicitly accounting for nonconvexity and uncertainty during optimization can avoid abnormal effects and often leads to remarkable gains. See, e.g., savings of 30 million $\text{\pounds}/\text{yr}$ for an antibody manufacturing plant in [2], or a \$3 billion increase in NPV for a natural gas network in [21].

Uncertainty in optimization models can be modeled in various ways, e.g., using random variables with specific probability distributions or a finite set of scenarios. This project focuses on uncertainty described by continuous random variables (RVs). Continuous RVs can represent uncertainties with a wide range of statistical distributions more precisely than a fixed number of sampled scenarios that might ignore some rare chance events.

At present, the most common approach for solving nonconvex stochastic programs is sample-average approximation (SAA), which approximates the expected value using fixed samples. This results in a deterministic program that can be solved globally using conventional B&B methods [22, 23]. However, SAA has several critical limitations. First, it only guarantees convergence to a global solution as the sample size tends to infinity [24]. Moreover, the number of scenarios required to achieve a high-quality solution in practice is unknown and can be quite large [25, 26, 27]. Thus, SAA often requires the global solution

of multiple deterministic problems that are too large to be handled effectively using standard B&B codes. An alternative approach is the stochastic branch-and-bound algorithm [3], which applies spatial-B&B only once using probabilistic upper and lower bounds in each node. However, since the computed bounds are probabilistic rather than deterministic, stochastic B&B only ensures convergence to a global solution when no fathoming is done, which is prohibitively expensive. Thus, the existing methods cannot provide guaranteed global solutions with reasonable efficiency for many problems of interest.

1.3.2 Contribution

To address the challenges outlined above, this thesis develops a novel B&B algorithm that is guaranteed to converge finitely to ϵ -global solutions of nonconvex stochastic programs with continuous random variables in a single run. First, in Chapter 2, we develop a new convex relaxation technique that can provide rigorous, deterministic lower bounds. Furthermore, these relaxations are proven to obey a second-order pointwise convergence property, which is sufficient for finite termination of branch-and-bound under standard assumptions. Empirical results are also shown for illustrating the convergence rate. In addition, we establish an extension of the relaxation technique that enables efficient computations with a wide variety of multivariate probability density functions.

Next, in Chapter 3, we present a new B&B algorithm to solve the nonconvex stochastic problem to ϵ -global optimality in finite time. Unlike the conventional B&B algorithm that only needs to explore the decision variable space, the new algorithm has an extra layer of complexity due to the need to partition the random variable space. We design an efficient rule that adaptively refines the uncertainty set partition as the B&B search proceeds. As a result, the algorithm is capable of using a coarse partition of the uncertainty space for the majority of the search space, and requires dense partitions only when close to the global solution. This leads to significant computational savings relative to sample-based approaches, which must use a fixed number of samples throughout the search. Compared

to the sample-based bounds in the stochastic B&B method, our method provides guaranteed bounds with no chance of fathoming optimal solutions. Compared to SAA, which has to run many repeats to test statistical significance of the solution and has to redo the whole process if a larger sample size is needed, our method only needs a single run to solve the problem with guaranteed convergence. This work is significant because it will enable the guaranteed solution of nonconvex stochastic programs without sampling error for the first time.

1.4 Nonconvex Stochastic Optimal Control Problems

This section introduces the stochastic optimal control problem studied in Chapter 4 of this thesis in more detail. The general stochastic optimal control problem is stated informally as

$$\min_{\mathbf{p} \in \bar{P} \subset \mathbb{R}^{n_p}} \mathbb{E}[g(\mathbf{p}, \boldsymbol{\omega}, \mathbf{x}(t_f, \mathbf{p}, \boldsymbol{\omega}))], \quad (1.2)$$

where \mathbb{E} and \mathbb{P} denote the expected value and probability over continuous random variables $\boldsymbol{\omega} \in \bar{\Omega} \subset \mathbb{R}^{n_\omega}$, respectively, and $\mathbf{x}(t_f, \mathbf{p}, \boldsymbol{\omega})$ is the solution of the nonlinear ordinary differential equations (ODEs)

$$\begin{aligned} \dot{\mathbf{x}}(t, \mathbf{p}, \boldsymbol{\omega}) &= \mathbf{f}(t, \mathbf{p}, \boldsymbol{\omega}, \mathbf{x}(t, \mathbf{p}, \boldsymbol{\omega})), \\ \mathbf{x}(t_0, \mathbf{p}, \boldsymbol{\omega}) &= \mathbf{x}_0(\mathbf{p}, \boldsymbol{\omega}). \end{aligned} \quad (1.3)$$

The functions g , \mathbf{f} , and \mathbf{x}_0 may be nonconvex with respect to all of their arguments. The decision vector \mathbf{p} may represent a parameterized open-loop control input, parameters in an explicit feedback controller embedded in (4.2), etc.

The objective is to develop a new method to compute guaranteed convex relaxations of the final-time expected-value objective function. Such relaxations offer a way to com-

pute rigorous upper and lower bounds that can be used within a B&B algorithm to find guaranteed global solution of this class of problems.

1.4.1 Motivation and Existing Methods

Stochastic optimal control is a crucial branch of decision-making under uncertainty and is widely used for advanced control of complex stochastic systems with constraints on states and control inputs. Well-established applications include optimal path planning [28], portfolio optimization [29], renewable energy systems [30] and chemical process control [31]. Since the dynamic behavior of many physical systems of practical interest can be modeled using systems of ordinary differential equations (ODEs) [32, 9], identifying the optimal decision for such systems under uncertainty becomes increasingly important.

For deterministic optimal control problems, many algorithms have been developed to obtain global solutions [33, 34, 35, 36, 37]. These methods are based on effective algorithms for enclosing the reachable set of the dynamics on subintervals of the decision space. With such an enclosure, it is possible to construct convex and concave relaxations of the optimal control problem on arbitrary subintervals of the decision space, and compute upper and lower bounds on the optimal objective value [37, 32, 38, 39, 40, 41, 42, 43, 44]. Finally, with rigorous bounds, we can use the spatial branch-and-bound (B&B) algorithm to obtain a global solution.

To the best of our knowledge, there is no existing algorithm that can find a guaranteed global solution for the stochastic optimal control problem in §1.4. The main challenge is that no existing method can compute a valid relaxation of the objective function, which involves both an expected value over continuous random variables and the solution of a nonlinear dynamic system. In practice, this problem is most commonly addressed by replacing the objective and constraints by sample-average approximations (SAA), resulting in a deterministic optimal control problem that can be solved using existing methods. However, SAA has several critical limitations that can lead to inaccurate solutions or excessive

computational cost. First, a sufficient sample size required to achieve a high-quality solution in practice is unknown [25, 26]. Theoretical sample size bounds are available [45], but are often very conservative and not generally computable. Moreover, it only guarantees convergence to a global solution as the sample size goes to infinity [24]. In addition, SAA needs to solve a large number of ODEs for independent samples and run many repeats to assess solution accuracy. Even worse, if a larger sample size is deemed necessary [26], we have to rerun the whole process until a predefined tolerance is satisfied. This is clearly problematic for nonconvex optimal control problems, where solving a single instance to global optimality is already demanding.

1.4.2 Contribution

In Chapter 4, we develop a new method for computing guaranteed convex and concave relaxations of nonlinear stochastic optimal control problems with final-time expected-value cost functions. This method is motivated by similar methods for deterministic optimal control problems, which have been successfully applied within spatial B&B techniques to obtain guaranteed global optima. Relative to those methods, a key challenge here is that the expected-value cost function cannot be expressed analytically in closed form. We develop the first ever algorithm that can provide guaranteed convex relaxations. These relaxations can be used to compute rigorous upper and lower bounds on the optimal objective value of such problems restricted to any given subinterval of the decision space, and hence enable deterministic global optimization for this class of problems.

1.5 AC Optimal Power Flow Problems

This section introduces the AC optimal power flow problems considered in Chapter 5 of this thesis in more detail. For a given power network, the ACOPF problem is to determine the real and reactive power outputs of all generators that minimize cost while meeting all demands, satisfying all operating constraints, and obeying the nonconvex steady-state AC

power flow equations. The objective is to develop an efficient global optimization algorithm for solving large-scale ACOPF problems.

1.5.1 Motivation and Existing Methods

AC optimal power flow problem and its various extensions are critical to power grid operations at all scales, including short-term generator dispatching, day-ahead unit commitment, and long-term network design and expansion planning [1, 4, 5, 6]. For a regional power network alone, there are more than three thousand buses, which results in ACOPF problems with tens of thousands of decision variables. Due to the size and complexity of these problems, grid operations today are much more commonly based on linear approximations of the ACOPF model [7], resulting in solutions that might be infeasible or potentially highly suboptimal. Alternatively, local methods can be used to find a local solution or stationary point of ACOPF very efficiently [46, 47]. However, ACOPF is a highly nonconvex problem. Therefore, local solvers may produce suboptimal solutions in many cases and provide no way of quantifying the degree of suboptimality. Moreover, although local solvers are known to often find global solutions in ACOPF test problems, there is significant evidence that local solutions are often highly suboptimal in practice. Indeed, the Energy Information Agency estimates that the ability to find the global solution of ACOPF could save the US 6 billion dollars annually in electricity markets [1]. Thus, finding global solutions of ACOPF is crucial for saving energy and providing affordable power to undeveloped areas.

Existing algorithms for globally solving ACOPF are based on constructing tight convex relaxations, including semi-definite programming (SDP) relaxations [48, 49], second-order cone programming (SOCP) relaxations [50, 51, 52] and convex quadratic programming (QP) relaxations [53, 54]. These methods can be categorized into two types: single relaxation methods and exhaustive search methods [55, 4, 5, 6]. The single convex relaxation approach aims to find an ϵ -global solution of ACOPF by solving one highly accurate convex relaxation. A solution of any convex relaxation provides a lower bound on the optimal

objective value of the original problem. Then, with an upper bound found by local methods or heuristics, we can quantify the quality of the obtained solution. If the convex relaxation solution is feasible, then it is a global solution. SDP relaxations have been proven to satisfy this in special cases [56, 57]. However, those conditions are often not met in practice and a major limitation of this approach is that it can lead to arbitrarily large global optimality gaps.

Alternatively, exhaustive search methods solve potentially many ACOPF relaxations within an iterative procedure that locates an ϵ -global solution of ACOPF in finite time, such as spatial B&B or nonconvex outer-approximation with piecewise convex relaxations [58, 52, 59]. But spatial B&B and outer approximations require exponential run-time scaling, thus cannot handle large-scale problems in general. However, it has been shown that applying iterative optimization-based bounds tightening (OBBT) techniques is highly effective at closing the global optimality gap for ACOPF problems [60, 59, 61]. OBBT is a greedy domain reduction technique that computes tight bounds on each decision variable by maximizing (for the upper bound) and minimizing (for the lower bound) each variable over the relaxed feasible set. Since the tightness of convex relaxations is relative to the width of bounds on the decision variables, this can lead to a substantially tighter relaxation in the next iteration. Even though this method cannot guarantee convergence, it works empirically on challenging ACOPF benchmark test cases. But OBBT is still costly because it requires solving two convex subproblems per decision variable in each iteration, which is prohibitive for large problems. A fast closed-form bounds tightening scheme was developed in [62], but the bounds do not result in competitive optimality gaps even with branching. Thus, while bounds-tightening has high potential for enabling the global solution of ACOPF problems, existing OBBT methods are too costly and existing closed-form methods are too conservative.

1.5.2 Contribution

This work makes three new contributions towards the global solution of ACOPF. We first prove the equivalence of a reformulation that is beneficial for constructing efficient convex relaxations. Second, we develop a new strengthened SOCP relaxation based on this reformulation with a concise structure. Third, using this relaxation, we establish a new OBBT scheme that performs bounds tightening on only a selected subset of variables. Among existing OBBT methods, the one that achieves the smallest optimality gaps on standard ACOPF test sets performs bounds tightening on all variables that appear in nonconvex terms [60]. Conversely, approaches that perform OBBT on only a subset of variables exhibit significantly larger gaps (although there are also differences in the relaxations used) [52]. In contrast, our results for the NESTA benchmarks, which are commonly used for the evaluation and validation of power system optimization algorithms, show that performing OBBT on a small subset of the variables in our new relaxation outperforms existing OBBT algorithms in terms of both optimality gaps and efficiency. Our new algorithm achieves 96.2% of the best optimality gaps achieved by all existing OBBT methods for NESTA benchmarks, where SDP, SOCP, and QC methods achieve the best gap in only 64.0%, 39.6%, and 71.7% of cases. We also do so with significantly higher efficiency, and about $5.1\times$ and $21.2\times$ faster than the SOCP and the QC methods on average.

CHAPTER 2
CONVEX RELAXATIONS FOR GLOBAL OPTIMIZATION UNDER
UNCERTAINTY DESCRIBED BY CONTINUOUS RANDOM VARIABLES

2.1 Introduction

This chapter presents a new method for automatically constructing convex underestimators and concave overestimators (i.e., convex and concave relaxations) of functions of the form $F(\mathbf{x}) \equiv \mathbb{E}[f(\mathbf{x}, \boldsymbol{\omega})]$, where $\mathbf{x} \in \bar{X} \subset \mathbb{R}^{n_x}$, \mathbb{E} denotes the expected value over continuous random variables $\boldsymbol{\omega} \in \bar{\Omega} \subset \mathbb{R}^{n_\omega}$, the domains \bar{X} and $\bar{\Omega}$ are compact n_x and n_ω -dimensional intervals, and f may be nonconvex in both arguments. The ability to construct convex and concave relaxations of nonconvex functions is central to algorithms for solving nonconvex optimization problems to guaranteed ϵ -global optimality [11, 15, 13, 63]. Here, we are specifically motivated by the following global optimization problem under uncertainty, where C is a compact feasible set contained in \bar{X} :

$$\min_{\mathbf{x} \in C} \mathbb{E}[f(\mathbf{x}, \boldsymbol{\omega})]. \quad (2.1)$$

Such problems arise broadly in chemical process design [31], structural design [64], renewable energy systems [30, 65], portfolio optimization [66], stochastic model predictive control [67, 68], discrete event systems [69], etc. Moreover, although we restrict our attention to single-stage problems in this chapter (i.e., problems with no recourse decisions), more flexible two-stage and multistage formulations can also be reduced to Problem (2.1) through the use of parameterized decision rules, which is an increasingly popular method for obtaining tractable approximate solutions [70].

In the applications above, many uncertainties are best modeled by continuous random variables, including process yields, material properties, renewable power generation, prod-

uct demands, returns on investments, etc. [64, 30, 65, 66]. However, when f is nonlinear with respect to ω , this very often precludes writing the function $F(\mathbf{x}) \equiv \mathbb{E}[f(\mathbf{x}, \omega)]$ analytically in closed form. Moreover, expressing $F(\mathbf{x})$ via quadrature rules quickly becomes intractable as the dimension of ω , i.e., n_ω , increases. In this situation, $F(\mathbf{x})$ must be evaluated by sampling, which fundamentally limits the applicability of guaranteed global optimization algorithms such as spatial branch-and-bound. Specifically, to perform an exhaustive global search, branch-and-bound requires the ability to compute guaranteed lower and upper bounds on the optimal value of Problem (2.1) restricted to any given n_x -dimensional subinterval $X \subset \bar{X}$. The lower bound is typically computed by minimizing a convex relaxation of F over X subject to the constraint that \mathbf{x} lies in a convex relaxation of the feasible set $X \cap C$, while the upper bound is computed by evaluating F at a feasible point in $X \cap C$ [11]. However, conventional methods for constructing convex relaxations are only applicable to functions that are known explicitly in closed form [11, 15, 13, 63]. Moreover, using only sample-based approximations of F , it is not even possible to bound its value at a single feasible point with finitely many computations.

At present, the most common approach for solving Problem (2.1) globally is sample-average approximation, which approximates F using fixed samples of the random variables chosen *prior* to optimization. This results in a deterministic optimization problem that can be solved globally using conventional methods [11, 15, 13, 63]. However, sample-average approximation has several critical limitations that often lead to inaccurate solutions or excessive computational cost for nonconvex problems. Most notably, it only guarantees convergence to a global solution (with probability one) as the sample size tends to infinity [24]. Moreover, the number of samples required to achieve a high-quality solution in practice is unknown and can be quite large [25] (also see ‘ill-conditioned’ problems in Linderoth et al. [26]). Perhaps more importantly, a sufficient sample size is typically not known *a priori*. Theoretical bounds are available [45], but are not generally computable and are often excessively large [24]. Instead, state-of-the-art methods determine an appropriate sample

size iteratively. For each fixed sample size N , the accuracy of the sample-average approximation is estimated by solving multiple instances of the approximation with independent sets of N samples [26]. For example, 10-40 independent instances are solved to estimate the approximation errors for the case studies in the articles [26, 71]. Notably, each instance must be solved to global optimality. Furthermore, this entire procedure must be repeated from scratch if a larger sample size N is deemed necessary [26]. This is clearly problematic for nonconvex problems, where solving just one instance to global optimality is already NP-hard.

An alternative approach is the stochastic branch-and-bound algorithm [3], which applies spatial branch-and-bound to Problem (2.1) using probabilistic upper and lower bounds on each node X based on a finite number of samples. Relative to sample-average approximation, a strength of this approach is that the sample size can be dynamically adapted as the search proceeds. However, since the computed bounds are only statistically valid, there is a nonzero probability of fathoming optimal solutions. Thus, stochastic branch-and-bound only ensures convergence to a global solution when no fathoming is done, and even then only in the limit of infinite branching.

In the case where f is convex, a number of deterministic (i.e., sample-free) methods are available for computing rigorous underestimators and overestimators of $F(\mathbf{x}) = \mathbb{E}[f(\mathbf{x}, \boldsymbol{\omega})]$ that can be used for globally solving Problem (2.1). The simplest underestimator is given by Jensen's inequality [72], which states that $\mathbb{E}[f(\mathbf{x}, \boldsymbol{\omega})] \geq f(\mathbf{x}, \mathbb{E}[\boldsymbol{\omega}])$ for convex f . This leads to a deterministic lower bounding problem for Problem (2.1) that can be solved using standard methods [73]. Moreover, $F(\mathbf{x})$ can be bounded above at any feasible point \mathbf{x} using, e.g., the Edmunson-Madansky upper bound [74], which uses values of $f(\mathbf{x}, \boldsymbol{\omega})$ at the extreme points of the uncertainty set $\bar{\Omega}$. Notably, these upper and lower bounds can be made arbitrarily tight using successively refined partitions of $\bar{\Omega}$, which allows Problem (2.1) to be solved to guaranteed ϵ -global optimality [73, 75]. Moreover, refinements of the Jensen and Edmunson-Madansky bounds using higher order moments

of ω have been studied in Dokov et al. and Edirisinghe et al. [76, 77]. However, all of these methods require f to be convex or, more generally, to satisfy a convex-concave saddle property. Moreover, achieving convergence by partitioning $\bar{\Omega}$ requires the ability to efficiently compute probabilities and conditional expectations on n_ω -dimensional subintervals of $\bar{\Omega}$, which severely limits the distributions of ω that can be handled efficiently (e.g., to multivariate uniform or Gaussian distributions with independent elements).

To address these limitations, this chapter presents a new method for computing deterministic convex and concave relaxations of $F(\mathbf{x}) = \mathbb{E}[f(\mathbf{x}, \omega)]$ on n_x -dimensional subintervals X of its domain \bar{X} . This method applies to arbitrary nonconvex functions f and a very general class of multivariate probability density functions for ω . In brief, nonconvexity is addressed through a novel combination of Jensen’s inequality and existing relaxation techniques for deterministic functions, such as McCormick’s technique [14]. Similarly, general multivariate densities are addressed by relaxing nonconvex transformations that relate ω to random variables with simpler distributions. We show that the resulting relaxations of F can be improved by partitioning $\bar{\Omega}$. More importantly, we establish second-order pointwise convergence (which implies second-order Hausdorff convergence [78]) of the relaxations to F as the diameter of X tends to 0, provided that the partition of $\bar{\Omega}$ is appropriately refined.

The proposed relaxations can be used to compute both upper and lower bounds for Problem (2.1) restricted to any given interval $X \subset \bar{X}$. In principle, this enables the global solution of Problem (2.1) by spatial branch-and-bound. We leave the details of this algorithm for future work. However, we note here some potentially significant advantages of this approach relative to existing methods. First, unlike the stochastic branch-and-bound algorithm, our relaxations provide deterministic upper and lower bounds for Problem (2.1) on any X , so there is zero probability of incorrectly fathoming an optimal solution during branch-and-bound. Second, the convergence of our relaxations as the diameter of X tends to 0 implies that spatial branch-and-bound will terminate finitely with an ϵ -global

solution under standard assumptions [11, 78]. This is in contrast to both stochastic branch-and-bound and sample-average approximation, which only converge in the limit of infinite sampling. In fact, the second-order convergence rate established here is known to be critical for avoiding the so-called *cluster effect* in branch-and-bound, and hence avoiding exponential run-time in practice [79]. Third, although refining the partition of $\bar{\Omega}$ is required for convergence, valid relaxations on X can be obtained using any partition of $\bar{\Omega}$, no matter how coarse. Thus, the partition of $\bar{\Omega}$ can be adaptively refined as the branch-and-bound search proceeds. This is potentially a very significant advantage over sample-average approximation, which must determine an appropriate number of samples *a priori*, and must solve the problem again from scratch if more samples are deemed necessary.

The remainder of this chapter is organized as follows. The next section establishes the necessary definitions and notation, followed by a formal problem statement. Next, the sections ‘Relaxations for Expected-Value Functions’ and ‘Convergence’ present the main theoretical results establishing the validity and convergence of the proposed relaxations, respectively. The section ‘Non-Uniform Random Variables’ develops an extension of the basic relaxation technique that enables efficient computations with a wide variety of multivariate probability density functions. Finally, the last section provides concluding remarks.

2.2 Preliminaries

Convex and concave relaxations are defined as follows.

Definition 1. Let $\bar{S} \subset \mathbb{R}^n$ and $h : \bar{S} \rightarrow \mathbb{R}$. For any convex $S \subset \bar{S}$, functions $h^{cv}, h^{cc} : S \rightarrow \mathbb{R}$ are *convex and concave relaxations of h on S* , respectively, if h^{cv} is convex on S , h^{cc} is concave on S , and

$$h^{cv}(\mathbf{s}) \leq h(\mathbf{s}) \leq h^{cc}(\mathbf{s}), \quad \forall \mathbf{s} \in S.$$

The following extension of Definition 1 is useful for convergence analysis. First, for

any $\mathbf{s}^L, \mathbf{s}^U \in \mathbb{R}^n$ with $\mathbf{s}^L \leq \mathbf{s}^U$, let $S = [\mathbf{s}^L, \mathbf{s}^U]$ denote the compact n -dimensional interval $\{\mathbf{s} \in \mathbb{R}^n : \mathbf{s}^L \leq \mathbf{s} \leq \mathbf{s}^U\}$. Moreover, for $\bar{S} \subset \mathbb{R}^n$, let $\mathbb{I}\bar{S}$ denote the set of all compact interval subsets S of \bar{S} . In particular, let $\mathbb{I}\mathbb{R}^n$ denote the set of all compact interval subsets of \mathbb{R}^n . Finally, denote the *diameter* of S by $\text{diam}(S) = \max_i |s_i^U - s_i^L|$.

Definition 2. Let $\bar{S} \subset \mathbb{R}^n$ and $h : \bar{S} \rightarrow \mathbb{R}$. A collection of functions $h_S^{cv}, h_S^{cc} : \bar{S} \rightarrow \mathbb{R}$ indexed by $S \in \mathbb{I}\bar{S}$ is called a *scheme of relaxations for h in \bar{S}* if, for every $S \in \mathbb{I}\bar{S}$, h_S^{cv} and h_S^{cc} are convex and concave relaxations of h on S .

Remark 3. The notion of a scheme of relaxations was first introduced in Bompadre et al. [78] with the alternative name *scheme of estimators*. Here, we use the term *relaxations* in place of *estimators* to avoid possible confusion with the common meaning of *estimation* in the stochastic setting.

The following notion of convergence for schemes of relaxations originates in Bompadre et al. [78].

Definition 4. Let $\bar{S} \subset \mathbb{R}^n$ and $h : \bar{S} \rightarrow \mathbb{R}$. A scheme of relaxations $(h_S^{cv}, h_S^{cc})_{S \in \mathbb{I}\bar{S}}$ for h in \bar{S} has *pointwise convergence of order γ* if $\exists \tau > 0$ such that

$$\sup_{\mathbf{s} \in S} |h_S^{cc}(\mathbf{s}) - h_S^{cv}(\mathbf{s})| \leq \tau \text{diam}(S)^\gamma, \quad \forall S \in \mathbb{I}\bar{S}.$$

Note that the constants γ and τ in Definition 4 may depend on \bar{S} , but not on S . First-order convergence is necessary for finite termination of spatial branch-and-bound algorithms, while second-order convergence is known to be critical for efficient branch-and-bound because it can eliminate the *cluster effect*, which refers to the accumulation of a large number of branch-and-bound nodes near a global solution [11, 78, 79]. Moreover, note that pointwise convergence of order γ is stronger than Hausdorff convergence of order γ (see Theorem 1 in Bompadre et al. [78]).

Several methods are available for automatically computing schemes of relaxations for *factorable functions*. A function h is called *factorable* if it is a finite recursive composition

of basic operations including $\{+, -, \times, \div\}$ and standard univariate functions such as x^n , e^x , $\sin x$, etc. Roughly, factorable functions include every function that can be written explicitly in computer code. Schemes of relaxations for factorable functions can be computed by the α BB method [63, 80], McCormick’s relaxation technique [13, 14], the addition of variables and constraints [15], and several advanced techniques [81, 82, 83, 84, 85]. Moreover, both α BB and McCormick relaxations are known to exhibit second-order pointwise convergence [78]. However, for functions h that are not known in closed form, and hence are not factorable, none of the aforementioned techniques apply. Some recent extensions of α BB and McCormick relaxations do address certain types of implicitly defined functions, such as the parametric solutions of fixed-point equations [86, 87], ordinary differential equations [88, 39], and differential-algebraic equations [40]. However, no techniques are currently available for relaxing the expected-value function of interest here.

2.3 Problem Statement

Let $\boldsymbol{\omega} \in \mathbb{R}^{n_\omega}$ be a vector of continuous random variables distributed according to a probability density function (PDF) $p : \mathbb{R}^{n_\omega} \rightarrow \mathbb{R}$. We assume throughout that p is zero outside of a compact n_ω -dimensional interval $\bar{\Omega} \subset \mathbb{R}^{n_\omega}$. Let $\bar{X} \subset \mathbb{R}^{n_x}$ be a compact n_x -dimensional interval, let $f : \bar{X} \times \bar{\Omega} \rightarrow \mathbb{R}$ be a potentially nonconvex function, and assume that the expected value $\mathbb{E}[f(\mathbf{x}, \boldsymbol{\omega})] \equiv \int_{\bar{\Omega}} f(\mathbf{x}, \boldsymbol{\omega})p(\boldsymbol{\omega})d\boldsymbol{\omega}$ exists for all $\mathbf{x} \in \bar{X}$. Moreover, define $F : \bar{X} \rightarrow \mathbb{R}$ by $F(\mathbf{x}) \equiv \mathbb{E}[f(\mathbf{x}, \boldsymbol{\omega})]$, $\forall \mathbf{x} \in \bar{X}$.

The objective of this chapter is to present a new scheme of relaxations for F in \bar{X} with second-order pointwise convergence. In particular, this scheme addresses the general case where F cannot be expressed explicitly as a factorable function of \mathbf{x} , and standard relaxation techniques cannot be applied. In such cases, F is most often approximated via sampling and, in general, $F(\mathbf{x})$ cannot even be evaluated exactly with finitely many computations. Critically, our new scheme consists of relaxations that provide bounds on F itself, rather than a finite approximation of F , but are nonetheless finitely computable.

Therefore, these relaxations can be used within a spatial branch-and-bound framework to solve Problem (2.1) to ϵ -global optimality without approximation errors.

A central assumption in the remainder of the chapter is that the integrand f is a factorable function, or that a scheme of relaxations is available by some other means.

Assumption 5. *A scheme of relaxations for f in $\bar{X} \times \bar{\Omega}$, denoted by $(f_{X \times \Omega}^{cv}, f_{X \times \Omega}^{cc})_{X \times \Omega \in \mathbb{I}\bar{X} \times \mathbb{I}\bar{\Omega}}$, is available. $f_{X \times \Omega}^{cv}$ and $f_{X \times \Omega}^{cc}$ denote convex and concave relaxations of f jointly on $X \times \Omega \in \mathbb{I}\bar{X} \times \mathbb{I}\bar{\Omega}$.*

Remark 6. We will sometimes make use of relaxations of f with respect to either \mathbf{x} or $\boldsymbol{\omega}$ independently, with the other treated as a constant. We denote these naturally by $f_X^{cv}(\mathbf{x}, \boldsymbol{\omega})$ and $f_\Omega^{cv}(\mathbf{x}, \boldsymbol{\omega})$. Within the scheme of Assumption 5, these relaxations are equivalent to the more cumbersome notations $f_X^{cv}(\mathbf{x}, \boldsymbol{\omega}) \equiv f_{X \times [\boldsymbol{\omega}, \boldsymbol{\omega}]}^{cv}(\mathbf{x}, \boldsymbol{\omega})$ and $f_\Omega^{cv}(\mathbf{x}, \boldsymbol{\omega}) \equiv f_{[\mathbf{x}, \mathbf{x}] \times \Omega}^{cv}(\mathbf{x}, \boldsymbol{\omega})$.

2.4 Relaxing Expected-Value Functions

This section presents a general approach for constructing finitely computable convex and concave relaxations of the expected value function $F(\mathbf{x}) = \mathbb{E}[f(\mathbf{x}, \boldsymbol{\omega})]$. Let $(f_{X \times \Omega}^{cv}, f_{X \times \Omega}^{cc})$ be a scheme of relaxations for f on $\bar{X} \times \bar{\Omega}$ as per Assumption 5 and choose any $X \in \mathbb{I}\bar{X}$. To begin, note that a direct application of integral monotonicity gives ([89], p.101)

$$\mathbb{E}[f_X^{cv}(\mathbf{x}, \boldsymbol{\omega})] \leq \mathbb{E}[f(\mathbf{x}, \boldsymbol{\omega})] \leq \mathbb{E}[f_X^{cc}(\mathbf{x}, \boldsymbol{\omega})], \quad \forall \mathbf{x} \in X, \quad (2.2)$$

which suggests defining relaxations of F by $F^{cv}(\mathbf{x}) \equiv \mathbb{E}[f_X^{cv}(\mathbf{x}, \boldsymbol{\omega})]$ and $F^{cc}(\mathbf{x}) \equiv \mathbb{E}[f_X^{cc}(\mathbf{x}, \boldsymbol{\omega})]$. However, although these functions are indeed convex and concave on X , respectively, they are not finitely computable because they need to be evaluated by sampling in general. To overcome this limitation, we apply Jensen's inequality, which is stated as follows.

Lemma 7. *Let $\Omega \subset \bar{\Omega}$ be convex and let $g : \Omega \rightarrow \mathbb{R}$. If g is convex and $\mathbb{E}[g(\boldsymbol{\omega})]$ exists, then $\mathbb{E}[g(\boldsymbol{\omega})] \geq g(\mathbb{E}[\boldsymbol{\omega}])$. If g is concave, then $\mathbb{E}[g(\boldsymbol{\omega})] \leq g(\mathbb{E}[\boldsymbol{\omega}])$.*

Proof. See Proposition 1.1 in Perlman et al. [72]. □

Although Jensen’s inequality is widely used to relax stochastic programs, it has so far only been applied in the case where $f(\mathbf{x}, \cdot)$ is convex on $\bar{\Omega}$ for all $\mathbf{x} \in X$, which we do not assume here. Instead, we propose to combine existing convex relaxation techniques such as McCormick relaxations with Jensen’s inequality. To do this, it is necessary to relax f jointly on $X \times \bar{\Omega}$. Then, integral monotonicity and Jensen’s inequality imply that

$$\mathbb{E}[f(\mathbf{x}, \boldsymbol{\omega})] \geq \mathbb{E}[f_{X \times \bar{\Omega}}^{cv}(\mathbf{x}, \boldsymbol{\omega})] \geq f_{X \times \bar{\Omega}}^{cv}(\mathbf{x}, \mathbb{E}[\boldsymbol{\omega}]), \quad (2.3)$$

$$\mathbb{E}[f(\mathbf{x}, \boldsymbol{\omega})] \leq \mathbb{E}[f_{X \times \bar{\Omega}}^{cc}(\mathbf{x}, \boldsymbol{\omega})] \leq f_{X \times \bar{\Omega}}^{cc}(\mathbf{x}, \mathbb{E}[\boldsymbol{\omega}]). \quad (2.4)$$

for all $\mathbf{x} \in X$. Note that the integrals $\mathbb{E}[f_{X \times \bar{\Omega}}^{cv}(\mathbf{x}, \boldsymbol{\omega})]$ and $\mathbb{E}[f_{X \times \bar{\Omega}}^{cc}(\mathbf{x}, \boldsymbol{\omega})]$ exist because the convexity and concavity of the integrands implies that they are continuous on the interior of $X \times \bar{\Omega}$, and the boundary of $X \times \bar{\Omega}$ has measure zero because $X \times \bar{\Omega}$ is an interval. The inequalities in Equations (2.3)–(2.4) suggest defining relaxations for F by $F^{cv}(\mathbf{x}) \equiv f_{X \times \bar{\Omega}}^{cv}(\mathbf{x}, \mathbb{E}[\boldsymbol{\omega}])$ and $F^{cc}(\mathbf{x}) \equiv f_{X \times \bar{\Omega}}^{cc}(\mathbf{x}, \mathbb{E}[\boldsymbol{\omega}])$. These relaxations are clearly convex and concave on X , respectively, and are finitely computable provided that $\mathbb{E}[\boldsymbol{\omega}]$ is known. However, a remaining difficulty is that the under/over-estimation caused by the use of Jensen’s inequality does not converge to zero as $\text{diam}(X) \rightarrow 0$, which is required for finite termination of spatial branch-and-bound. We address this problem by considering relaxations constructed on interval partitions of $\bar{\Omega}$.

Definition 8. A collection $\mathcal{P} = \{\Omega_i\}_{i=1}^n$ of n_ω -dimensional compact intervals $\Omega_i \in \mathbb{I}\bar{\Omega}$ is called an *interval partition of $\bar{\Omega}$* if $\bar{\Omega} = \cup_{i=1}^n \Omega_i$ and $\text{int}(\Omega_i) \cap \text{int}(\Omega_j) = \emptyset$ for all distinct i and j .

Definition 9. For any measurable $\Omega \subset \bar{\Omega}$, let $\mathbb{P}(\Omega)$ denote the probability of the event $\boldsymbol{\omega} \in \Omega$, and let $\mathbb{E}[\cdot|\Omega]$ denote the conditional expected-value conditioned on the event $\boldsymbol{\omega} \in \Omega$.

The following theorem extends the relaxations defined above to partitions of $\overline{\Omega}$.

Theorem 10. *Let $\mathcal{P} = \{\Omega_i\}_{i=1}^n$ be an interval partition of $\overline{\Omega}$. For every $X \in \mathbb{I}\overline{X}$ and every $\mathbf{x} \in X$, define*

$$F_{X \times \mathcal{P}}^{cv}(\mathbf{x}) \equiv \sum_{i=1}^n \mathbb{P}(\Omega_i) f_{X \times \Omega_i}^{cv}(\mathbf{x}, \mathbb{E}[\boldsymbol{\omega} | \Omega_i]), \quad (2.5)$$

$$F_{X \times \mathcal{P}}^{cc}(\mathbf{x}) \equiv \sum_{i=1}^n \mathbb{P}(\Omega_i) f_{X \times \Omega_i}^{cc}(\mathbf{x}, \mathbb{E}[\boldsymbol{\omega} | \Omega_i]). \quad (2.6)$$

With these definitions, $F_{X \times \mathcal{P}}^{cv}$ and $F_{X \times \mathcal{P}}^{cc}$ are convex and concave relaxations of F on X , respectively.

Proof. By the law of total expectation (Proposition 5.1 in Ross et al. [90]),

$$F(\mathbf{x}) = \mathbb{E}[f(\mathbf{x}, \boldsymbol{\omega})] = \sum_{i=1}^n \mathbb{P}(\Omega_i) \mathbb{E}[f(\mathbf{x}, \boldsymbol{\omega}) | \Omega_i], \quad (2.7)$$

for all $\mathbf{x} \in \overline{X}$. Thus, for any $X \in \mathbb{I}\overline{X}$ and any $\mathbf{x} \in X$, integral monotonicity and Jensen's inequality give,

$$F(\mathbf{x}) \geq \sum_{i=1}^n \mathbb{P}(\Omega_i) \mathbb{E}[f_{X \times \Omega_i}^{cv}(\mathbf{x}, \boldsymbol{\omega}) | \Omega_i], \quad (2.8)$$

$$\geq \sum_{i=1}^n \mathbb{P}(\Omega_i) f_{X \times \Omega_i}^{cv}(\mathbf{x}, \mathbb{E}[\boldsymbol{\omega} | \Omega_i]), \quad (2.9)$$

$$= F_{X \times \mathcal{P}}^{cv}(\mathbf{x}). \quad (2.10)$$

Moreover, $F_{X \times \mathcal{P}}^{cv}$ is convex on X because it is a sum of convex functions. Thus, $F_{X \times \mathcal{P}}^{cv}$ is a convex relaxation of F on X , and the proof for $F_{X \times \mathcal{P}}^{cc}$ is analogous. \square

The relaxations defined in Equations (2.5)–(2.6) are finitely computable provided that the probabilities $\mathbb{P}(\Omega_i)$ and conditional expectations $\mathbb{E}[\boldsymbol{\omega} | \Omega_i]$ are computable for any subinterval $\Omega_i \subset \overline{\Omega}$. This is trivial when $\boldsymbol{\omega}$ is uniformly distributed, but requires difficult multidimensional integrations even for Gaussian random variables. We develop a general approach

for avoiding such integrals for a broad class of random variables called *factorable random variables* in the section ‘Non-Uniform Random Variables’ below. Given these probabilities and expected values, the required relaxations of the integrand f can be computed using any standard technique. In the following example we apply McCormick relaxations [13, 14]. In this case, we call the relaxations in Equation (2.5)–(2.6) *Jensen-McCormick relaxations*.

Example 1. Let $\bar{X} \equiv [-1, 1] \times [-1, 1]$, let $\boldsymbol{\omega} = (\omega_1, \omega_2)$ be uniformly distributed in $\bar{\Omega} \equiv [0, 1] \times [0, 2]$, and define $F : \bar{X} \rightarrow \mathbb{R}$ by $F(\mathbf{x}) \equiv \mathbb{E}[f(\mathbf{x}, \boldsymbol{\omega})]$ with

$$f(\mathbf{x}, \boldsymbol{\omega}) \equiv \frac{x_1 x_2 \ln(3 + x_1 \omega_1 \omega_2) - (x_1^2 - 1)(x_2^2 - 1)\omega_2^2}{2 + \omega_1 x_1}.$$

The nonlinearity of f with respect to $\boldsymbol{\omega}$ makes it difficult if not impossible to evaluate F analytically. Nonetheless, a rigorous convex relaxation for F can be constructed using Theorem 10. Figure 2.1 shows the relaxation $F_{\bar{X} \times \mathcal{P}}^{cv}(\mathbf{x})$ computed using three different partitions \mathcal{P} of $\bar{\Omega}$ with 1, 16, and 64 uniform subintervals each. The required relaxations $f_{\bar{X} \times \Omega_i}^{cv}$ were automatically constructed on each $\bar{X} \times \Omega_i$ by McCormick’s relaxation technique [13, 14]. Figure 2.1 also shows simulated $f(\mathbf{x}, \boldsymbol{\omega})$ values and a sample-average approximation of F using 100 samples. Clearly, the Jensen-McCormick relaxations are convex and underestimate the expected value $F(\mathbf{x})$. Interestingly, however, they do not underestimate $f(\mathbf{x}, \boldsymbol{\omega})$ for every $\boldsymbol{\omega} \in \bar{\Omega}$. Figure 2.1 also shows that $F_{\bar{X} \times \mathcal{P}}^{cv}(\mathbf{x})$ gets significantly tighter as the partition of $\bar{\Omega}$ is refined from 1 subinterval to 16, while the additional improvement from 16 to 64 is small. This shows that sharp results are obtained with few subintervals in this case. Note that $F_{\bar{X} \times \mathcal{P}}^{cv}(\mathbf{x})$ will not converge to $F(\mathbf{x})$ under further $\bar{\Omega}$ partitioning unless \bar{X} is also partitioned, as in spatial branch-and-bound. \square

Spatial branch-and-bound algorithms compute a lower bound on the optimal objective value in a given subinterval X by minimizing a convex relaxation of the objective function, while an upper bound is most often obtained by simply evaluating the objective at a feasible point. Theorem 10 provides a suitable convex relaxation for the lower bounding

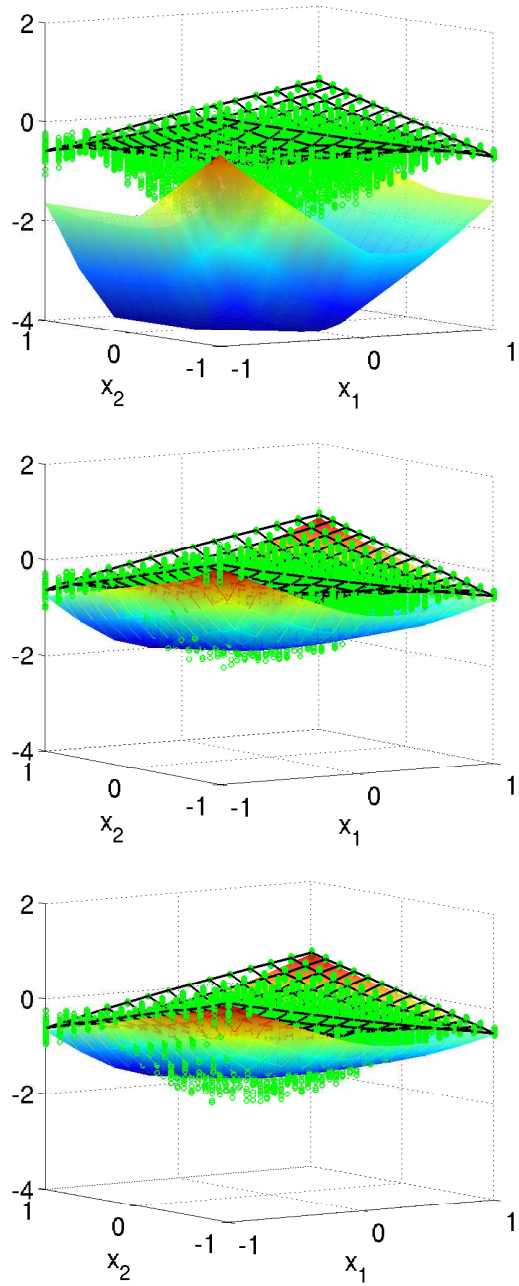


Figure 2.1: Jensen-McCormick convex relaxations of F in Example 1 (shaded surfaces) with partitions of $\bar{\Omega}$ into 1 (top), 16 (middle), and 64 (bottom) uniform subintervals, along with simulated values of $f(\mathbf{x}, \omega)$ at sampled ω values (\circ) and a sample-average approximation of F with 100 samples (black mesh).

problem. However, in the presence of continuous random variables, computing a valid upper bound becomes nontrivial because, in general, F cannot be evaluated finitely. One possible solution is to evaluate the concave relaxation $F_{X \times \mathcal{P}}^{cc}$ instead. However, this is unnecessarily conservative. Instead, rigorous upper (and lower) bounds can be computed at feasible points, without sampling error, by the following simple corollary of Theorem 10.

Corollary 11. *Let $\mathcal{P} = \{\Omega_i\}_{i=1}^n$ be an interval partition of $\bar{\Omega}$. For any $\mathbf{x} \in \bar{X}$, the following bounds hold:*

$$F(\mathbf{x}) \geq \sum_{i=1}^n \mathbb{P}(\Omega_i) f_{\Omega_i}^{cv}(\mathbf{x}, \mathbb{E}[\boldsymbol{\omega}|\Omega_i]), \quad (2.11)$$

$$F(\mathbf{x}) \leq \sum_{i=1}^n \mathbb{P}(\Omega_i) f_{\Omega_i}^{cc}(\mathbf{x}, \mathbb{E}[\boldsymbol{\omega}|\Omega_i]). \quad (2.12)$$

Proof. The result follows by simply applying Theorem 10 with the degenerate interval $X = [\mathbf{x}, \mathbf{x}]$. □

Clearly, the need to exhaustively partition $\bar{\Omega}$ in Theorem 10 and Corollary 11 is potentially prohibitive for problems with high-dimensional uncertainty spaces. However, it is essential for obtaining deterministic bounds on F , rather than bounds that are only statistically valid. Moreover, Theorem 10 and Corollary 11 provide valid bounds on F for any choice of partition \mathcal{P} , no matter how coarse, and this has significant implications in the context of spatial branch-and-bound. Specifically, since valid bounds are obtained with any \mathcal{P} , it is possible to fathom a given node X with certainty using only a coarse partition of $\bar{\Omega}$. In other words, if X is proven to be infeasible or suboptimal based on such a coarse description of uncertainty, then this decision cannot be overturned at any later stage based on a more detailed representation (i.e., a finer partition). This is distinctly different from the case with sample-based bounds, where bounds based on few samples can always be invalidated by additional samples in the future. Thus, when using the bounds and relaxations of Theorem 10 and Corollary 11 in branch-and-bound, it is possible to refine the partition of

$\bar{\Omega}$ adaptively as the search proceeds. It is therefore conceivable that, in some cases, much of the search space could be ruled out using only coarse partitions at low cost, while fine partitions are required only in the vicinity of global solutions. We leave the development and testing of such an adaptive branch-and-bound scheme for future work. However, as a step in this direction, we now turn to the study of the convergence behavior of $F_{X \times \mathcal{P}}^{cv}$ and $F_{X \times \mathcal{P}}^{cc}$ as both X and the elements of \mathcal{P} are refined towards degeneracy.

2.5 Convergence

Consider any $X \in \mathbb{I}\bar{X}$ and any interval partition $\mathcal{P} = \{\Omega_i\}_{i=1}^n$ of $\bar{\Omega}$, and let the relaxations $F_{X \times \mathcal{P}}^{cv}$ and $F_{X \times \mathcal{P}}^{cc}$ be defined as in Theorem 10. This section considers the convergence of these relaxations to $F(\mathbf{x}) = \mathbb{E}[f(\mathbf{x}, \boldsymbol{\omega})]$ as the diameters of X and the elements Ω_i of \mathcal{P} tend towards zero. We require the following assumption on the scheme of relaxations used for f .

Assumption 12. *The scheme of relaxations $(f_{X \times \Omega}^{cv}, f_{X \times \Omega}^{cc})$ from Assumption 5 has second-order pointwise convergence in $\mathbb{I}\bar{X} \times \mathbb{I}\bar{\Omega}$; i.e., $\exists \tau > 0$ such that*

$$\sup_{(\mathbf{x}, \boldsymbol{\omega}) \in X \times \Omega} |f_{X \times \Omega}^{cc}(\mathbf{x}, \boldsymbol{\omega}) - f_{X \times \Omega}^{cv}(\mathbf{x}, \boldsymbol{\omega})| \leq \tau \text{diam}(X \times \Omega)^2,$$

for all $(X \times \Omega) \in \mathbb{I}\bar{X} \times \mathbb{I}\bar{\Omega}$.

Both McCormick and α BB relaxations are known to satisfy Assumption 12 [78]. We now show that this implies a convergence bound for $F_{X \times \mathcal{P}}^{cv}$ and $F_{X \times \mathcal{P}}^{cc}$ in terms of $\text{diam}(X)^2$ and the ‘average’ square-diameter of partition elements $\Omega_i \in \mathcal{P}$.

Lemma 13. *If Assumption 12 holds with $\tau > 0$, then, for any $X \in \mathbb{I}\bar{X}$ and any interval partition $\mathcal{P} = \{\Omega_i\}_{i=1}^n$ of $\bar{\Omega}$,*

$$\sup_{\mathbf{x} \in X} |F_{X \times \mathcal{P}}^{cc}(\mathbf{x}) - F_{X \times \mathcal{P}}^{cv}(\mathbf{x})| \leq \tau \left[\text{diam}(X)^2 + \sum_{i=1}^n \mathbb{P}(\Omega_i) \text{diam}(\Omega_i)^2 \right].$$

Proof. Choose any $X \in \mathbb{I}\bar{X}$ and any $\mathbf{x} \in X$. Moreover, choose any interval partition $\mathcal{P} = \{\Omega_i\}_{i=1}^n$ of $\bar{\Omega}$ and define the shorthand $\hat{\omega}_i \equiv \mathbb{E}[\boldsymbol{\omega}|\Omega_i]$. From Equations (2.5)–(2.6), we have

$$\sup_{\mathbf{x} \in X} |F_{X \times \mathcal{P}}^{cc}(\mathbf{x}) - F_{X \times \mathcal{P}}^{cv}(\mathbf{x})| \quad (2.13)$$

$$= \sup_{\mathbf{x} \in X} \sum_{i=1}^n \mathbb{P}(\Omega_i) |f_{X \times \Omega_i}^{cc}(\mathbf{x}, \hat{\omega}_i) - f_{X \times \Omega_i}^{cv}(\mathbf{x}, \hat{\omega}_i)|, \quad (2.14)$$

$$\leq \sum_{i=1}^n \mathbb{P}(\Omega_i) \sup_{\mathbf{x} \in X} |f_{X \times \Omega_i}^{cc}(\mathbf{x}, \hat{\omega}_i) - f_{X \times \Omega_i}^{cv}(\mathbf{x}, \hat{\omega}_i)|, \quad (2.15)$$

$$\leq \sum_{i=1}^n \mathbb{P}(\Omega_i) \tau \text{diam}(X \times \Omega_i)^2, \quad (2.16)$$

$$\leq \sum_{i=1}^n \mathbb{P}(\Omega_i) \tau (\text{diam}(X)^2 + \text{diam}(\Omega_i)^2), \quad (2.17)$$

$$\leq \tau \left(\text{diam}(X)^2 + \sum_{i=1}^n \mathbb{P}(\Omega_i) \text{diam}(\Omega_i)^2 \right). \quad (2.18)$$

□

In order to use the relaxations $F_{X \times \mathcal{P}}^{cv}$ and $F_{X \times \mathcal{P}}^{cc}$ in a spatial branch-and-bound algorithm, it is important that the relaxation error $\sup_{\mathbf{x} \in X} |F_{X \times \mathcal{P}}^{cc}(\mathbf{x}) - F_{X \times \mathcal{P}}^{cv}(\mathbf{x})|$ converges to zero as $\text{diam}(X) \rightarrow 0$ [11]. However, Lemma 13 suggests that this will not occur if \mathcal{P} remains constant, since the term $\sum_{i=1}^n \mathbb{P}(\Omega_i) \text{diam}(\Omega_i)^2$ will not converge to zero. However, convergence as $\text{diam}(X) \rightarrow 0$ can be achieved if \mathcal{P} is refined appropriately as X diminishes. We formalize this next.

Definition 14. For every $X \in \mathbb{I}\bar{X}$, let $\Phi(X) = \{\Omega_i\}_{i=1}^n$ denote an interval partition of $\bar{\Omega}$ satisfying the condition

$$\sum_{i=1}^n \mathbb{P}(\Omega_i) \text{diam}(\Omega_i)^2 \leq K \text{diam}(X)^2, \quad (2.19)$$

for some constant $K > 0$ that is independent of X . Moreover, let $(\mathcal{F}_X^{cv}, \mathcal{F}_X^{cc})_{X \in \mathbb{I}\bar{X}}$ be a

scheme of relaxations for F defined for all $X \in \overline{\mathbb{I}X}$ by

$$\mathcal{F}_X^{cv}(\mathbf{x}) \equiv F_{X \times \Phi(X)}^{cv}(\mathbf{x}), \quad \forall \mathbf{x} \in X, \quad (2.20)$$

$$\mathcal{F}_X^{cc}(\mathbf{x}) \equiv F_{X \times \Phi(X)}^{cc}(\mathbf{x}), \quad \forall \mathbf{x} \in X, \quad (2.21)$$

where $F_{X \times \Phi(X)}^{cv}$ and $F_{X \times \Phi(X)}^{cc}$ are defined as in Equations (2.5)–(2.6).

Theorem 15. *The scheme of relaxations $(\mathcal{F}_X^{cv}, \mathcal{F}_X^{cc})_{X \in \overline{\mathbb{I}X}}$ for F has second-order pointwise convergence; i.e., there exists $\hat{\tau} > 0$ such that*

$$\sup_{\mathbf{x} \in X} |\mathcal{F}_X^{cc}(\mathbf{x}) - \mathcal{F}_X^{cv}(\mathbf{x})| \leq \hat{\tau} \text{diam}(X)^2, \quad \forall X \in \overline{\mathbb{I}X}.$$

Proof. Let $\tau > 0$ satisfy Assumption 12 and choose any $X \in \overline{\mathbb{I}X}$. By Definition 14 and Lemma 13,

$$\begin{aligned} \sup_{\mathbf{x} \in X} |\mathcal{F}_X^{cc}(\mathbf{x}) - \mathcal{F}_X^{cv}(\mathbf{x})| &= \sup_{\mathbf{x} \in X} |F_{X \times \Phi(X)}^{cc}(\mathbf{x}) - F_{X \times \Phi(X)}^{cv}(\mathbf{x})| \\ &\leq \tau \left[\text{diam}(X)^2 + \sum_{i=1}^n \mathbb{P}(\Omega_i) \text{diam}(\Omega_i)^2 \right], \end{aligned}$$

where $\Phi(X) = \{\Omega_i\}_{i=1}^n$. Applying Equation (2.19),

$$\sup_{\mathbf{x} \in X} |\mathcal{F}_X^{cc}(\mathbf{x}) - \mathcal{F}_X^{cv}(\mathbf{x})| \leq \tau(1 + K) \text{diam}(X)^2, \quad (2.22)$$

which proves the result with $\hat{\tau} = \tau(1 + K)$. \square

The partitioning condition Equation (2.19) is easily satisfied in practice. For example, choosing any $K > 0$, it is satisfied by simply partitioning $\overline{\Omega}$ uniformly until each element satisfies $\text{diam}(\Omega_i)^2 \leq K \text{diam}(X)^2$. The following example demonstrates the convergence result of Theorem 15 using this simple scheme. Although this scheme is likely to generate much larger partitions than are necessary for convergence, we leave the issue of efficient

adaptive partitioning schemes for future work.

Example 2. Let $\bar{X} \equiv [24, 26]$, let ω be uniformly distributed in $\bar{\Omega} \equiv [10, 13]$, and define $F : \bar{X} \rightarrow \mathbb{R}$ by $F(x) \equiv \mathbb{E}[f(x, \omega)]$ with

$$f(x, \omega) \equiv \frac{(\omega - 10)^2 \ln(x) + (x - 5)^2}{\omega}.$$

Consider the sequence of intervals $X_\epsilon \equiv [25 - \epsilon, 25 + \epsilon] \subset \bar{X}$ with $\epsilon \rightarrow 0$, so that $\text{diam}(X_\epsilon) \rightarrow 0$. For every X_ϵ , let $\Phi(X_\epsilon) = \{\Omega_i\}_{i=1}^n$ be generated by uniformly partitioning $\bar{\Omega}$ until $\text{diam}(\Omega_i) \leq 10\text{diam}(X_\epsilon) = 20\epsilon$, which verifies Equation (2.19) with $K = 100$. Moreover, define the relaxations $\mathcal{F}_{X_\epsilon}^{cv}$ and $\mathcal{F}_{X_\epsilon}^{cc}$ of F on X_ϵ as in Definition 14, where McCormick's relaxations are used to compute $(f_{X_\epsilon \times \Omega}^{cv}, f_{X_\epsilon \times \Omega}^{cc})$ satisfying Assumptions 5 and 12. Figure 2.2 shows the pointwise relaxation error $|\mathcal{F}_{X_\epsilon}^{cc}(x) - \mathcal{F}_{X_\epsilon}^{cv}(x)|$ versus ϵ for the point $x = 25$. The observed slope of 2 on log-log axes indicates that the convergence is indeed second-order. \square

2.6 Non-Uniform Random Variables

The relaxation theory presented in the previous sections puts two significant restrictions on the random variables ω . First, ω must be compactly supported in the interval $\bar{\Omega} \in \mathbb{IR}^{n_\omega}$. Therefore, if we wish to use, e.g., normal random variables, we must use a truncated density function. However, this is not a major limitation since the truncated distribution can be made arbitrarily close to the original by choosing $\bar{\Omega}$ large. Second, computing the relaxations $F_{X \times \mathcal{P}}^{cv}$ and $F_{X \times \mathcal{P}}^{cc}$ for a given partition \mathcal{P} of $\bar{\Omega}$ requires the ability to compute the probability $\mathbb{P}(\Omega)$ and conditional expectation $\mathbb{E}[\omega|\Omega]$ for any given subinterval Ω of $\bar{\Omega}$. While this is trivial for uniform random variables, it may involve very cumbersome multidimensional integrals for other types of random variables. In this section, we address this issue in two steps. First, we compile a library of so-called *primitive* random variables for which the required probabilities and expectations are easily computed by well-known

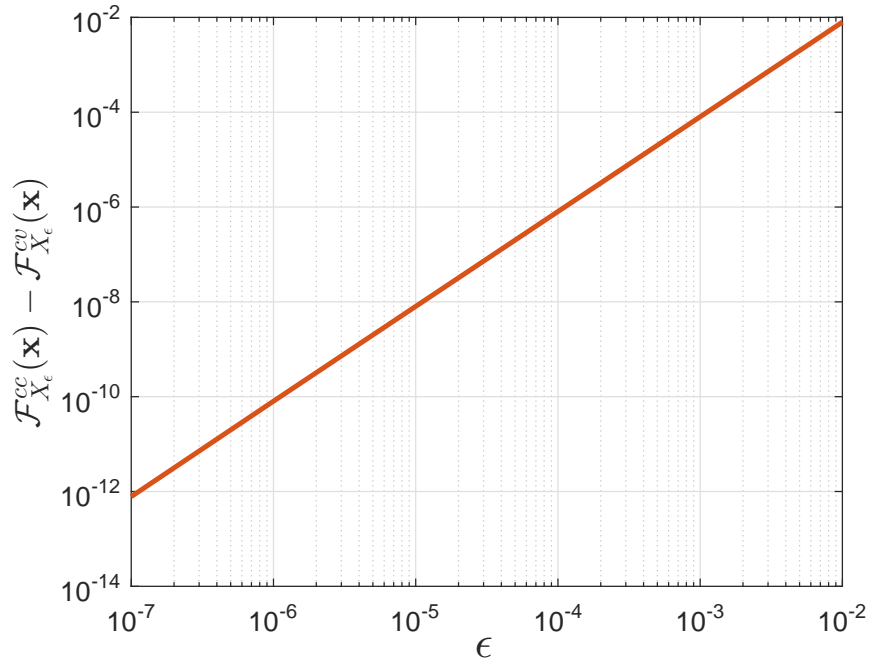


Figure 2.2: Second-order pointwise convergence of Jensen-McCormick relaxations with respect to $\frac{1}{2}\text{diam}(X_\epsilon) = \epsilon$ for Example 2 under a uniform $\bar{\Omega}$ partitioning rule satisfying Equation (2.19) with $K = 100$. Plotted values are for $x = \text{mid}(X_\epsilon) = 25$.

formulas. Second, we extend our relaxation theory to problems with *factorable* random variables, which are those random variables that can be transformed into primitive random variables by a factorable function. We then provide some general strategies for finding such transformations.

2.6.1 Primitive Random Variables

Recall that ω is a vector of random variables with PDF $p : \mathbb{R}^{n_\omega} \rightarrow \mathbb{R}$ compactly supported in the interval $\bar{\Omega} \in \mathbb{I}\mathbb{R}^{n_\omega}$. We will call ω a *primitive* random vector if, for any $\Omega \in \mathbb{I}\bar{\Omega}$, the quantities $\mathbb{P}(\Omega)$ and $\mathbb{E}[\omega|\Omega]$ can be computed efficiently through simple formulas. Clearly, uniformly distributed random variables are primitive. Moreover, if the elements of $\omega = (\omega_1, \dots, \omega_{n_\omega})$ are independent, then several other distributions for each ω_i result in a primitive ω . To see this, let $\bar{\Omega} = \bar{W}_1 \times \dots \times \bar{W}_{n_\omega}$ and let $\Omega = W_1 \times \dots \times W_{n_\omega} \in \mathbb{I}\bar{\Omega}$.

With this notation, independence implies that

$$\mathbb{P}(\Omega) = \prod_{i=1}^{n_\omega} \mathbb{P}(W_i), \quad (2.23)$$

$$\mathbb{E}[\boldsymbol{\omega}|\Omega] = (\mathbb{E}[\omega_1|W_1], \dots, \mathbb{E}[\omega_{n_\omega}|W_{n_\omega}]). \quad (2.24)$$

Thus, $\boldsymbol{\omega}$ is primitive if formulas are known for the one-dimensional probabilities $\mathbb{P}(W_i)$ and expectations $\mathbb{E}[\omega_i|W_i]$. Such formulas are well known for many common distributions. However, recall that distributions with non-interval supports must be truncated to \overline{W}_i here. The following lemma provides a means to translate formulas for $\mathbb{P}(W_i)$ and $\mathbb{E}[\omega_i|W_i]$ for an arbitrary one-dimensional distribution to corresponding formulas for the same distribution truncated on \overline{W}_i .

Lemma 16. *Let η be a random variable with probability density function (PDF) $p_\eta : \mathbb{R} \rightarrow \mathbb{R}$, and let \mathbb{P}_η and \mathbb{E}_η denote the probability and expected value with respect to p_η , respectively. Moreover, choose any $\overline{W} \in \mathbb{I}\mathbb{R}$ and let ω be a random variable with the truncated PDF $p : \mathbb{R} \rightarrow \mathbb{R}$ defined by*

$$p(\omega) \equiv p_\eta(\omega|\overline{W}) = \begin{cases} p_\eta(\omega)/\mathbb{P}_\eta(\overline{W}) & \text{if } \omega \in \overline{W} \\ 0 & \text{otherwise} \end{cases}.$$

Let \mathbb{P} and \mathbb{E} denote the probability and expected value with respect to p . For any $W \in \mathbb{I}\overline{W}$, the following relations hold:

$$\mathbb{P}(W) = \mathbb{P}_\eta(W)/\mathbb{P}_\eta(\overline{W}), \quad (2.25)$$

$$\mathbb{E}[\omega|W] = \mathbb{E}_\eta[\omega|W], \quad (2.26)$$

Proof. For any $W \in \mathbb{I}\overline{W}$,

$$\mathbb{P}(W) = \int_W p(\omega) d\omega = \int_W \frac{p_\eta(\omega)}{\mathbb{P}_\eta(\overline{W})} d\omega = \frac{\mathbb{P}_\eta(W)}{\mathbb{P}_\eta(\overline{W})}, \quad (2.27)$$

Table 2.1: Primitive one-dimensional distributions on $\overline{W} = [\overline{\omega}^L, \overline{\omega}^U]$ with formulas for the CDFs $P(\omega)$ and the conditional expectations $\mathbb{E}[\omega|W]$ with $\omega \in W = [\omega^L, \omega^U] \in \mathbb{I}\overline{W}$. Normal and Gamma distributions are truncated to \overline{W} [92]. Formulas for the Beta distribution are for $\overline{W} = [0, 1]$, but arbitrary \overline{W} can be achieved by linear transformation of the random variable (see §2.6.2).

Distribution	Notation	$P(\omega)$	$\mathbb{E}[\omega W]$
Uniform $U(\overline{\omega}^L, \overline{\omega}^U)$		$\frac{\omega - \overline{\omega}^L}{\overline{\omega}^U - \overline{\omega}^L}$	$\frac{\omega^L + \omega^U}{2}$
Truncated Normal $\mathcal{N}(\mu, \sigma^2, \overline{\omega}^L, \overline{\omega}^U)$	$\phi(\xi) \equiv \frac{1}{\sqrt{2\pi}} \exp(-\frac{1}{2}\xi^2)$ $\Phi(\xi) \equiv \frac{1}{2}(1 + \operatorname{erf}(\xi/\sqrt{2}))$	$\frac{\Phi(\frac{\omega - \mu}{\sigma}) - \Phi(\frac{\overline{\omega}^L - \mu}{\sigma})}{\Phi(\frac{\overline{\omega}^U - \mu}{\sigma}) - \Phi(\frac{\overline{\omega}^L - \mu}{\sigma})}$	$\mu + \frac{\phi(\frac{\omega^L - \mu}{\sigma}) - \phi(\frac{\omega^U - \mu}{\sigma})}{\Phi(\frac{\omega^U - \mu}{\sigma}) - \Phi(\frac{\omega^L - \mu}{\sigma})} \sigma$
Truncated Gamma $\Gamma(\alpha, \beta, \overline{\omega}^L, \overline{\omega}^U)$ $\alpha > 0, \beta > 0$	$\Gamma(a, z) \equiv \int_z^\infty t^{a-1} e^{-t} dt$	$\frac{\Gamma(\alpha, \frac{\omega}{\beta}) - \Gamma(\alpha, \frac{\overline{\omega}^L}{\beta})}{\Gamma(\alpha, \frac{\overline{\omega}^U}{\beta}) - \Gamma(\alpha, \frac{\overline{\omega}^L}{\beta})}$	$\frac{\beta(\Gamma(\alpha + 1, \frac{\omega^U}{\beta}) - \Gamma(\alpha + 1, \frac{\omega^L}{\beta}))}{\Gamma(\alpha, \frac{\omega^U}{\beta}) - \Gamma(\alpha, \frac{\omega^L}{\beta})}$
Beta ($\overline{W} = [0, 1]$) $B(\alpha, \beta)$ $\alpha > 0, \beta > 0$	$B(a, b, c) \equiv \int_0^c t^{a-1} (1-t)^{b-1} dt$	$\frac{B(\alpha, \beta, \omega)}{B(\alpha, \beta, 1)}$	$\frac{B(1 + \alpha, \beta, \omega^U) - B(1 + \alpha, \beta, \omega^L)}{B(\alpha, \beta, \omega^U) - B(\alpha, \beta, \omega^L)}$

which proves Equation (2.25). Similarly,

$$\mathbb{E}[\omega|W] = \frac{1}{\mathbb{P}(W)} \int_W \omega p(\omega) d\omega, \quad (2.28)$$

$$= \frac{1}{\mathbb{P}(W)} \int_W \omega \frac{p_\eta(\omega)}{\mathbb{P}_\eta(W)} d\omega. \quad (2.29)$$

Applying Equation (2.25),

$$\mathbb{E}[\omega|W] = \frac{1}{\mathbb{P}_\eta(W)} \int_W \omega p_\eta(\omega) d\omega = \mathbb{E}_\eta[\omega|W]. \quad (2.30)$$

□

Table 2.1 lists formulas for the cumulative probability distributions (CDFs) P and conditional expectations $\mathbb{E}[\omega|W]$ for several common one-dimensional distributions. When necessary, distributions are truncated to an interval $\overline{W} = [\overline{\omega}^L, \overline{\omega}^U]$. The listed CDFs can be used to compute $\mathbb{P}(W)$ via $\mathbb{P}(W) = P(\omega^U) - P(\omega^L)$. The formulas in Table 2.1 follow directly from Lemma 16 and standard formulas for probabilities and conditional expectations [91, 92].

2.6.2 Factorable Random Variables

We now extend our relaxation method to a flexible class of non-primitive random variables. For the following definition, recall the definition of a *factorable function* discussed at the end of the section ‘Preliminaries’ above.

Definition 17. The random vector ω is called *factorable* if there exists an open set $\Gamma_0 \subset \mathbb{R}^{n_\omega}$, an interval $\bar{\Gamma} \in \mathbb{I}\Gamma_0$, and a function $\psi : \Gamma_0 \rightarrow \mathbb{R}^{n_\omega}$ such that (i) ψ is continuously differentiable on Γ_0 and $\det\left(\frac{\partial\psi}{\partial\gamma}(\gamma)\right) \neq 0, \forall \gamma \in \Gamma_0$; (ii) ψ is one-to-one on Γ_0 , and hence invertible on the image set $\psi(\Gamma_0)$; (iii) ω has zero probability density outside of $\psi(\bar{\Gamma})$; (iv) $\gamma = \psi^{-1}(\omega)$ is a primitive random variable; and (v) ψ can be expressed as a factorable function on $\bar{\Gamma}$.

Remark 18. A standard result in probability theory (Section 6.7 in Ross et al. [90]) shows that, under the conditions of Definition 17, $\gamma = \psi^{-1}(\omega)$ obeys the PDF $p_\gamma : \mathbb{R}^{n_\omega} \rightarrow \mathbb{R}$ defined by

$$p_\gamma(\gamma) = \begin{cases} p(\psi(\gamma)) \left| \det\left(\frac{\partial\psi}{\partial\gamma}(\gamma)\right) \right| & \text{if } \gamma \in \bar{\Gamma} \\ 0 & \text{otherwise.} \end{cases}, \quad (2.31)$$

where p is the PDF of ω . Thus, the fourth condition of Definition 17 is equivalent to the statement that p_γ is the PDF of a primitive random variable.

The following theorem shows that the expected value $F(\mathbf{x}) = \mathbb{E}[f(\mathbf{x}, \omega)]$ of a factorable function f with respect to a factorable random variable ω can be reformulated as an equivalent expected value over a primitive random variable γ , and the reformulated integrand is again a factorable function.

Theorem 19. Assume that ω is factorable and let $\psi, \bar{\Gamma}, \gamma$, and p_γ be defined as in Definition 17 and Remark 18. Moreover, denote the expected value with respect to p_γ by \mathbb{E}_γ . If

$\hat{f} : \bar{X} \times \bar{\Gamma} \rightarrow \mathbb{R}$ is defined by $\hat{f}(\mathbf{x}, \gamma) = f(\mathbf{x}, \psi(\gamma))$, then \hat{f} is a factorable function and

$$\mathbb{E}[f(\mathbf{x}, \boldsymbol{\omega})] = \mathbb{E}_\gamma[\hat{f}(\mathbf{x}, \gamma)]. \quad (2.32)$$

Proof. By condition (v) of Definition 17, \hat{f} is a composition of factorable functions, and is therefore factorable [13]. Now, by condition (iii) of Definition 17, $p(\boldsymbol{\omega}) = 0$ for all $\boldsymbol{\omega} \notin \psi(\bar{\Gamma})$. Therefore,

$$\mathbb{E}[f(\mathbf{x}, \boldsymbol{\omega})] = \int_{\psi(\bar{\Gamma})} f(\mathbf{x}, \boldsymbol{\omega}) p(\boldsymbol{\omega}) d\boldsymbol{\omega}.$$

Conditions (i) and (ii) imply that ψ is a diffeomorphism from Γ_0 to $\psi(\Gamma_0)$. Since the boundary of $\bar{\Gamma}$ has measure zero, it follows that the boundary of $\psi(\bar{\Gamma})$ has measure zero (Lemma 18.1 in Munkres et al. [93]) and can be excluded from the integral above. Moreover, ψ is a valid change-of-variables from $\boldsymbol{\omega}$ in the open set $\text{int}(\psi(\bar{\Gamma}))$ to γ in the open set $\psi^{-1}(\text{int}(\psi(\bar{\Gamma})))$ (p.147 in Munkres et al. [93]). Furthermore, the latter set is equivalent to $\text{int}(\bar{\Gamma})$ by Theorem 18.2 in Munkres et al. [93]. Then, applying the Change of Variables Theorem 17.2 in Munkres et al. [93] and noting that the boundary of $\bar{\Gamma}$ has measure zero,

$$\mathbb{E}[f(\mathbf{x}, \boldsymbol{\omega})] = \int_{\bar{\Gamma}} f(\mathbf{x}, \psi(\gamma)) p(\psi(\gamma)) \left| \det \left(\frac{\partial \psi}{\partial \gamma}(\gamma) \right) \right| d\gamma.$$

Then, using Equation (2.31),

$$\mathbb{E}[f(\mathbf{x}, \boldsymbol{\omega})] = \int_{\bar{\Gamma}} f(\mathbf{x}, \psi(\gamma)) p_\gamma(\gamma) d\gamma = \mathbb{E}_\gamma[\hat{f}(\mathbf{x}, \gamma)].$$

□

When $\boldsymbol{\omega}$ is factorable, Theorem 19 implies that valid relaxations for $F(\mathbf{x}) = \mathbb{E}[f(\mathbf{x}, \boldsymbol{\omega})]$ can be obtained by relaxing the equivalent representation $F(\mathbf{x}) = \mathbb{E}_\gamma[\hat{f}(\mathbf{x}, \gamma)]$. Relaxations of the latter expression can be readily computed as described previously since \hat{f} is

factorable and γ is a primitive random variable. Specifically, letting $\mathcal{P} = \{\Gamma_i\}_{i=1}^n$ denote an interval partition of $\overline{\Gamma}$, valid relaxations are given by

$$F_{X \times \mathcal{P}}^{cv}(\mathbf{x}) \equiv \sum_{i=1}^n \mathbb{P}_\gamma(\Gamma_i) \hat{f}_{X \times \Gamma_i}^{cv}(\mathbf{x}, \mathbb{E}_\gamma[\gamma | \Gamma_i]), \quad (2.33)$$

$$F_{X \times \mathcal{P}}^{cc}(\mathbf{x}) \equiv \sum_{i=1}^n \mathbb{P}_\gamma(\Gamma_i) \hat{f}_{X \times \Gamma_i}^{cc}(\mathbf{x}, \mathbb{E}_\gamma[\gamma | \Gamma_i]). \quad (2.34)$$

Thus, relaxations can be computed without explicitly computing $\mathbb{P}(\Omega)$ and $\mathbb{E}[\omega | \Omega]$ for non-primitive distributions.

In the following subsections, we discuss several methods for computing the factorable transformation ψ required by Definition 17. We first consider one-dimensional transformations that can be used to handle random variables ω with more general distributions than in Table 2.1, but still restricted to having independent elements. Subsequently, we show how random variables with independent elements can be transformed into random variables with any desired covariance matrix.

2.6.3 The Inverse Transform Method

Let $P : \mathbb{R} \rightarrow [0, 1]$ be the cumulative distribution function (CDF) for ω . It is well known that the random variable defined by $\gamma = P(\omega)$ is uniformly distributed on $[0, 1]$ [94]. Thus, γ is a primitive random variable, and $\omega = P^{-1}(\gamma)$ is a factorable random variable as per Definition 17 under the following assumptions.

Assumption 20. *Let ω be compactly supported in the interval $\overline{W} \in \mathbb{IR}$. Assume that P is continuously differentiable on \overline{W} and satisfies $\frac{dP}{d\omega}(\omega) = p(\omega) > 0$ for all $\omega \in \overline{W}$. Moreover, assume that P^{-1} is a factorable function.*

Under Assumption 20, it is always possible to define an open set W_0 containing \overline{W} and a continuously differentiable function $\psi^{-1} : W_0 \rightarrow \mathbb{R}$ that agrees with P on \overline{W} and satisfies $\frac{d\psi^{-1}}{d\omega}(\omega) > 0$ for all $\omega \in W_0$. This last condition ensures that ψ^{-1} has an inverse

ψ defined on $\Gamma_0 \equiv \psi^{-1}(W_0)$, which contains the interval $\bar{\Gamma} \equiv \psi^{-1}(\bar{W}) = P(\bar{W}) = [0, 1]$. By Theorem 8.2 in [93], Γ_0 is open and ψ is continuously differentiable on Γ_0 . Moreover, an application of the chain rule to the identity $\psi^{-1}(\psi(\gamma)) = \gamma$ gives

$$\frac{d\psi}{d\gamma}(\gamma) = \left[\frac{d\psi^{-1}}{d\omega}(\psi(\gamma)) \right]^{-1} > 0, \quad \gamma \in \Gamma_0. \quad (2.35)$$

Thus, conditions (i) and (ii) of Definition 17 are satisfied. Condition (iii) states that $\psi(\bar{\Gamma}) = P^{-1}([0, 1])$ contains the support of ω , which holds by definition of P . Condition (iv) holds because, by Remark 18 and Equation (2.35),

$$p_\gamma(\gamma) = p(\psi(\gamma)) \left[\frac{d\psi^{-1}}{d\omega}(\psi(\gamma)) \right]^{-1} \quad (2.36)$$

$$= p(\psi(\gamma)) \left[\frac{dP}{d\omega}(\psi(\gamma)) \right]^{-1}, \quad (2.37)$$

$$= p(\psi(\gamma)) [p(\psi(\gamma))]^{-1}, \quad (2.38)$$

$$= 1, \quad (2.39)$$

for all $\gamma \in \bar{\Gamma}$, and $p_\gamma(\gamma) = 0$ otherwise. Thus, γ is uniform. Finally, condition (v) of Definition 17 holds by the assumption that P^{-1} is factorable. Thus, ω is a factorable random variable under the transformation $\omega = P^{-1}(\gamma)$.

For example, let $\omega \sim W(\alpha, \beta, \bar{\omega}^L, \bar{\omega}^U)$ be a truncated Weibull random variable with coefficients α and β . The standard (untruncated) Weibull CDF and inverse CDF are given by

$$P_\eta(\eta) = 1 - e^{-(\eta/\alpha)^\beta}, \quad (2.40)$$

$$P_\eta^{-1}(\gamma) = \alpha \sqrt[\beta]{-\ln(1 - \gamma)}. \quad (2.41)$$

The CDF of the truncated distribution is given by

$$P(\omega) = \frac{P_\eta(\omega) - P_\eta(\bar{\omega}^L)}{P_\eta(\bar{\omega}^U) - P_\eta(\bar{\omega}^L)}, \quad \forall \omega \in \bar{W}, \quad (2.42)$$

and hence

$$\begin{aligned} P^{-1}(\gamma) &= P_\eta^{-1} [P_\eta(\bar{\omega}^L) + (P_\eta(\bar{\omega}^U) - P_\eta(\bar{\omega}^L))\gamma], \\ &= \alpha \sqrt[\beta]{-\ln \left[e^{-(\frac{\bar{\omega}^L}{\alpha})^\beta} + (e^{-(\frac{\bar{\omega}^U}{\alpha})^\beta} - e^{-(\frac{\bar{\omega}^L}{\alpha})^\beta})\gamma \right]}. \end{aligned} \quad (2.43)$$

This gives the desired factorable transformation $\omega = \psi(\gamma) = P^{-1}(\gamma)$. Similar transformations for several common distributions are collected in Table 2.2.

2.6.4 Other Transformations

For many common random variables, explicit transformations from simpler random variables have been developed for the purpose of generating samples computationally. One example is the Box-Muller transformation, which transforms the two-dimensional uniform random variable γ on $(0, 1] \times [0, 1]$ into two independent standard normal random variables ω via

$$\begin{aligned} \omega_1 &= \sqrt{-2 \ln \gamma_1} \cos(2\pi\gamma_2), \\ \omega_2 &= \sqrt{-2 \ln \gamma_1} \sin(2\pi\gamma_2). \end{aligned} \quad (2.44)$$

According to Martino et al. [95], the Box-Muller transform can also be used to generate independent bivariate normal random variables truncated on a disc of radius \bar{r} ; i.e., with $\bar{\Omega} \equiv \{\omega \in \mathbb{R}^2 : \omega_1^2 + \omega_2^2 \leq \bar{r}^2\}$. This is accomplished by simply setting $\bar{\gamma}_1^L = \exp(-\frac{\bar{r}^2}{2})$, $\bar{\Gamma} = [\bar{\gamma}_1^L, 1] \times [0, 1]$, and defining γ on $\bar{\Gamma}$ by Equation (2.44), which is clearly factorable.

Many other factorable transformations can be readily devised. Naturally, we can replace log-normal random variables by the log of normal random variables, χ^2 random variables

Table 2.2: Some common random variables ω that are factorable in the sense of Definition 17 with γ uniformly distributed on $\bar{\Gamma} = [0, 1]$ and factorable transformations $\psi(\gamma) = P^{-1}(\gamma)$ given by inverse CDFs. All random variables ω are truncated on the interval $\bar{W} = [\bar{\omega}^L, \bar{\omega}^U]$. $P_\eta^{-1}(\gamma)$ is the inverse CDF of the corresponding untruncated random variable, so that $P^{-1}(\gamma) = P_\eta^{-1}[P_\eta(\bar{\omega}^L) + (P_\eta(\bar{\omega}^U) - P_\eta(\bar{\omega}^L))\gamma]$.

Distribution	$P_\eta^{-1}(\gamma)$	$P^{-1}(\gamma)$
Truncated Exponential $Exp(\lambda, \bar{\omega}^L, \bar{\omega}^U)$ $\lambda > 0$	$-\frac{1}{\lambda} \ln(1 - \gamma)$	$-\frac{1}{\lambda} \ln[e^{-\lambda\bar{\omega}^L} + (e^{-\lambda\bar{\omega}^U} - e^{-\lambda\bar{\omega}^L})\gamma]$
Truncated Weibull $W(\alpha, \beta, \bar{\omega}^L, \bar{\omega}^U)$ $\alpha, \beta > 0$	$\alpha \sqrt[\beta]{-\ln(1 - \gamma)}$	$\alpha \sqrt[\beta]{-\ln \left[e^{-(\frac{\bar{\omega}^L}{\alpha})^\beta} + (e^{-(\frac{\bar{\omega}^U}{\alpha})^\beta} - e^{-(\frac{\bar{\omega}^L}{\alpha})^\beta})\gamma \right]}$
Truncated Cauchy $C(\alpha, \beta, \bar{\omega}^L, \bar{\omega}^U)$	$\beta \tan((\gamma - \frac{1}{2})\pi) + \alpha$	$\beta \tan[\arctan(\frac{\bar{\omega}^L - \alpha}{\beta}) + (\arctan(\frac{\bar{\omega}^U - \alpha}{\beta}) - \arctan(\frac{\bar{\omega}^L - \alpha}{\beta}))\gamma] + \alpha$
Truncated Rayleigh $Ra(\sigma, \bar{\omega}^L, \bar{\omega}^U)$ $\sigma > 0$	$\sqrt{-2\sigma^2 \ln(1 - \gamma)}$	$\sqrt{-2\sigma^2 \ln[e^{-\frac{(\bar{\omega}^L)^2}{2\sigma^2}} + (e^{-\frac{(\bar{\omega}^U)^2}{2\sigma^2}} - e^{-\frac{(\bar{\omega}^L)^2}{2\sigma^2}})\gamma]}$
Truncated Pareto $Pa(m, \alpha, \bar{\omega}^L, \bar{\omega}^U)$ $m, \alpha > 0$	$m(1 - \gamma)^{-\frac{1}{\alpha}}$	$m[(\frac{m}{\bar{\omega}^L})^\alpha + ((\frac{m}{\bar{\omega}^U})^\alpha - (\frac{m}{\bar{\omega}^L})^\alpha)\gamma]^{-\frac{1}{\alpha}}$

by summations of squared standard normal random variables, etc.

2.6.5 Dependent Random Variables

Using the techniques outlined in the previous subsections, factorable random vectors can be generated with elements obeying a wide variety of common distributions, but all elements must be independent. Let $\hat{\omega}$ denote such a random vector, so that $\text{Cov}(\hat{\omega}) = \mathbf{I}$. In this subsection, we show that another factorable (in fact linear) transformation can be used to generate a random vector ω from $\hat{\omega}$ with any desired mean \mathbf{d} and positive definite covariance matrix \mathbf{C} . For any such \mathbf{C} , positive definiteness implies that there exists a unique positive definite matrix $\mathbf{C}^{1/2}$ such that $(\mathbf{C}^{1/2})^2 = \mathbf{C}$. Thus, defining $\omega = \mathbf{d} + \mathbf{C}^{1/2}(\hat{\omega} - \mathbb{E}[\hat{\omega}])$, we readily obtain $\mathbb{E}[\omega] = \mathbf{d}$ and

$$\text{Cov}(\omega) = \mathbb{E}[(\omega - \mathbb{E}[\omega])(\omega - \mathbb{E}[\omega])^T], \quad (2.45)$$

$$= \mathbb{E}[\mathbf{C}^{1/2}(\hat{\omega} - \mathbb{E}[\hat{\omega}])(\hat{\omega} - \mathbb{E}[\hat{\omega}])^T(\mathbf{C}^{1/2})^T], \quad (2.46)$$

$$= \mathbf{C}^{1/2}\text{Cov}(\hat{\omega})\mathbf{C}^{1/2}, \quad (2.47)$$

$$= \mathbf{C}, \quad (2.48)$$

as desired. Note that this linear transformation can be applied directly to any of the primitive random variables listed in Table 2.1 (e.g., to obtain a multivariate normal distribution with mean \mathbf{d} and covariance \mathbf{C}) or to more general factorable random variables constructed via the methods in the previous subsections.

Example 3. To demonstrate the use of non-primitive factorable random variables, we consider relaxing the objective function of the following stochastic optimization problem modified from Ryoo et al. [96], which considers the optimal design of two consecutive contin-

uous stirred-tank reactors of volumes x_1 and x_2 carrying out the reactions $A \rightleftharpoons B \rightleftharpoons C$:

$$\begin{aligned}
\min_{\mathbf{x}} \quad & - \mathbb{E} \left[\frac{k_{f,2}x_2(1 + k_{r,1}x_1) + k_{f,1}x_1(1 + k_{f,2}x_2)}{(1 + k_{f,1}x_1)(1 + k_{f,2}x_2)(1 + k_{r,1}x_1)(1 + k_{r,2}x_2)} \right] \\
\text{s.t.} \quad & x_1^{0.5} + x_2^{0.5} \leq 4 \\
& 0 \leq x_1, x_2 \leq 16 \\
& k_{r,1} = 0.99k_{f,1} \\
& k_{r,2} = 0.90k_{f,2} \\
& \begin{bmatrix} k_{f,1} \\ k_{f,2} \end{bmatrix} = \begin{bmatrix} 0.097 \\ 0.039 \end{bmatrix} + \begin{bmatrix} 0.0072 & 0.0006 \\ 0.0006 & 0.0036 \end{bmatrix} \begin{bmatrix} \gamma_1 \\ \gamma_2 \end{bmatrix} \\
& \gamma_1 \sim \mathcal{N}(\mu_1, \sigma_1^2, \bar{\gamma}_1^L, \bar{\gamma}_1^U) \\
& \gamma_2 \sim \mathcal{N}(\mu_2, \sigma_2^2, \bar{\gamma}_2^L, \bar{\gamma}_2^U)
\end{aligned}$$

The objective is to maximize the expected value of the concentration of product B in the exit stream of the second reactor. We assume that the forward reaction rates $(k_{f,1}, k_{f,2})$ follow a bivariate normal distribution with

$$\mathbf{d} = \mathbb{E} \left(\begin{bmatrix} k_{f,1} \\ k_{f,2} \end{bmatrix} \right) = \begin{bmatrix} 0.097 \\ 0.039 \end{bmatrix}, \quad (2.49)$$

$$\mathbf{C}^{1/2} = \sqrt{\text{Cov} \left(\begin{bmatrix} k_{f,1} \\ k_{f,2} \end{bmatrix} \right)} = \begin{bmatrix} 0.0072 & 0.0006 \\ 0.0006 & 0.0036 \end{bmatrix}. \quad (2.50)$$

To avoid computing probabilities and conditional expected values of this distribution over subintervals, we introduce a primitive random vector γ consisting of two independent random variables (γ_1, γ_2) satisfying standard normal distributions ($\mu_1 = \mu_2 = 0$ and $\sigma_1 = \sigma_2 = 1$) truncated at plus and minus five standard deviations, giving the truncation

bounds

$$[\bar{\gamma}_1^L, \bar{\gamma}_1^U] = [\bar{\gamma}_2^L, \bar{\gamma}_2^U] = [-5, 5]. \quad (2.51)$$

After truncation, $\text{Var}(\gamma_1) = \text{Var}(\gamma_2) = 0.9999 \approx 1$. We then transform (γ_1, γ_2) into a bivariate normal random variable $(k_{f,1}, k_{f,2})$ with the desired mean and covariance as discussed in the subsection ‘Dependent Random Variables’ above. With these definitions, Figure 2.3 shows convex relaxations for the objective function on $X \equiv [2.5, 4] \times [2.5, 4]$ computed as in Equation (2.33) with partitions $\mathcal{P} = \{\Gamma_i\}_{i=1}^{n_\omega}$ of $\bar{\Gamma}$ consisting of 1, 16, and 64 elements. The required relaxations of $\hat{f}(\mathbf{x}, \boldsymbol{\gamma}) = f(\mathbf{x}, \mathbf{d} + \mathbf{C}^{1/2}\boldsymbol{\gamma})$ on each $X \times \Gamma_i$ were computed using McCormick relaxations [13]. Figure 2.3 shows that the relaxation computed with a partition consisting of only one element is fairly weak, but improves significantly with 16 elements. On the other hand, the additional improvement achieved with 64 elements is minor.

Figure 2.4 shows the pointwise convergence of the computed relaxations on a sequence of intervals $X_\epsilon \equiv [5 - \epsilon, 5 + \epsilon] \times [6 - \epsilon, 6 + \epsilon]$ as $\epsilon \rightarrow 0$. Specifically, Figure 2.4 shows the convergence of the scheme of relaxations $(\mathcal{F}_X^{cv}, \mathcal{F}_X^{cc})$ defined analogously to Equations (2.20)–(2.21) by imposing an X -dependent uniform partitioning rule to $\bar{\Gamma}$ such that

$$\sum_{i=1}^n \mathbb{P}(\Gamma_i) \text{diam}(\Gamma_i)^2 \leq K \text{diam}(X)^2. \quad (2.52)$$

Again, the observed slope of 2 on log-log axes verifies the theoretical second-order pointwise convergence ensured by Theorem 15. □

2.7 Conclusions

In this chapter, we developed a new method for computing convex and concave relaxations of nonconvex expected-value functions over continuous random variables. These relaxations can provide rigorous lower and upper bounds for use in spatial branch-and-bound

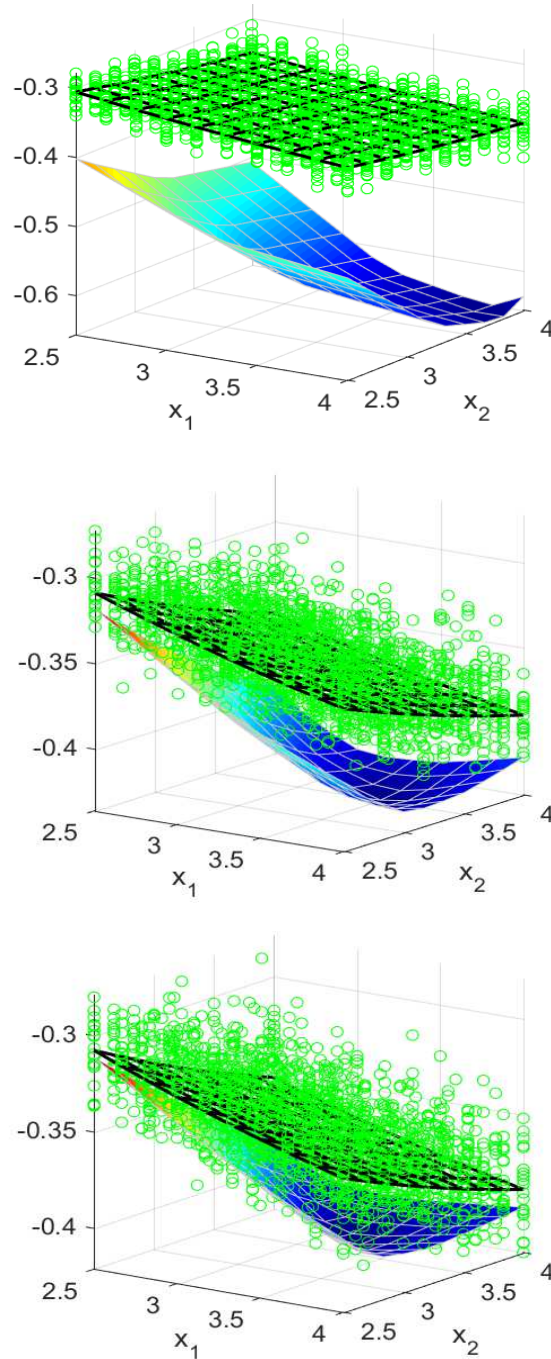


Figure 2.3: Jensen-McCormick convex relaxations of the objective function F in Example 3 (shaded surfaces) with partitions of $\bar{\Gamma}$ into 1 (top), 16 (middle), and 64 (bottom) uniform subintervals, along with simulated values of $f(\mathbf{x}, \omega)$ at sampled ω values (\circ) and a sample average approximation of F with 100 samples (black mesh).

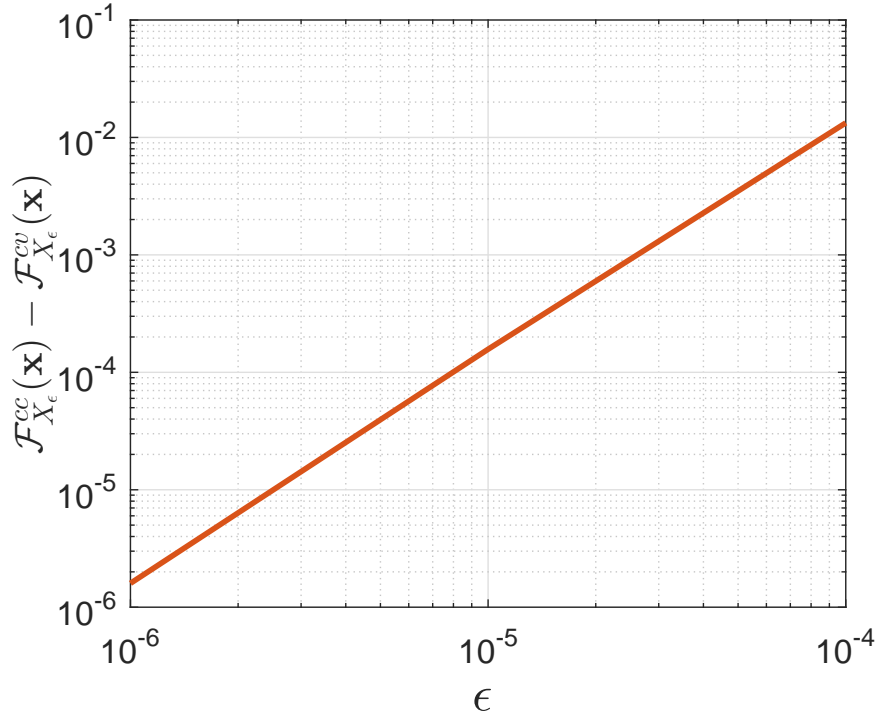


Figure 2.4: Second-order pointwise convergence of Jensen-McCormick relaxations with respect to $\frac{1}{2}\text{diam}(X_\epsilon) = \epsilon$ for Example 3 under a uniform $\bar{\Gamma}$ partitioning rule satisfying Equation (2.52) with $K = 10^8$. Plotted values are for $\mathbf{x} = \text{mid}(X_\epsilon) = (5, 6)$.

algorithms, thereby enabling the global solution of nonconvex optimization problems subject to continuous uncertainties (e.g., process yields, renewable resources, product demands, etc.). Importantly, these relaxations are not sample-based. Instead, they make use of an exhaustive partition of the uncertainty set. As a consequence, they can be evaluated finitely, even when the original expected-value cannot be. Empirical results with simple uniform partitions showed that tight relaxations can be obtained with fairly coarse partitions. Moreover, when the uncertainty partition is refined appropriately, we established second-order pointwise convergence of the relaxations to the true expected value as the relaxation domain tends to a singleton. Such convergence is critical for ensuring finite termination of spatial branch-and-bound and avoiding the cluster effect. Finally, using the notion of *factorable random variables*, we extended our relaxation technique to a wide variety of multivariate probability distributions in a manner that avoids the need to com-

pute any difficult multidimensional integrals. In Chapter 3, we plan to develop a complete spatial branch-and-bound algorithm for nonconvex optimization problems with continuous uncertainties by combining the relaxations developed here with efficient, adaptive uncertainty partitioning strategies.

CHAPTER 3

GUARANTEED GLOBAL OPTIMIZATION OF EXPECTED-VALUE MINIMIZATION PROBLEMS WITH CONTINUOUS RANDOM VARIABLES

3.1 Introduction

This chapter presents a new algorithm for globally solving an important class of nonconvex stochastic programs. Specifically, we consider stochastic programs of the following form, where $\mathbf{x} \in \bar{X} \subset \mathbb{R}^{n_x}$, \mathbb{E} denotes the expected value over continuous random variables (RVs) $\boldsymbol{\omega} \in \bar{\Omega} \subset \mathbb{R}^{n_\omega}$, the domains \bar{X} and $\bar{\Omega}$ are compact n_x and n_ω -dimensional intervals, and f and g can be nonconvex with respect to both \mathbf{x} and $\boldsymbol{\omega}$:

$$\begin{aligned} \min_{\mathbf{x} \in \bar{X}} \quad & \mathbb{E}[f(\mathbf{x}, \boldsymbol{\omega})] \\ \text{s.t.} \quad & \mathbf{g}(\mathbf{x}) \leq \mathbf{0}. \end{aligned} \tag{3.1}$$

Problems of this form are critical in many applications, including engineering design [31, 64], renewable energy systems [30, 65], financial optimization [66], stochastic optimal control [67, 68], discrete event systems [69], etc. In particular, nonconvex f and g functions arise commonly in models of chemical processes, water and gas networks, AC power systems, etc. [97, 18], and continuous random variables are widely used to characterize uncertainty in, e.g., product demands, returns on investments, and renewable energy resources [30]. In addition, although we focus on single-stage problems in this chapter, more flexible two-stage and multistage formulations can also be reduced to Problem (3.1) through parameterized decision rules, which is an increasingly popular method for obtaining tractable approximate solutions [70].

In principle, Problem (3.1) can be solved to guaranteed global optimality using a spatial

branch-and-bound (B&B) search. However, B&B requires the ability to compute guaranteed lower and upper bounds on the optimal value of Problem (3.1) restricted to any given n_x -dimensional subinterval $X \subset \bar{X}$. The lower bound is typically computed by minimizing a convex relaxation of (3.1) over $X \subset \bar{X}$, while the upper bound is computed by evaluating the objective function at a feasible point \mathbf{x} [11]. Unfortunately, neither of these common bounding procedures can be directly applied to Problem (3.1) because, in general, the objective function $F(\mathbf{x}) \equiv \mathbb{E}[f(\mathbf{x}, \boldsymbol{\omega})]$ cannot be expressed analytically in closed-form. Instead, only estimates of $F(\mathbf{x})$ obtained by sampling or quadrature are generally available. Clearly, estimating $F(\mathbf{x})$ in this way does not provide a rigorous upper bound. Moreover, obtaining accurate estimates can be prohibitively expensive, especially when n_ω is large, given the fact that a global optimization algorithm might require F to be evaluated thousands of times. Obtaining a rigorous lower bound for Problem (3.1) is even more problematic because all existing general-purpose methods for constructing the needed convex relaxation are only applicable to functions that are known explicitly in closed form [11, 15, 13, 63].

In the existing literature, Problem (3.1) is most commonly solved by sample-average approximation (SAA). In this approach, F is approximated using a finite number of sampled scenarios determined prior to optimization. This results in a deterministic approximation of Problem (3.1) that can be solved by conventional methods. In particular, a global solution of this approximation can be obtained by standard B&B algorithms [11, 15, 13, 63]. However, SAA often provides an unworkable compromise between accuracy and efficiency for nonconvex programs. On the one hand, using too few scenarios can result in inaccurate solutions that are highly suboptimal or even infeasible. On the other hand, increasing the number of scenarios leads to higher computational cost. Moreover, verifying the accuracy of a solution generally requires solving 10–40 repeats of the deterministic problem with independent samples, and the entire problem needs to be resolved from scratch if a larger sample size is needed [26, 71]. This leads to an unmanageable

computational burden for many nonconvex problems because solving a single instance to global optimality is already very demanding. Another common approach is the so-called stochastic branch-and-bound (B&B) algorithm [3]. Unlike standard B&B algorithms, the upper and lower bounds used in stochastic B&B are based on a finite number of samples and are only valid in a probabilistic sense. The key advantage of this approach is that the sample size can be adapted dynamically during the B&B search, leading to significant computational savings. However, since the bounds are only probabilistically valid, there is a nonzero probability of discarding optimal solutions using standard B&B fathoming rules. As a consequence, stochastic B&B is only guaranteed to converge to a global solution when no fathoming is done, which is computationally prohibitive.

To address these challenges, this chapter develops a complete spatial branch-and-bound (B&B) algorithm for solving Problem (3.1) to guaranteed ϵ -global optimality. In this algorithm, both the upper and lower bounding procedures are enabled by the Jensen-McCormick relaxation technique developed in Chapter 2, which provides guaranteed convex and concave relaxations of $F(\mathbf{x}) \equiv \mathbb{E}[f(\mathbf{x}, \boldsymbol{\omega})]$ with any factorable nonconvex function f and a wide variety of multivariate probability density functions for $\boldsymbol{\omega}$. For a given B&B node $X_k \subset \bar{X}$, our algorithm computes a rigorous lower bound by solving a convex relaxation on X_k constructed using Jensen-McCormick relaxations, and computes a rigorous upper bound by locating a feasible point \mathbf{x} and using a Jensen-McCormick concave relaxation to compute an upper bound on $F(\mathbf{x})$. A key issue for both computations is that the Jensen-McCormick relaxations rely on a partition of the uncertainty space $\bar{\Omega}$ and only converge as this partition is refined. Therefore, a major outstanding task is to determine how to refine the partition of $\bar{\Omega}$ during spatial B&B so as to guarantee convergence while also managing computational cost. For this purpose, we develop an intelligent uncertainty set partitioning rule that is guided by heuristic estimates of how much the relaxations in node X_k would be improved by refining the partition of $\bar{\Omega}$ relative to how much they would be improved by bisecting X_k . This rule determines not only when to refine the partition,

but also where in $\bar{\Omega}$ it will be most effective to refine. With this rule, the B&B algorithm may execute many successive bisections of the decision variable space without increasing or only slightly increasing the size of the uncertainty set partition, which plays a major role in maintaining tractability of the lower bounding procedure. In addition, we develop novel numerical methods for efficiently storing and manipulating large partitions, as well as a new affine relaxation technique for efficiently evaluating, refining, and minimizing Jensen-McCormick relaxations built on large partitions.

A critical feature of our approach is that the upper and lower bounds computed in each node are always rigorous, regardless of how coarse or fine the uncertainty set partition is when the node is processed. This implies that fathoming and termination decisions are made with certainty, which enables the uncertainty set to be adaptively refined as B&B proceeds without loss of rigor. This is in contrast to the existing stochastic B&B algorithm proposed in [3], which applies spatial-B&B using probabilistic upper and lower bounds and therefore has a nonzero probability of inadvertently fathoming global solutions. With our proposed partitioning rule, large regions of the search space can often be fathomed using only coarse partitions, while very fine partitions are only required in few nodes near a global solution. This is a significant advantage compared to state-of-the-art SAA approaches, where the expected-value objective is approximated using a fixed (typically large) number samples that remains constant throughout the B&B search. Moreover, the number of scenarios required to achieve a high-quality solution from SAA is not known in advance, so solution quality must be tested by solving the optimization problem multiple times with independent sample sets. Therefore, another significant advantage of our method is that we only need a single run to solve the problem to guaranteed global optimality without sampling errors. Numerical examples show that our method is more than one order of magnitude faster than SAA for the considered test problems.

The remainder of this chapter is organized as follows. First, Section 3.2 and Section 3.3 introduce necessary definitions, notations, and a formal problem statement. Next, our

novel spatial branch-and-bound algorithm is presented in Section 3.4. In addition, Section 3.5 provides the convergence rate analysis of our presented relaxations scheme. In Section 3.6, we demonstrate our proposed global optimization algorithm in a case study. Finally, Section 3.7 provides concluding remarks.

3.2 Preliminaries

The proposed branch-and-bound algorithm makes use of convex and concave relaxations, defined as follows.

Definition 21. Let $\bar{S} \subset \mathbb{R}^n$ and $h : \bar{S} \rightarrow \mathbb{R}$. For any convex $S \subset \bar{S}$, functions $h^{cv}, h^{cc} : S \rightarrow \mathbb{R}$ are *convex and concave relaxations of h on S* , respectively, if h^{cv} is convex on S , h^{cc} is concave on S , and

$$h_S^{cv}(\mathbf{s}) \leq h(\mathbf{s}) \leq h_S^{cc}(\mathbf{s}), \quad \forall \mathbf{s} \in S.$$

The following extension of Definition 21 is useful for convergence analysis. First, for any $\mathbf{s}^L, \mathbf{s}^U \in \mathbb{R}^n$ with $\mathbf{s}^L \leq \mathbf{s}^U$, let $S = [\mathbf{s}^L, \mathbf{s}^U]$ denote the compact n -dimensional interval $\{\mathbf{s} \in \mathbb{R}^n : \mathbf{s}^L \leq \mathbf{s} \leq \mathbf{s}^U\}$. Moreover, for $\bar{S} \subset \mathbb{R}^n$, let $\mathbb{I}\bar{S}$ denote the set of all compact interval subsets S of \bar{S} . In particular, let $\mathbb{I}\mathbb{R}^n$ denote the set of all compact interval subsets of \mathbb{R}^n . Finally, denote the *diameter* of S by $\text{diam}(S) = \max_i |s_i^U - s_i^L|$.

Definition 22. Let $\bar{S} \subset \mathbb{R}^n$ and $h : \bar{S} \rightarrow \mathbb{R}$. A collection of functions $h_S^{cv}, h_S^{cc} : \bar{S} \rightarrow \mathbb{R}$ indexed by $S \in \mathbb{I}\bar{S}$ is called a *scheme of relaxations for h in \bar{S}* if, for every $S \in \mathbb{I}\bar{S}$, h_S^{cv} and h_S^{cc} are convex and concave relaxations of h on S .

Remark 23. The notion of a scheme of relaxations was first introduced in Bompadre et al. [78] with the alternative name *scheme of estimators*. Here, we use the term *relaxations* in place of *estimators* to avoid possible confusion with the common meaning of *estimation* in the stochastic setting.

Definition 24. Let $S \subset \mathbb{R}^{n_s}$ be a nonempty convex set, let $h^{cv} : S \rightarrow \mathbb{R}$ be convex, and let $h^{cc} : S \rightarrow \mathbb{R}$ be concave. A vector $\nabla \mathbf{h}^{cv}(\mathbf{s}_0) \in \mathbb{R}^{n_s}$ is called a *subgradient* of h^{cv} at $\mathbf{s}_0 \in S$ if

$$h^{cv}(\mathbf{s}) \geq h^{cv}(\mathbf{s}_0) + (\nabla \mathbf{h}^{cv}(\mathbf{s}_0))^T(\mathbf{s} - \mathbf{s}_0), \quad \forall \mathbf{s} \in S.$$

A vector $\nabla \mathbf{h}^{cc}(\mathbf{s}_0) \in \mathbb{R}^{n_s}$ is called a *subgradient* of h^{cc} at $\mathbf{s}_0 \in S$ if

$$h^{cc}(\mathbf{s}) \leq h^{cc}(\mathbf{s}_0) + (\nabla \mathbf{h}^{cc}(\mathbf{s}_0))^T(\mathbf{s} - \mathbf{s}_0), \quad \forall \mathbf{s} \in S.$$

Existence of subgradients on the interior of S is guaranteed, and for differentiable convex and concave functions, the unique subgradient is the gradient.

3.3 Problem Statement

Let $\boldsymbol{\omega} \in \mathbb{R}^{n_\omega}$ be a vector of continuous random variables distributed according to a probability density function (PDF) $p : \mathbb{R}^{n_\omega} \rightarrow \mathbb{R}$. We assume throughout that p is zero outside of a compact n_ω -dimensional interval $\bar{\Omega} \subset \mathbb{R}^{n_\omega}$. Let $\bar{X} \subset \mathbb{R}^{n_x}$ be a compact n_x -dimensional interval, let $f : \bar{X} \times \bar{\Omega} \rightarrow \mathbb{R}$ and $\mathbf{g} : \bar{X} \rightarrow \mathbb{R}^{n_{sc}}$ be potentially nonconvex functions, and assume that the expected value $\mathbb{E}[f(\mathbf{x}, \boldsymbol{\omega})]$ exists for all $\mathbf{x} \in \bar{X}$. Moreover, define $F : \bar{X} \rightarrow \mathbb{R}$ by $F(\mathbf{x}) \equiv \mathbb{E}[f(\mathbf{x}, \boldsymbol{\omega})]$, $\forall \mathbf{x} \in \bar{X}$.

The objective of this chapter is to develop a novel spatial branch-and-bound algorithm for solving Problem (3.1) to guaranteed global optimality. In particular, we consider the general case where F cannot be expressed explicitly as a factorable function of \mathbf{x} . This implies that none of the existing relaxation techniques used to obtain rigorous lower bounds in B&B algorithms can be applied. Furthermore, it implies that F cannot even be evaluated exactly with finitely many computations and must be approximated via sampling. Therefore, even the rigorous upper bounds needed for B&B cannot be obtained in the usual way (i.e., by evaluating F at feasible points). We will address both problems using the Jensen-

McCormick relaxation technique developed in Chapter 2. To apply this technique, we require a scheme of relaxations for the integrand f with certain properties. These are formalized in the following assumptions, which hold for the remainder of this chapter. If f is factorable, then suitable relaxations can be easily obtained using the standard McCormick relaxation technique [13].

Assumption 25. A scheme of relaxations for f in $\bar{X} \times \bar{\Omega}$ is available, and is denoted by $(f_{X \times \Omega}^{cv}, f_{X \times \Omega}^{cc})_{X \times \Omega \in \mathbb{I}\bar{X} \times \mathbb{I}\bar{\Omega}}$. Here, $f_{X \times \Omega}^{cv}$ and $f_{X \times \Omega}^{cc}$ denote convex and concave relaxations of f jointly on $X \times \Omega \in \mathbb{I}\bar{X} \times \mathbb{I}\bar{\Omega}$.

Remark 26. We will sometimes make use of relaxations of f with respect to either \mathbf{x} or $\boldsymbol{\omega}$ independently, with the other treated as a constant. We denote these naturally by $f_X^{cv}(\mathbf{x}, \boldsymbol{\omega})$ and $f_\Omega^{cv}(\mathbf{x}, \boldsymbol{\omega})$. Within the scheme of Assumption 25, these relaxations are equivalent to the more cumbersome notations $f_X^{cv}(\mathbf{x}, \boldsymbol{\omega}) \equiv f_{X \times [\boldsymbol{\omega}, \boldsymbol{\omega}]}^{cv}(\mathbf{x}, \boldsymbol{\omega})$ and $f_\Omega^{cv}(\mathbf{x}, \boldsymbol{\omega}) \equiv f_{[\mathbf{x}, \mathbf{x}] \times \Omega}^{cv}(\mathbf{x}, \boldsymbol{\omega})$.

Assumption 27. The scheme of relaxations $(f_{X \times \Omega}^{cv}, f_{X \times \Omega}^{cc})$ from Assumption 25 has second-order pointwise convergence in $\mathbb{I}\bar{X} \times \mathbb{I}\bar{\Omega}$; i.e., $\exists \tau > 0$ such that

$$\sup_{(\mathbf{x}, \boldsymbol{\omega}) \in X \times \Omega} |f_{X \times \Omega}^{cc}(\mathbf{x}, \boldsymbol{\omega}) - f_{X \times \Omega}^{cv}(\mathbf{x}, \boldsymbol{\omega})| \leq \tau \text{diam}(X \times \Omega)^2,$$

for all $(X \times \Omega) \in \mathbb{I}\bar{X} \times \mathbb{I}\bar{\Omega}$.

Both McCormick and α BB relaxations are known to satisfy Assumption 27 [78].

Definition 28. Let X and Y compact subsets of \mathbb{R}^n . The *Hausdorff distance* between X and Y is defined as

$$d_H(X, Y) \equiv \max \left(\sup_{\mathbf{x} \in X} \inf_{\mathbf{y} \in Y} \|\mathbf{x} - \mathbf{y}\|_\infty, \sup_{\mathbf{y} \in Y} \inf_{\mathbf{x} \in X} \|\mathbf{x} - \mathbf{y}\|_\infty \right).$$

If X and Y are intervals with $X = [\mathbf{x}^L, \mathbf{x}^U]$ and $Y = [\mathbf{y}^L, \mathbf{y}^U]$, then $d_H(X, Y)$ simplifies

to

$$d_H(X, Y) \equiv \max (\|\mathbf{x}^L - \mathbf{y}^L\|_\infty, \|\mathbf{x}^U - \mathbf{y}^U\|_\infty) .$$

Assumption 29. *The convex relaxations $f_{X \times \Omega}^{cv}$ from Assumption 25 are Lipschitz continuous; i.e., $\exists L > 0$ such that*

$$\begin{aligned} & |f_{X_1 \times \Omega_1}^{cv}(\mathbf{x}_1, \boldsymbol{\omega}_1) - f_{X_2 \times \Omega_2}^{cv}(\mathbf{x}_2, \boldsymbol{\omega}_2)| \\ & \leq L \max (\|(\mathbf{x}_1, \boldsymbol{\omega}_1) - (\mathbf{x}_2, \boldsymbol{\omega}_2)\|_\infty, d_H(X_1 \times \Omega_1, X_2 \times \Omega_2)) , \end{aligned}$$

for every $X_1, X_2 \in \overline{X}$, $\Omega_1, \Omega_2 \in \overline{\Omega}$, $(\mathbf{x}_1, \boldsymbol{\omega}_1) \in X_1 \times \Omega_1$, and $(\mathbf{x}_2, \boldsymbol{\omega}_2) \in X_2 \times \Omega_2$.

McCormick relaxations are known to satisfy Assumption 29 (see Corollary 2.5.41 in [98]).

3.4 A Novel Spatial Branch-and-Bound Algorithm

This section presents a complete spatial branch-and-bound (B&B) algorithm for solving Problem (3.1) to guaranteed global optimality. Based on the Jensen-McCormick relaxation technique we previously developed in Chapter 2, we formalize a general lower bounding approach, an efficient adaptive uncertainty set partitioning rule, and a general upper bounding approach for the overall B&B algorithm.

3.4.1 Upper and Lower Bounding Problems

Given a generic subinterval $X \subset \overline{X}$, the spatial-B&B algorithm requires methods for computing valid upper and lower bounds on the optimal value of (3.1) restricted to X . The upper bound is typically obtained by evaluating the objective at a feasible point (sometimes located by solving a so-called *upper bounding problem*), while the lower bound is typically obtained by solving a convex or affine relaxation called the *lower bounding problem*. We

compute both bounds here using the Jensen-McCormick relaxation technique developed in Chapter 2. The key definitions are reproduced below.

Definition 30. A collection $\mathcal{P} = \{\Omega_i\}_{i=1}^n$ of n_ω -dimensional intervals is called a *partition* of $\bar{\Omega}$ if:

1. $\bar{\Omega} = \cup_{i=1}^n \Omega_i$,
2. $\text{int}(\Omega_i) \cap \text{int}(\Omega_j) = \emptyset$ for all distinct i and j .

Lemma 31. Let $\mathcal{P} = \{\Omega_i\}_{i=1}^n$ be a partition of $\bar{\Omega}$. For every $X \in \mathbb{I}\bar{X}$ and every $\mathbf{x} \in X$, define

$$F_{X \times \mathcal{P}}^{cv}(\mathbf{x}) \equiv \sum_{i=1}^n \mathbb{P}(\Omega_i) f_{X \times \Omega_i}^{cv}(\mathbf{x}, \mathbb{E}[\boldsymbol{\omega} | \Omega_i]), \quad (3.2)$$

$$F_{X \times \mathcal{P}}^{cc}(\mathbf{x}) \equiv \sum_{i=1}^n \mathbb{P}(\Omega_i) f_{X \times \Omega_i}^{cc}(\mathbf{x}, \mathbb{E}[\boldsymbol{\omega} | \Omega_i]). \quad (3.3)$$

With these definitions, $F_{X \times \mathcal{P}}^{cv}$ and $F_{X \times \mathcal{P}}^{cc}$ are convex and concave relaxations of F on X , respectively.

Proof. See Theorem 31 in Chapter 2. □

Let X be a subinterval of \bar{X} and let $\mathcal{P} = \{\Omega_i\}_{i=1}^n$ be a partition of $\bar{\Omega}$. To obtain a valid upper bound, we first identify a candidate point $\mathbf{x} \in X$. If \mathbf{x} is infeasible, then the upper bound is set to $+\infty$. Alternatively, if \mathbf{x} is feasible, then the upper bound is computed by

$$\text{UB} = F_{[\mathbf{x}, \mathbf{x}] \times \mathcal{P}}^{cc}(\mathbf{x}) = \sum_{\Omega \in \mathcal{P}} \mathbb{P}(\Omega) f_{\Omega}^{cc}(\mathbf{x}, \mathbb{E}[\boldsymbol{\omega} | \Omega]). \quad (3.4)$$

The use of F^{cc} here provides a rigorous upper bound on $F(\mathbf{x})$ by Lemma 31, whereas simply evaluating $F(\mathbf{x})$ by sample average approximation would not be rigorous due to sampling error. Note that the relaxation $F_{[\mathbf{x}, \mathbf{x}] \times \mathcal{P}}^{cc}$ is used above, not $F_{X \times \mathcal{P}}^{cc}$. In other words, we only relax f with respect to $\boldsymbol{\omega}$ in the computation of the upper bound, which leads

to a much less conservative bound than relaxing with respect to both \mathbf{x} and $\boldsymbol{\omega}$. In our implementation, we choose the candidate point \mathbf{x} as the solution of the lower bounding problem defined below. However, many other choices are possible, such as the midpoint of X . We could also generate a candidate point by solving a sample-average approximation problem, which might be worth the additional expense particularly in the root node.

To formulate the lower bounding problem, let $\mathbf{g}_X^{cv} : X \rightarrow \mathbb{R}^{n_{sc}}$ be a convex relaxation of \mathbf{g} on X . A valid lower bounding problem for (3.1) on X is given by,

$$\begin{aligned} \min_{\mathbf{x} \in X} \quad & F_{X \times \mathcal{P}}^{cv}(\mathbf{x}) \\ \text{s.t.} \quad & \mathbf{g}_X^{cv}(\mathbf{x}) \leq \mathbf{0} \end{aligned} \tag{3.5}$$

This problem is convex and can be easily solved to global optimality to obtain the required lower bound. To enhance efficiency, in our numerical implementation we choose to use schemes of relaxations for f and \mathbf{g} in which each $f_{X \times \Omega_i}^{cv}$, $f_{X \times \Omega_i}^{cc}$, and \mathbf{g}_X^{cv} is affine with respect to both \mathbf{x} and $\boldsymbol{\omega}$. Such relaxations can be readily constructed as linearizations of standard McCormick relaxations computed using well-known subgradient propagation rules [84]. As a result, the lower bounding problem is a linear program that can be solved more efficiently and reliably than a general convex program. This efficiency boost is particularly pronounced when the partition size is large because, for general convex relaxations, the sum over partition elements in (3.2) needs to be computed every time the objective of (3.5) is evaluated. In contrast, for affine relaxations, only a single evaluation of the sum is needed to compute the coefficients of the linear programming formulation of (3.5).

In order to ensure finite termination of a spatial-B&B algorithm based on the upper and lower bounding procedures above, it is necessary that the relaxation error $\sup_{\mathbf{x} \in X} |F_{X \times \mathcal{P}}^{cc}(\mathbf{x}) - F_{X \times \mathcal{P}}^{cv}(\mathbf{x})|$ converges to zero as $\text{diam}(X) \rightarrow 0$ [11]. To ensure this, the partition $\mathcal{P} = \{\Omega_i\}_{i=1}^n$ must be refined as $\text{diam}(X) \rightarrow 0$, and a major task is to determine how to do this effectively. In Theorem 15 of Chapter 2, an uniform partition rule was proposed and

it was shown that the resulting scheme of relaxations satisfies a second-order convergence property that guarantees finite termination of spatial B&B. This rule requires the partition \mathcal{P} to obey the following condition:

$$\sum_{i=1}^n \mathbb{P}(\Omega_i) \text{diam}(\Omega_i)^2 \leq K \text{diam}(X)^2. \quad (3.6)$$

At each B&B node X_k , a simple approach to satisfy the rule above is to uniformly partition $\bar{\Omega}$ until $\text{diam}(\Omega_i) \leq K \text{diam}(X_k)$, where K is an algorithm parameter. However, this rule tends to generate a massive number of partition elements because $\text{diam}(X)$ often becomes very small when searching close to the global solution. Therefore, in the next subsection, we design an efficient adaptive uncertainty set partitioning rule that achieves the desired convergence property with much smaller partition sizes, which maintains tractability of the lower bounding problem.

3.4.2 Uncertainty Set $\bar{\Omega}$ Partition Rule

The convergence and accuracy of the upper and lower bounding procedures depend on both the branching of the decision variable space \bar{X} and the partitioning of the random variable space $\bar{\Omega}$. Balancing these two operations is the key to computational efficiency. The inefficient uniform partition rule for $\bar{\Omega}$ mentioned above only considers the width of the current node X_k and the intervals in the uncertainty set partition. Alternatively, the $\bar{\Omega}$ partition refinement could be more efficiently guided by estimating how much a refinement would improve the accuracy of the bounding procedures relative to the improvement achieved by bisecting X_k . We develop such a partitioning rule below.

In order to represent large partitions of $\bar{\Omega}$ concisely, we restrict our partitioning rule to use *Cartesian partitions* defined next. These are partitions that are generated by one-dimensional partitions along each coordinate direction. More precisely, every element of a Cartesian partition is a Cartesian product of elements in the one-dimensional coordinate

partitions.

Definition 32. Let $\bar{\Omega} = W_1 \times \cdots \times W_{n_\omega}$, where W_1, \dots, W_{n_ω} are one-dimensional intervals.

A collection $\mathcal{P} = \{\Omega_i\}_{i=1}^n$ is called a *Cartesian partition of $\bar{\Omega}$* if:

1. $\mathcal{P} = \{\Omega_i\}_{i=1}^n$ is a partition of $\bar{\Omega}$,
2. There exist one-dimensional partitions $\mathcal{P}_{W_1}, \dots, \mathcal{P}_{W_{n_\omega}}$ of W_1, \dots, W_{n_ω} , respectively, such that $\mathcal{P} = \{I_1 \times \cdots \times I_{n_\omega} : I_j \in \mathcal{P}_{W_j}, \forall j = 1, \dots, n_\omega\}$.

We now define some key notation used in the proposed partitioning rule.

Definition 33. For any set $\Omega = W_1 \times \cdots \times W_{n_\omega} \in \mathbb{I}\mathbb{R}^{n_\omega}$, where W_1, \dots, W_{n_ω} are one-dimensional intervals, define the *projection of Ω onto dimension $m \in \{1, \dots, n_\omega\}$* as $\pi_m(\Omega) \equiv W_m$. Similarly, for any vector $\mathbf{v} = (v_1, \dots, v_n) \in \mathbb{R}^n$, define the *projection of \mathbf{v} onto dimension m* as $\pi_m(\mathbf{v}) \equiv v_m$.

Definition 34. For any set $\Omega = [\omega_1^L, \omega_1^U] \times \cdots \times [\omega_{n_\omega}^L, \omega_{n_\omega}^U] \in \mathbb{I}\mathbb{R}^{n_\omega}$, define the *bisection of Ω along dimension $m \in \{1, \dots, n_\omega\}$* as the set of two intervals $\text{bisect}(\Omega, m) \equiv \{Q_1, Q_2\}$, where

$$\begin{aligned} Q_1 &= [\omega_1^L, \omega_1^U] \times \cdots \times \left[\omega_m^L, \frac{\omega_m^L + \omega_m^U}{2} \right] \times \cdots \times [\omega_{n_\omega}^L, \omega_{n_\omega}^U], \\ Q_2 &= [\omega_1^L, \omega_1^U] \times \cdots \times \left[\frac{\omega_m^L + \omega_m^U}{2}, \omega_m^U \right] \times \cdots \times [\omega_{n_\omega}^L, \omega_{n_\omega}^U]. \end{aligned}$$

Definition 35. For any set $X = [x_1^L, x_1^U] \times \cdots \times [x_n^L, x_n^U] = [\mathbf{x}^L, \mathbf{x}^U]$, define the *middle point of X* as $\text{mid}(X) = \left[\frac{x_1^L + x_1^U}{2}, \dots, \frac{x_n^L + x_n^U}{2} \right]$.

Definition 36. Let $\mathcal{P} = \{\Omega_i\}_{i=1}^n$ be a Cartesian partition of $\bar{\Omega} \in \mathbb{I}\mathbb{R}^{n_\omega}$. For any $W \in \mathbb{I}\mathbb{R}$, the *slice of \mathcal{P} in dimension m induced by W* is the set of all $\Omega \in \mathcal{P}$ whose projection onto dimension m equals W , which is defined as $S_{\mathcal{P}}(m, W) \equiv \{\Omega \in \mathcal{P} : \pi_m(\Omega) = W\}$. Note that if $W \notin \mathcal{P}_{W_m}$, then $S_{\mathcal{P}}(m, W) = \emptyset$.

Definition 37. Let \mathcal{P} be a Cartesian partition of $\overline{\Omega} \in \mathbb{I}\mathbb{R}^{n_\omega}$, let $W \in \mathbb{I}\mathbb{R}$, and let $m \in \{1, \dots, n_\omega\}$. For every $\Omega \in \mathcal{P}$ and $\mathbf{x} \in \overline{X}$, define *the type-one error on Ω* by

$$\text{err1}(\Omega, \mathbf{x}) \equiv \mathbb{P}(\Omega) (f_\Omega^{cc}(\mathbf{x}, \mathbb{E}[\boldsymbol{\omega}|\Omega]) - f_\Omega^{cv}(\mathbf{x}, \mathbb{E}[\boldsymbol{\omega}|\Omega])). \quad (3.7)$$

The type-one error on a slice $S_{\mathcal{P}}(m, W)$ and on the partition \mathcal{P} are defined as the sum of all type-one errors over $\Omega \in S_{\mathcal{P}}(m, W)$ and $\Omega \in \mathcal{P}$, respectively:

$$\text{err1}(S_{\mathcal{P}}(m, W), \mathbf{x}) \equiv \sum_{\Omega \in S_{\mathcal{P}}(m, W)} \text{err1}(\Omega, \mathbf{x}), \quad (3.8)$$

$$\text{err1}(\mathcal{P}, \mathbf{x}) \equiv \sum_{\Omega \in \mathcal{P}} \text{err1}(\Omega, \mathbf{x}). \quad (3.9)$$

For every $\Omega \in \mathcal{P}$, $X \in \mathbb{I}\overline{X}$, and $\mathbf{x}, \mathbf{x}_0 \in X$, define *the type-two error on Ω* by

$$\text{err2}(\Omega, \mathbf{x}_0, \mathbf{x}, X) \equiv \mathbb{P}(\Omega) (f_\Omega^{cc}(\mathbf{x}_0, \mathbb{E}[\boldsymbol{\omega}|\Omega]) - f_{\Omega \times X}^{cv}(\mathbf{x}, \mathbb{E}[\boldsymbol{\omega}|\Omega])). \quad (3.10)$$

The type-two error on a slice $S_{\mathcal{P}}(m, W)$ and on the partition \mathcal{P} are defined as the sum of all type-two errors over $\Omega \in S_{\mathcal{P}}(m, W)$ and $\Omega \in \mathcal{P}$, respectively:

$$\text{err2}(S_{\mathcal{P}}(m, W), \mathbf{x}_0, \mathbf{x}, X) \equiv \sum_{\Omega \in S_{\mathcal{P}}(m, W)} \text{err2}(\Omega, \mathbf{x}_0, \mathbf{x}, X), \quad (3.11)$$

$$\text{err2}(\mathcal{P}, \mathbf{x}_0, \mathbf{x}, X) \equiv \sum_{\Omega \in \mathcal{P}} \text{err2}(\Omega, \mathbf{x}_0, \mathbf{x}, X). \quad (3.12)$$

The type-one error is a measure of the error induced by relaxing f only with respect to the uncertainty using the partition \mathcal{P} . In contrast, the type-two error is a measure of the error induced by relaxing f with respect to both the uncertainty and the decision variables. Given any B&B node $X \subset \overline{X}$ and a Cartesian partition \mathcal{P} , the proposed partitioning rule uses these two error estimates to estimate what fraction of the current relaxation error is due the uncertainty. Specifically, the error induced by relaxing over \mathcal{P} is evaluated at the lower

bounding solution \mathbf{x}_0^* by $\text{err1}(\mathcal{P}, \mathbf{x}_0^*)$, and the error induced by relaxing over both \mathcal{P} and X is evaluated at the lower bounding solution \mathbf{x}_0^* by $\text{err2}(\mathcal{P}, \mathbf{x}_0^*, \mathbf{x}_0^*, X)$. In the proposed partitioning rule, we only refine the partition \mathcal{P} when the relaxation error over \mathcal{P} is greater than a certain fraction of the total relaxation error. When this is true, \mathcal{P} is refined by bisecting all partition elements that lie in the slice of \mathcal{P} that has the highest type-one error. The lower bounding problem is then solved again with the updated partition \mathcal{P} to determine a new lower bounding solution, \mathbf{x}^* . This procedure is repeated until either $\text{err1}(\mathcal{P}, \mathbf{x}_0^*)$ is less than a fixed fraction of $\text{err2}(\mathcal{P}, \mathbf{x}_0^*, \mathbf{x}^*, X)$, or $\text{err2}(\mathcal{P}, \mathbf{x}_0^*, \mathbf{x}^*, X)$ is less than a fixed fraction of $\text{diam}(X)$. This uncertainty set partitioning rule is described in Algorithm 1. Two distinct points \mathbf{x} and \mathbf{x}_0 are used in evaluating the type-two error in Algorithm 1 due to technical details in the proof of the convergence result given in Theorem 42 below.

Algorithm 1 Uncertainty Set $\overline{\Omega}$ Partition Rule 1

```

1: function REFINE PARTITION 1( $\mathcal{P}, X, \alpha_1, \alpha_2$ )
2:    $\mathbf{x}_0^* \leftarrow \underset{\mathbf{x} \in X}{\text{argmin}} F_{X \times \mathcal{P}}^{cv}(\mathbf{x})$ 
3:    $\mathbf{x}^* \leftarrow \mathbf{x}_0^*$ 
4:   while  $\text{err1}(\mathcal{P}, \mathbf{x}_0^*) > \alpha_1 \text{err2}(\mathcal{P}, \mathbf{x}_0^*, \mathbf{x}^*, X)$  and  $\text{err2}(\mathcal{P}, \mathbf{x}_0^*, \mathbf{x}^*, X) > \alpha_2 \text{diam}(X)$  do
5:      $(m^*, W^*) \leftarrow \underset{W \in \mathcal{P}_m}{\text{argmax}}_{m \in \{1, \dots, n_\omega\}} \text{err1}(S_{\mathcal{P}}(m, W), \mathbf{x}_0^*)$ 
6:     Refine  $\mathcal{P}$  by removing every  $\Omega \in S_{\mathcal{P}}(m^*, W^*)$  and replacing it with  $\text{bisect}(\Omega, m^*)$ 
7:      $\mathbf{x}^* \leftarrow \underset{\mathbf{x} \in X}{\text{argmin}} F_{X \times \mathcal{P}}^{cv}(\mathbf{x})$ 
8:   end while
9:   return ( $\mathcal{P}$ )
10: end function

```

3.4.3 The Overall Spatial Branch-and-Bound Scheme

Putting together the pieces from the last two subsections, a complete branch-and-bound algorithm is formalized in the following pseudocode.

1. **(Initialization)** Let $X_0 = \overline{X}$, $\mathcal{P} = \{\overline{\Omega}\}$, $\text{LB} = \text{LB}_0 = -\infty$, $\text{UB} = \text{UB}_0 = +\infty$, $k = 1$, $\mathbf{x}^* = \mathbf{x}_0^* = \text{mid}(\overline{X})$, $N = \{(X_0, \text{LB}_0)\}$.
2. **(Termination Test)** If $\text{UB} - \text{LB} \leq \epsilon_1 \text{UB} + \epsilon_2$, terminate. The point \mathbf{x}^* is a global solution.

3. **(Node Selection)** Select and delete a node (X_k, LB_k) from N that has the smallest lower bound value LB_k .
4. **(Lower Bounding)** Build and solve a convex relaxation of the form (3.5) on X_k and \mathcal{P} . Store the optimal solution and objective value as \mathbf{x}_k^* and $F_k^{cv,*}$, respectively. Update the nodal lower bound by $LB_k \leftarrow \max(LB_k, F_k^{cv,*})$.
5. **(Uncertainty Set Partition Refinement)** Refine the uncertainty set partition by $\mathcal{P} \leftarrow \text{RefinePartition1}(\mathcal{P}, X_k, \alpha_1, \alpha_2)$, where RefinePartition1 is defined by Algorithm 1. Update the nodal lower bound LB_k with respect to the new \mathcal{P} if possible. Update the global lower bound LB as the smallest lower bound over all existing nodes.
6. **(Upper Bounding)** If the lower bounding solution \mathbf{x}_k^* is feasible, calculate UB_k through (3.4). Otherwise, set $UB_k = +\infty$. If $UB_k < UB$, update $UB \leftarrow UB_k$ and set $\mathbf{x}^* \leftarrow \mathbf{x}_k^*$.
7. **(Fathoming)** Delete all nodes in N whose lower bound is greater than UB . If $LB_k > UB$, go to Step 2.
8. **(Branching)** For every dimension m , define the *sensitivity*

$$\text{sen}(m, \mathbf{x}_k^*, X_k, \mathcal{P}) = \left(\frac{|\pi_m(\nabla F_{X_k \times \mathcal{P}}^{cv}(\mathbf{x}_k^*))|}{\|\nabla F_{X_k \times \mathcal{P}}^{cv}(\mathbf{x}_k^*)\|_1} + \delta \right) \cdot \text{diam}(\pi_m(X_k)),$$

where δ is a predefined positive constant. Choose the dimension m with maximum sensitivity $\text{sen}(m, \mathbf{x}_k^*, X_k, \mathcal{P})$ and generate two child nodes X' and X'' by bisecting X_k along its m^{th} dimension. Set $LB' = LB'' = LB_k$, add nodes (X', LB') and (X'', LB'') to N , then set $k = k + 1$, and go to Step 2.

3.5 Convergence

In this Section, we prove the finite termination property for our presented uncertainty set partitioning rule in Algorithm 1. Moreover, we provide analysis for the convergence rate

of the relaxation scheme using this new uncertainty set partitioning rule.

3.5.1 Finite Termination of the Uncertainty Set Partition Rule

Lemma 38. *Let $X \in \mathbb{I}\bar{X}$, let $\alpha_1, \alpha_2 \in (0, 1)$, and let \mathcal{P}_0 be a Cartesian partition of $\bar{\Omega}$. Suppose Algorithm 1 is called with the arguments $(\mathcal{P}_0, X, \alpha_1, \alpha_2)$ and let \mathcal{P}_k denote the updated partition of $\bar{\Omega}$ after k iterations of the algorithm. Choose any $\Omega \in \mathcal{P}_0$ and any $m \in \{1, \dots, n_\omega\}$ and let $W = \pi_m(\Omega)$. If Algorithm 1 does not terminate finitely, then exactly one of the following two cases happens:*

- (1) (m, W) will be selected by line 5 of Algorithm 1 after finitely many iterations.
- (2) $\lim_{k \rightarrow \infty} \text{err1}(S_{\mathcal{P}_k}(m, W), \mathbf{x}_0^*) = 0$, where \mathbf{x}_0^* is defined in Algorithm 1 as the initial lower bounding solution.

Proof. To arrive at a contradiction, suppose that Algorithm 1 does not terminate finitely, (m, W) is never selected by line 5 of Algorithm 1, and $\lim_{k \rightarrow \infty} \text{err1}(S_{\mathcal{P}_k}(m, W), \mathbf{x}_0^*) = a > 0$. Since Algorithm 1 chooses and bisects one slice in every iteration, the failure of termination implies that there exists at least one dimension $n \in \{1, \dots, n_\omega\}$ that is bisected infinitely many times. Therefore, there exists at least one nested sequence $\{\Omega_k\}$, with $\Omega_k \in \mathcal{P}_k$ for all $k \in \mathbb{N}$, such that $\lim_{k \rightarrow \infty} \text{diam}(\pi_n(\Omega_k)) = 0$. Moreover, by the definition of $S_{\mathcal{P}_k}(n, \pi_n(\Omega_k))$, we have $\text{diam}(\pi_n(\Omega)) \leq \text{diam}(\pi_n(\Omega_k))$, for every $\Omega \in S_{\mathcal{P}_k}(n, \pi_n(\Omega_k))$ and every $k \in \mathbb{N}$.

Furthermore,

$$\begin{aligned}
\lim_{k \rightarrow \infty} \sum_{\Omega \in S_{\mathcal{P}_k}(n, \pi_n(\Omega_k))} \mathbb{P}(\Omega) &= \lim_{k \rightarrow \infty} \sum_{\Omega \in S_{\mathcal{P}_k}(n, \pi_n(\Omega_k))} \int_{\Omega} p(\boldsymbol{\omega}) d\boldsymbol{\omega}, \\
&\leq \lim_{k \rightarrow \infty} \sum_{\Omega \in S_{\mathcal{P}_k}(n, \pi_n(\Omega_k))} \int_{\Omega} 1 d\boldsymbol{\omega}, \\
&= \lim_{k \rightarrow \infty} \sum_{\Omega \in S_{\mathcal{P}_k}(n, \pi_n(\Omega_k))} \text{diam}(\pi_n(\Omega)) \left(\prod_{j \neq n} \text{diam}(\pi_j(\Omega)) \right), \\
&\leq \lim_{k \rightarrow \infty} \text{diam}(\pi_n(\Omega_k)) \left(\prod_{j \neq n} \text{diam}(\pi_j(\bar{\Omega})) \right), \\
&= 0.
\end{aligned}$$

By definition,

$$\begin{aligned}
&\lim_{k \rightarrow \infty} \text{err1}(S_{\mathcal{P}_k}(n, \pi_n(\Omega_k)), \mathbf{x}_0^*) \\
&= \lim_{k \rightarrow \infty} \sum_{\Omega \in S_{\mathcal{P}_k}(n, \pi_n(\Omega_k))} \mathbb{P}(\Omega) (f_{\Omega}^{cc}(\mathbf{x}_0^*, \mathbb{E}[\boldsymbol{\omega}|\Omega]) - f_{\Omega}^{cv}(\mathbf{x}_0^*, \mathbb{E}[\boldsymbol{\omega}|\Omega])).
\end{aligned}$$

By Assumption 27, there exist $\tau > 0$, such that

$$\begin{aligned}
&\lim_{k \rightarrow \infty} \text{err1}(S_{\mathcal{P}_k}(n, \pi_n(\Omega_k)), \mathbf{x}_0^*) \\
&\leq \lim_{k \rightarrow \infty} \sum_{\Omega \in S_{\mathcal{P}_k}(n, \pi_n(\Omega_k))} \mathbb{P}(\Omega) \tau \text{diam}(\Omega)^2, \\
&\leq \tau \text{diam}(\bar{\Omega})^2 \lim_{k \rightarrow \infty} \sum_{\Omega \in S_{\mathcal{P}_k}(n, \pi_n(\Omega_k))} \mathbb{P}(\Omega) = 0.
\end{aligned}$$

Thus we have shown that there exists a sequence of slices $\{S_{\mathcal{P}_k}(n, \pi_n(\Omega_k))\}$, such that

- (i) $\lim_{k \rightarrow \infty} \text{err1}(S_{\mathcal{P}_k}(n, \pi_n(\Omega_k)), \mathbf{x}_0^*) = 0$,
- (ii) Elements in the sequence $\{(n, \pi_n(\Omega_k))\}$ will be selected by line 5 of Algorithm 1 infinitely many times (with infinitely many different k).

Since line 5 of Algorithm 1 always chooses the slice with maximum err1 , if (m, W) is not

selected after finitely many iterations, it follows that

$$\text{err1}(S_{\mathcal{P}_k}(m, W), \mathbf{x}_0^*) \leq \text{err1}(S_{\mathcal{P}_k}(n, \pi_n(\Omega_k)), \mathbf{x}_0^*), \quad \forall k.$$

Therefore,

$$a = \lim_{k \rightarrow \infty} \text{err1}(S_{\mathcal{P}_k}(m, W), \mathbf{x}_0^*) \leq \lim_{k \rightarrow \infty} \text{err1}(S_{\mathcal{P}_k}(n, \pi_n(\Omega_k)), \mathbf{x}_0^*) = 0, \quad \forall \mathbf{x} \in X.$$

But this contradicts the fact that $a > 0$. □

Lemma 39. *Let $X \in \mathbb{I}\bar{X}$, let $\alpha_1, \alpha_2 \in (0, 1)$, and let \mathcal{P}_0 be a Cartesian partition of $\bar{\Omega}$. Suppose Algorithm 1 is called with arguments $(\mathcal{P}_0, X, \alpha_1, \alpha_2)$ and let \mathcal{P}_k denote the updated partition of $\bar{\Omega}$ after k iterations of the algorithm. Let \mathbf{x}_0^* be the initial lower bounding solution computed in Algorithm 1. Choose any $\Omega \in \mathcal{P}_0$ and let $m^* = \underset{m}{\text{argmax}} \text{diam}(\pi_m(\Omega))$ and $W^* = \pi_{m^*}(\Omega)$. If Algorithm 1 does not terminate finitely, then exactly one of the following cases happens:*

- (1) (m^*, W^*) will be selected by line 5 of Algorithm 1 after finite number of iterations k .
- (2) $\lim_{k \rightarrow \infty} \text{err1}(S_{\mathcal{P}_k}(m^*, W^*), \mathbf{x}_0^*) = 0$.

Proof. The result follows directly by applying Lemma 38 to m^* and W^* . □

Theorem 40. *Let $X \in \mathbb{I}\bar{X}$, let $\alpha_1, \alpha_2 \in (0, 1)$, and let \mathcal{P}_0 be a Cartesian partition of $\bar{\Omega}$. Suppose Algorithm 1 is called with arguments $(\mathcal{P}_0, X, \alpha_1, \alpha_2)$ and let \mathcal{P}_k denote the updated partition of $\bar{\Omega}$ after k iterations of the algorithm. Let \mathbf{x}_0^* be the initial lower bounding solution computed in Algorithm 1. If Algorithm 1 does not terminate finitely, then*

$$\lim_{k \rightarrow \infty} \sum_{\Omega \in \mathcal{P}_k} \text{err1}(\Omega, \mathbf{x}_0^*) = 0.$$

Proof. The summation of $\text{err1}(\cdot, \mathbf{x}_0^*)$ over all $\bar{\Omega}$ partition elements equals the summation

over nonzero ones. Defining $T(\mathcal{P}_k) \equiv \{\Omega_i \in \mathcal{P}_k : \text{err1}(\Omega_i, \mathbf{x}_0^*) \neq 0\}$, we have

$$\lim_{k \rightarrow \infty} \sum_{\Omega \in \mathcal{P}_k} \text{err1}(\Omega, \mathbf{x}_0^*) = \lim_{k \rightarrow \infty} \sum_{\Omega \in T(\mathcal{P}_k)} \text{err1}(\Omega, \mathbf{x}_0^*). \quad (3.13)$$

By Assumption 27, there exist $\tau > 0$, such that

$$\lim_{k \rightarrow \infty} \sum_{\Omega \in \mathcal{P}_k} \text{err1}(\Omega, \mathbf{x}_0^*) \leq \tau \lim_{k \rightarrow \infty} \sum_{\Omega \in T(\mathcal{P}_k)} \mathbb{P}(\Omega) \text{diam}(\Omega)^2, \quad (3.14)$$

$$\leq \tau \lim_{k \rightarrow \infty} \left(\max_{\Omega \in T(\mathcal{P}_k)} \text{diam}(\Omega)^2 \right) \sum_{\Omega \in T(\mathcal{P}_k)} \mathbb{P}(\Omega), \quad (3.15)$$

$$\leq \tau \lim_{k \rightarrow \infty} \left(\max_{\Omega \in T(\mathcal{P}_k)} \text{diam}(\Omega)^2 \right). \quad (3.16)$$

Let m^* be the widest dimension over all elements in $T(\mathcal{P}_k)$; i.e.,

$$\begin{aligned} (m^*, \Omega^*) &\in \operatorname{argmax}_{m, \Omega} \text{diam}(\pi_m(\Omega)) \\ &\text{s.t. } \Omega \in T(\mathcal{P}_k). \end{aligned}$$

Moreover, let $W^* = \pi_{m^*}(\Omega^*)$. From Lemma 39, we know that either (m^*, W^*) will be selected by line 5 of Algorithm 1 after finite number of iterations, or all elements in $S_{\mathcal{P}_k}(m^*, W^*)$ will leave $T(\mathcal{P}_k)$ in a limit, since $\lim_{k \rightarrow \infty} \text{err1}(S_{\mathcal{P}_k}(m^*, W^*), \mathbf{x}_0^*) = 0$. This means the widest dimension over elements in $T(\mathcal{P}_k)$ will either be bisected after finite number of iterations, or the element with the widest dimension will be eliminated from $T(\mathcal{P}_k)$ in a limit. Thus, in a limit, the widest dimension over elements in $T(\mathcal{P}_k)$ will go to 0; i.e.,

$$\lim_{k \rightarrow \infty} \max_{\Omega \in T(\mathcal{P}_k)} \text{diam}(\Omega) = 0. \quad (3.17)$$

Combine Equation (3.16) and (3.17), we get

$$0 \leq \lim_{k \rightarrow \infty} \sum_{\Omega \in \mathcal{P}_k} \text{err1}(\Omega, \mathbf{x}_0^*) \leq \tau \lim_{k \rightarrow \infty} \left(\max_{\Omega \in T(\mathcal{P}_k)} \text{diam}(\Omega)^2 \right) = 0.$$

Therefore, $\lim_{k \rightarrow \infty} \sum_{\Omega \in \mathcal{P}_k} \text{err1}(\Omega, \mathbf{x}_0^*) = 0$. □

By Theorem 40, if Algorithm 1 does not terminate finitely, the summation of relaxation error over $\bar{\Omega}$ partitions will converge to 0. Thus, for any given relaxation error tolerance, Algorithm 1 will terminate finitely.

3.5.2 Convergence of the Relaxation Scheme

Definition 41. For every $X \in \mathbb{I}\bar{X}$, let $\Phi(X) \equiv \text{RefinePartition1}(\mathcal{P}, X, \alpha_1, \alpha_2)$ be a partition produced by Algorithm 1 using any initial Cartesian partition \mathcal{P} and any $\alpha_1, \alpha_2 \in (0, 1)$. Moreover, let $(\mathcal{F}_X^{cv}, \mathcal{F}_X^{cc})_{X \in \mathbb{I}\bar{X}}$ be a scheme of relaxations for F defined for all $X \in \mathbb{I}\bar{X}$ by

$$\mathcal{F}_X^{cv}(\mathbf{x}) \equiv F_{X \times \Phi(X)}^{cv}(\mathbf{x}), \quad \forall \mathbf{x} \in X, \quad (3.18)$$

$$\mathcal{F}_X^{cc}(\mathbf{x}) \equiv F_{X \times \Phi(X)}^{cc}(\mathbf{x}), \quad \forall \mathbf{x} \in X. \quad (3.19)$$

Theorem 42. *The scheme of relaxations $(\mathcal{F}_X^{cv}, \mathcal{F}_X^{cc})_{X \in \mathbb{I}\bar{X}}$ has first-order Hausdorff convergence; i.e., there exists $\tau > 0$ such that*

$$\left| \inf_{\mathbf{x} \in X} F(\mathbf{x}) - \inf_{\mathbf{x} \in X} F_{X \times \Phi(X)}^{cv}(\mathbf{x}) \right| \leq \tau \text{diam}(X), \quad \forall X \in \mathbb{I}\bar{X}. \quad (3.20)$$

Proof. Choose any $X \in \mathbb{I}\bar{X}$. Let $\mathbf{x}_0^*, \mathbf{x}^* \in X$ be the values of \mathbf{x}_0^* and \mathbf{x}^* in Algorithm 1

when the algorithm terminates. Since \mathbf{x}^* minimizes $F_{X \times \Phi(X)}^{cv}(\mathbf{x})$ over X , we have

$$\left| \inf_{\mathbf{x} \in X} F(\mathbf{x}) - \inf_{\mathbf{x} \in X} F_{X \times \Phi(X)}^{cv}(\mathbf{x}) \right| \quad (3.21)$$

$$= \left| \inf_{\mathbf{x} \in X} \left(\sum_i \mathbb{P}(\Omega_i) \mathbb{E}[f(\mathbf{x}, \boldsymbol{\omega}) | \Omega_i] \right) - \inf_{\mathbf{x} \in X} \left(\sum_i \mathbb{P}(\Omega_i) f_{X \times \Omega_i}^{cv}(\mathbf{x}, \mathbb{E}[\boldsymbol{\omega} | \Omega_i]) \right) \right|, \quad (3.22)$$

$$\leq \sum_i \mathbb{P}(\Omega_i) \mathbb{E}[f(\mathbf{x}_0^*, \boldsymbol{\omega}) | \Omega_i] - \sum_i \mathbb{P}(\Omega_i) f_{X \times \Omega_i}^{cv}(\mathbf{x}_0^*, \mathbb{E}[\boldsymbol{\omega} | \Omega_i]), \quad (3.23)$$

$$\leq \sum_i \mathbb{P}(\Omega_i) \left(f_{\Omega_i}^{cc}(\mathbf{x}_0^*, \mathbb{E}[\boldsymbol{\omega} | \Omega_i]) - f_{X \times \Omega_i}^{cv}(\mathbf{x}_0^*, \mathbb{E}[\boldsymbol{\omega} | \Omega_i]) \right), \quad (3.24)$$

$$= \sum_i \mathbb{P}(\Omega_i) \left(f_{\Omega_i}^{cc}(\mathbf{x}_0^*, \mathbb{E}[\boldsymbol{\omega} | \Omega_i]) - f_{\Omega_i}^{cv}(\mathbf{x}_0^*, \mathbb{E}[\boldsymbol{\omega} | \Omega_i]) + f_{\Omega_i}^{cv}(\mathbf{x}_0^*, \mathbb{E}[\boldsymbol{\omega} | \Omega_i]) - \right. \quad (3.25)$$

$$\left. f_{X \times \Omega_i}^{cv}(\mathbf{x}_0^*, \mathbb{E}[\boldsymbol{\omega} | \Omega_i]) \right). \quad (3.26)$$

Upon termination of the \mathcal{P} refinement Algorithm 1, we must have $\text{err}2(\mathcal{P}, \mathbf{x}_0^*, \mathbf{x}^*, X) \leq \alpha_2 \text{diam}(X)$ or $\text{err}1(\mathcal{P}, \mathbf{x}_0^*) \leq \alpha_1 \text{err}2(\mathcal{P}, \mathbf{x}_0^*, \mathbf{x}^*, X)$. If $\text{err}2(\mathcal{P}, \mathbf{x}_0^*, \mathbf{x}^*, X) \leq \alpha_2 \text{diam}(X)$, from Equation (3.24), we directly get

$$\left| \inf_{\mathbf{x} \in X} F(\mathbf{x}) - \inf_{\mathbf{x} \in X} F_{X \times \Phi(X)}^{cv}(\mathbf{x}) \right| \leq \alpha_2 \text{diam}(X) \leq \tau \text{diam}(X), \quad \forall \tau \geq \alpha_2. \quad (3.27)$$

Otherwise, if $\text{err}1(\mathcal{P}, \mathbf{x}_0^*) \leq \alpha_1 \text{err}2(\mathcal{P}, \mathbf{x}_0^*, \mathbf{x}^*, X)$, we have

$$\sum_i \mathbb{P}(\Omega_i) \left(f_{\Omega_i}^{cc}(\mathbf{x}_0^*, \mathbb{E}[\boldsymbol{\omega} | \Omega_i]) - f_{\Omega_i}^{cv}(\mathbf{x}_0^*, \mathbb{E}[\boldsymbol{\omega} | \Omega_i]) \right), \quad (3.28)$$

$$\leq \alpha_1 \sum_i \mathbb{P}(\Omega_i) \left(f_{\Omega_i}^{cc}(\mathbf{x}_0^*, \mathbb{E}[\boldsymbol{\omega} | \Omega_i]) - f_{X \times \Omega_i}^{cv}(\mathbf{x}_0^*, \mathbb{E}[\boldsymbol{\omega} | \Omega_i]) \right), \quad (3.29)$$

$$= \alpha_1 \sum_i \mathbb{P}(\Omega_i) \left(f_{\Omega_i}^{cc}(\mathbf{x}_0^*, \mathbb{E}[\boldsymbol{\omega} | \Omega_i]) - f_{\Omega_i}^{cv}(\mathbf{x}_0^*, \mathbb{E}[\boldsymbol{\omega} | \Omega_i]) + f_{\Omega_i}^{cv}(\mathbf{x}_0^*, \mathbb{E}[\boldsymbol{\omega} | \Omega_i]) - \right. \quad (3.30)$$

$$\left. f_{X \times \Omega_i}^{cv}(\mathbf{x}_0^*, \mathbb{E}[\boldsymbol{\omega} | \Omega_i]) \right). \quad (3.31)$$

Therefore,

$$(1 - \alpha_1) \sum_i \mathbb{P}(\Omega_i) \left(f_{\Omega_i}^{cc}(\mathbf{x}_0^*, \mathbb{E}[\boldsymbol{\omega}|\Omega_i]) - f_{\Omega_i}^{cv}(\mathbf{x}_0^*, \mathbb{E}[\boldsymbol{\omega}|\Omega_i]) \right), \quad (3.32)$$

$$\leq \alpha_1 \sum_i \mathbb{P}(\Omega_i) \left(f_{\Omega_i}^{cv}(\mathbf{x}_0^*, \mathbb{E}[\boldsymbol{\omega}|\Omega_i]) - f_{X \times \Omega_i}^{cv}(\mathbf{x}^*, \mathbb{E}[\boldsymbol{\omega}|\Omega_i]) \right). \quad (3.33)$$

Combining Equation (3.26) and Equation (3.33), we have

$$\left| \inf_{\mathbf{x} \in X} F(\mathbf{x}) - \inf_{\mathbf{x} \in X} F_{X \times \Phi(X)}^{cv}(\mathbf{x}) \right|, \quad (3.34)$$

$$\leq \left(1 + \frac{\alpha_1}{1 - \alpha_1}\right) \sum_i \mathbb{P}(\Omega_i) \left(f_{\Omega_i}^{cv}(\mathbf{x}_0^*, \mathbb{E}[\boldsymbol{\omega}|\Omega_i]) - f_{X \times \Omega_i}^{cv}(\mathbf{x}^*, \mathbb{E}[\boldsymbol{\omega}|\Omega_i]) \right). \quad (3.35)$$

By Assumption 29, there exists $L > 0$, such that

$$\left| \inf_{\mathbf{x} \in X} F(\mathbf{x}) - \inf_{\mathbf{x} \in X} F_{X \times \Phi(X)}^{cv}(\mathbf{x}) \right| \leq \left(1 + \frac{\alpha_1}{1 - \alpha_1}\right) L \text{diam}(X) \leq \tau \text{diam}(X), \quad (3.36)$$

where $\tau = L\left(1 + \frac{\alpha_1}{1 - \alpha_1}\right) > 0$. □

3.6 Numerical Results

In this section, we test the performance of our novel B&B algorithm, with the uncertainty set partitioning rule proposed in the previous section. For the case study, we compare against the same B&B algorithm with a naïve uniform uncertainty set partitioning rule, and against sample-average approximation (SAA). All algorithms were implemented in Matlab R2020b on a 2.6 GHz 6-Core Intel Core i7 MacPro. Lower bounding problems were solved using CPLEX V12.10.0 [99].

3.6.1 A Chemical Reactor Design Problem

Consider the following single-stage stochastic program modified from Ryoo et al. [96], which involves the optimal sizing of two continuous stirred-tank reactors of volumes x_1

and x_2 in series carrying out the reactions $A \rightleftharpoons B \rightleftharpoons C$:

$$\begin{aligned}
\min_{\mathbf{x}} \quad & -\mathbb{E} \left[\frac{k_{f,2}x_2(1+k_{r,1}x_1) + k_{f,1}x_1(1+k_{f,2}x_2)}{(1+k_{f,1}x_1)(1+k_{f,2}x_2)(1+k_{r,1}x_1)(1+k_{r,2}x_2)} \right] \\
\text{s.t.} \quad & x_1^{0.5} + x_2^{0.5} \leq 4 \\
& 10^{-5} \leq x_1, x_2 \leq 16 \\
& k_{r,1} = 0.99k_{f,1} \\
& k_{r,2} = 0.90k_{f,2} \\
& \begin{bmatrix} k_{f,1} \\ k_{f,2} \end{bmatrix} = \begin{bmatrix} 0.9 & 0.1 \\ 0.1 & 0.9 \end{bmatrix} \begin{bmatrix} \gamma_1 \\ \gamma_2 \end{bmatrix} \\
& \gamma_1 \sim \mathcal{N}(\mu_1, \sigma_1^2, \bar{\gamma}_1^L, \bar{\gamma}_1^U) \\
& \gamma_2 \sim \mathcal{N}(\mu_2, \sigma_2^2, \bar{\gamma}_2^L, \bar{\gamma}_2^U)
\end{aligned}$$

The objective is to maximize the expected value of the concentration of product B in the exit stream of the second reactor. The forward reaction rates $(k_{f,1}, k_{f,2})$ are correlated random variables described by a linear transformation of two independent random variables γ_1 and γ_2 following truncated normal distributions with means $\mu_1 = 0.097$ and $\mu_2 = 0.039$, standard deviations $\sigma_1 = 0.002$ and $\sigma_2 = 0.002$, and truncation bounds corresponding to plus and minus three standard deviations; i.e., $\bar{\gamma}_1^L = 0.091$, $\bar{\gamma}_1^U = 0.103$, $\bar{\gamma}_2^L = 0.033$, and $\bar{\gamma}_2^U = 0.045$.

Table 3.1 shows the results of the B&B algorithm described in §3.4 with two different uncertainty set partitioning rules. The relative tolerance ϵ used for the B&B termination test was 10^{-3} . A key observation from the numerical results in Table 3.1 is that the adaptive uncertainty set partitioning rule in Algorithm 1 significantly increases the computational efficiency of the B&B algorithm relative to uniform partitioning. With the adaptive partitioning rule, it only takes about 0.9s to solve the problem. In contrast, using the uniform $\bar{\Omega}$ partitioning rule, the algorithm does not terminate within 1000s. This dramatic speed-up

Table 3.1: Computational times for solving the reactor design problem using our novel B&B algorithm with two different uncertainty set partitioning rules and using sample-average approximation (SAA).

Method	Time (s)	Settings
B&B	1.22	Partitioning rule - Algorithm 1 with $\alpha = 0.5$
B&B	0.93	Partitioning rule - Algorithm 1 with $\alpha = 0.6$
B&B	0.91	Partitioning rule - Algorithm 1 with $\alpha = 0.7$
B&B	>1000	Partitioning rule - uniform, $\text{diam}(\Omega_i) \leq 10\text{diam}(X_k), \forall i$
B&B	>1000	Partitioning rule - uniform, $\text{diam}(\Omega_i) \leq 100\text{diam}(X_k), \forall i$
SAA	13.78	$N = 120, N' = 4000, M = 30$
SAA	11.21	$N = 150, N' = 4000, M = 20$
SAA	10.71	$N = 200, N' = 4000, M = 15$

is achieved by more effective management of the $\bar{\Omega}$ partition size. To illustrate this clearly, Figure 3.1 shows the subintervals of the decision space (i.e, nodes) visited by the B&B algorithm color coded by the size of the $\bar{\Omega}$ partition at the time each node was fathomed. The data in the figure are for Algorithm 1 with $\alpha = 0.7$. The figure shows that the vast majority of the search space is successfully fathomed using very small $\bar{\Omega}$ partitions. Over 56% of the visited nodes are fathomed using partitions with 6 or fewer elements. Moreover, fewer than 1.4% of the visited nodes were fathomed with the maximum partition size of 56. The nodes requiring large partitions are predominantly clustered near the global solution or the active constraint boundary. In contrast, using a uniform uncertainty set partitioning rule that satisfies $\text{diam}(\Omega_i) \leq 100\text{diam}(X_k)$ produces much larger partitions when $\text{diam}(X_k)$ becomes small, leading to higher computational times. This result clearly illustrates that our new uncertainty set partitioning rule can achieve higher efficiency than the uniform partitioning rule by an effective control of the partition size.

Table 3.1 also compares the results of our B&B method with several implementations of sample-average approximation (SAA), which is the most common approach for solving stochastic programs. SAA was implemented according to the standard procedure described in [100]. In this procedure, first a sample size N is chosen and the expected-value objective function is approximated using N fixed samples of the random variables. This deterministic

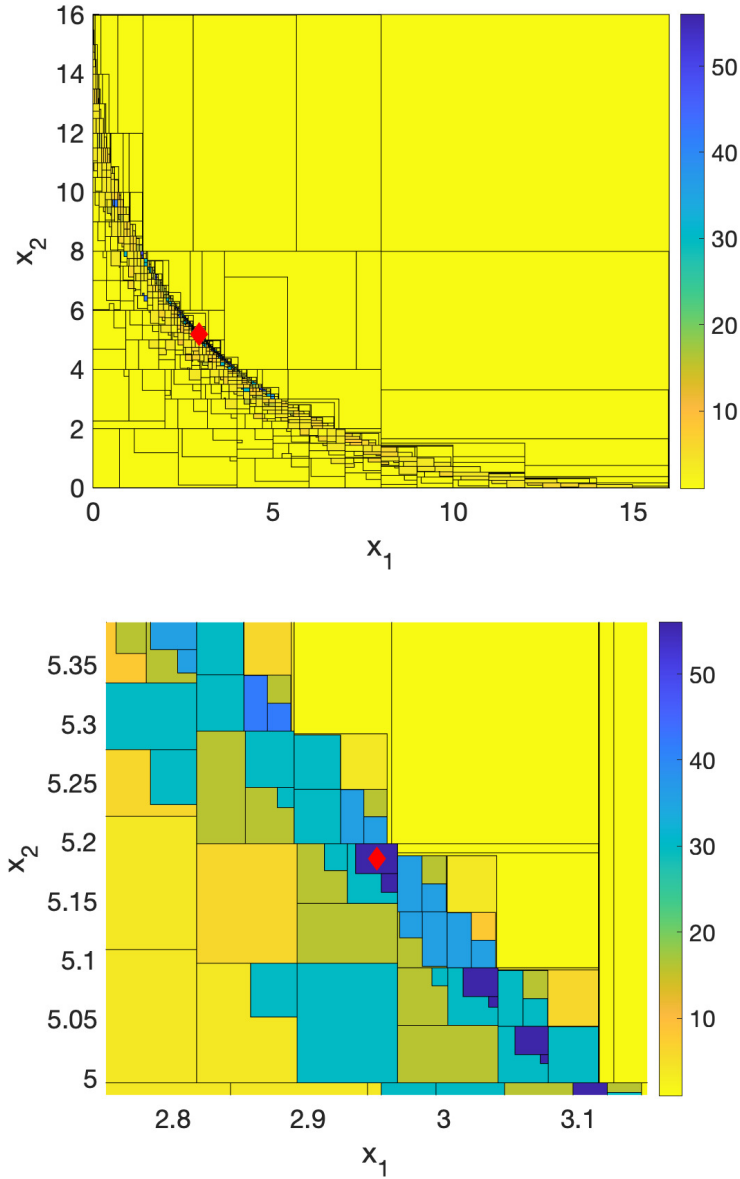


Figure 3.1: Upper: Nodes X_k visited by the B&B algorithm using the uncertainty set partitioning rule in Algorithm 1 with $\alpha = 0.7$ for the reactor design problem, color coded by the size of the partition of $\bar{\Omega}$ when each node was fathomed (color bar). Lower: Close-up view near an ϵ -optimal solution (red diamond).

approximation is then solved to global optimality. Second, a larger sample size N' is used to obtain an accurate estimate of the objective function value at the optimal solution. Third, M replicates of the problem are solved with independent samples and the variance of the optimality gap estimator is calculated. If the optimality gap estimator does not meet the required tolerance, the sample size N is increased by ΔN , the sample size N' is increased by $\Delta N'$, and the number of replicates M is increased by ΔM . Finally, the entire process is repeated until a predefined relative tolerance is reached, which we chose as 10^{-3} . To enable a fair comparison that isolates the key differences in how SAA and our proposed algorithm handle uncertainty, we solved all of the deterministic subproblems generated by SAA using the same basic B&B algorithm as for our methods. Upper bounds were obtained using simple objective function evaluations and lower bounds were obtained by constructing standard McCormick-based affine relaxations and solving them using CPLEX V12.10.0, exactly as in our algorithm. We tested SAA for various choices of the parameters N , N' , M , ΔN , $\Delta N'$, and ΔM . The best result are shown in Table 3.1. With these choices of N , N' , and M , the optimality gap estimator satisfies the specified tolerance in the first attempt, so the values of ΔN , $\Delta N'$, and ΔM are irrelevant. This represents a best case scenario for SAA by effectively assuming that the correct sample size is guessed on the first attempt. Nevertheless, the fastest SAA implementation required 11.21s to solve the problem. Therefore, even though we have omitted the cost of determining an appropriate sample size, which can be very costly, our method is still more than one order of magnitude faster than SAA. At the same time, our algorithm provides a rigorous ϵ -global solution of the original problem with no sampling error, while SAA only provides an ϵ -global solution of an approximation. These results clearly indicate that our proposed algorithm provides significant advantages relative to SAA for nonconvex stochastic programs, both in terms of computational effort and solution accuracy.

3.7 Conclusion

In this chapter, we developed a novel branch-and-bound algorithm for locating guaranteed global solutions of expected-value minimization problems with continuous random variables. The accuracy of the lower bounding and upper bounding procedures depend on the branching of the decision variable space as well as the partition of the random variable space. We presented an efficient uncertainty set partitioning rule that adaptively refines the $\bar{\Omega}$ partition as the B&B search proceeds. The resulting algorithm is capable of using a coarse partition of the uncertainty space for fathoming the majority of the search space, and requires dense partitions only when close to the global solution, leading to significant reductions in computational cost. Moreover, all computed bounds are rigorous at all stages of the algorithm, regardless of how coarse or fine the uncertainty set partition is. Thus, fathoming and termination decisions can be made with certainty at any time without loss of rigor. As a result, the algorithm provides guaranteed global solutions of the original stochastic program with no sampling or approximation error. The presented case study shows that our algorithm is significantly faster than the uniform partition rule and the standard SAA method.

CHAPTER 4
CONVEX RELAXATIONS FOR NONLINEAR STOCHASTIC OPTIMAL
CONTROL PROBLEMS

4.1 Introduction

This chapter concerns the guaranteed global solution of the stochastic optimal control problem stated informally as

$$\begin{aligned} \min_{\mathbf{p} \in \overline{P} \subset \mathbb{R}^{n_p}} \quad & \mathbb{E}[g(\mathbf{p}, \boldsymbol{\omega}, \mathbf{x}(t_f, \mathbf{p}, \boldsymbol{\omega}))], \\ \text{s.t.} \quad & \mathbb{P}[\mathbf{h}(\mathbf{p}, \boldsymbol{\omega}, \mathbf{x}(t_f, \mathbf{p}, \boldsymbol{\omega})) \leq \mathbf{0}] \geq 1 - \alpha, \end{aligned} \tag{4.1}$$

where \mathbb{E} and \mathbb{P} denote the expected value and probability over continuous random variables $\boldsymbol{\omega} \in \overline{\Omega} \subset \mathbb{R}^{n_\omega}$, respectively, and $\mathbf{x}(t_f, \mathbf{p}, \boldsymbol{\omega})$ is the solution of the nonlinear ordinary differential equations (ODEs)

$$\begin{aligned} \dot{\mathbf{x}}(t, \mathbf{p}, \boldsymbol{\omega}) &= \mathbf{f}(t, \mathbf{p}, \boldsymbol{\omega}, \mathbf{x}(t, \mathbf{p}, \boldsymbol{\omega})), \\ \mathbf{x}(t_0, \mathbf{p}, \boldsymbol{\omega}) &= \mathbf{x}_0(\mathbf{p}, \boldsymbol{\omega}). \end{aligned} \tag{4.2}$$

The functions g , \mathbf{h} , \mathbf{f} , and \mathbf{x}_0 may be nonconvex with respect to all of their arguments. The decision vector \mathbf{p} may represent a parameterized open-loop control input, parameters in an explicit feedback controller embedded in (4.2), etc. Such problems arise in stochastic model predictive control [68], renewable energy systems [30], trajectory planning [28], chemical process control [31], and many other applications.

For optimal control problems with deterministic objectives and constraints, a number of algorithms have recently been developed that can provide guaranteed global solutions [33, 34, 35, 36, 37]. In brief, these methods are predicated on effective algorithms for

enclosing the reachable set of the dynamics on subintervals of the decision space. These enclosures can take the form of fixed interval bounds or other fixed sets [35, 36], but are more commonly described by bounds that depend affinely or convexly on the decisions \mathbf{p} [37, 32, 38, 39, 40, 41, 42, 43, 44]. With such an enclosure, it is possible to construct convex relaxations of the optimal control problem on arbitrary subintervals of the decision space, and using these, to compute bounds on the optimal objective value on such subintervals. Finally, these bounds can be used within a generic spatial branch-and-bound (B&B) algorithm [11] to obtain a rigorous global solution.

To the best of our knowledge, no such guaranteed global optimization algorithm is available for the stochastic problem (4.1). In this case, a critical new challenge is that it is typically not possible to express the expected-value and probability appearing in the objective and constraints as closed-form functions of \mathbf{p} . In particular, doing so would require both an analytical solution of the nonlinear ODEs, and an analytical expression for the multidimensional integrals defining \mathbb{E} and \mathbb{P} . In the context of the optimization approach outlined above, the absence of such analytical expressions is problematic because without them it is no longer possible to obtain guaranteed bounds on the optimal objective value. In fact, using either sample-based or quadrature type approximations of \mathbb{E} and \mathbb{P} , it is not even possible to bound the objective and constraint values at a given feasible point with finitely many computations.

In practice, this problem is most commonly addressed by replacing the objective and constraints in (4.1) by sample-average approximations (SAA), resulting in a deterministic optimal control problem that can be solved using existing methods. However, SAA has several critical limitations that can lead to inaccurate solutions or excessive computational cost. First, it only guarantees convergence to a global solution as the sample size tends to infinity [24]. Moreover, the number of samples required to achieve a high-quality solution in practice is unknown and can be quite large [25, 26]. More importantly, a sufficient sample size is not known in advance. Theoretical sample size bounds are available [45],

but are very conservative and not generally computable. Thus, it is often necessary to solve several SAA problems with independent samples to assess solution accuracy, and to repeat the entire process if a larger sample size is deemed necessary [26]. This is clearly problematic for nonconvex optimal control problems, where solving a single instance to global optimality is already demanding.

In this chapter, we take a first step towards extending the rigorous global optimization methods outlined above to the stochastic problem (4.1). Specifically, our main contribution is a new method for computing guaranteed convex and concave relaxations of the final-time expected-value objective function. As with the deterministic methods above, we rely on an existing method for computing time-varying bounds on the solutions of (4.2) [38]. However, we modify the method here to obtain lower and upper bounds that are convex and concave, respectively, with respect to both \mathbf{p} and ω . Through an application of Jensen’s inequality, we then obtain a time-varying, \mathbf{p} -dependent convex enclosure of the mapping $t \mapsto \mathbb{E}[g(\mathbf{p}, \omega, \mathbf{x}(t, \mathbf{p}, \omega))]$. The use of Jensen’s inequality to compute rigorous lower bounds for convex stochastic programs is well known. However, the combination of Jensen’s inequality with automated, general purpose convex relaxation techniques to address nonconvex stochastic programs was first proposed in Chapter 2. Here, we extend this approach to dynamic optimization problems. This relaxation method is similar in spirit to the so-called *probability bounds* for dynamic systems in [101, 102], but these works do not consider expected-value bounds and have not been applied in the context of optimization.

In the absence of chance constraints, the relaxation technique presented here can provide both lower and upper bounds on the optimal objective value of (4.1), without resorting to sample-based or quadrature approximations. In principle, this enables the application of spatial B&B to solve (4.1) to guaranteed global optimality with no approximation error. However, we leave the details of such a B&B algorithm, as well as the treatment of chance constraints, for future work.

The remainder of this chapter is organized as follows. First, Section 4.2 gives a formal

problem statement. Our new relaxation theory is then developed in two steps in Sections 4.3 and 4.4. In Section 4.5, we apply the developed relaxations to obtain computable upper and lower bounds on the optimal objective value of (4.1) in the absence of chance constraints. In Section 4.6, we demonstrate the proposed relaxation technique on a simple case study. Finally, Section 4.7 provides concluding remarks.

4.2 Problem Statement

Let $I = [t_0, t_f] \subset \mathbb{R}$ be a time horizon of interest, let $\bar{P} \subset \mathbb{R}^{n_p}$ be a compact n_p -dimensional interval of decision variables \mathbf{p} , and let $\boldsymbol{\omega}$ be a random vector with probability density function (PDF) $p : \mathbb{R}^{n_\omega} \rightarrow \mathbb{R}$. Specifically, $\boldsymbol{\omega}$ is a time-invariant random vector, rather than a random process. We assume that p is zero outside of a compact interval $\bar{\Omega} \subset \mathbb{R}^{n_\omega}$. Let $\mathbf{x}_0 : \mathbb{R}^{n_p} \times \mathbb{R}^{n_\omega} \rightarrow \mathbb{R}^{n_x}$ and $\mathbf{f} : \mathbb{R} \times \mathbb{R}^{n_p} \times \mathbb{R}^{n_\omega} \times \mathbb{R}^{n_x} \rightarrow \mathbb{R}^{n_x}$ be locally Lipschitz continuous functions defining the dynamics (4.2). We assume that (4.2) has a unique solution $\mathbf{x}(\cdot, \mathbf{p}, \boldsymbol{\omega})$ on all of I for every $(\mathbf{p}, \boldsymbol{\omega}) \in \bar{P} \times \bar{\Omega}$. Note that the derivative $\dot{\mathbf{x}}(t, \mathbf{p}, \boldsymbol{\omega})$ in (4.2) is well-defined in the usual sense because \mathbf{f} is continuous and $\boldsymbol{\omega}$ is time-invariant. Finally, let $g : \mathbb{R}^{n_p} \times \mathbb{R}^{n_\omega} \times \mathbb{R}^{n_x} \rightarrow \mathbb{R}$ and define

$$\mathcal{G}(\mathbf{p}) \equiv \mathbb{E}[g(\mathbf{p}, \boldsymbol{\omega}, \mathbf{x}(t_f, \mathbf{p}, \boldsymbol{\omega}))], \quad (4.3)$$

$$= \int_{\bar{\Omega}} g(\mathbf{p}, \boldsymbol{\omega}, \mathbf{x}(t_f, \mathbf{p}, \boldsymbol{\omega})) p(\boldsymbol{\omega}) d\boldsymbol{\omega}, \quad (4.4)$$

which is assumed to exist for every $\mathbf{p} \in \bar{P}$. We do not impose any convexity assumptions on the functions \mathbf{x}_0 , \mathbf{f} , or g .

The objective of this chapter is to develop a method for computing convex and concave relaxations of \mathcal{G} on any given subinterval of \bar{P} . Specifically, we are interested in relaxations of \mathcal{G} itself, rather than any finite approximation of \mathcal{G} via sampling, quadrature, etc. At the same time, the relaxations themselves must be finitely computable to be of value in the context of spatial B&B.

The following general notation is used in the remainder of the chapter. For any $\mathbf{s}^L, \mathbf{s}^U \in \mathbb{R}^n$ with $\mathbf{s}^L \leq \mathbf{s}^U$, let $S = [\mathbf{s}^L, \mathbf{s}^U]$ denote the compact n -dimensional interval $\{\mathbf{s} \in \mathbb{R}^n : \mathbf{s}^L \leq \mathbf{s} \leq \mathbf{s}^U\}$. Let $\mathbb{I}\mathbb{R}^n$ denote the set of all compact interval subsets of \mathbb{R}^n . Similarly, for $\bar{S} \subset \mathbb{R}^n$, let $\mathbb{I}\bar{S}$ denote the set of all compact interval subsets of \bar{S} , $\mathbb{I}\bar{S} \equiv \{S \in \mathbb{I}\mathbb{R}^n : S \subset \bar{S}\}$.

Definition 43. Let $S \subset \mathbb{R}^n$ be convex and $h : S \rightarrow \mathbb{R}$. Functions $h^{cv}, h^{cc} : S \rightarrow \mathbb{R}$ are *convex and concave relaxations of h on S* , respectively, if h^{cv} is convex on S , h^{cc} is concave on S , and

$$h^{cv}(\mathbf{s}) \leq h(\mathbf{s}) \leq h^{cc}(\mathbf{s}), \quad \forall \mathbf{s} \in S.$$

4.3 Relaxing the Dynamics on $P \times \Omega$

The first step in our relaxation procedure is to compute convex and concave relaxations of the function $G : \mathbb{R}^{n_p} \times \mathbb{R}^{n_\omega} \rightarrow \mathbb{R}$ defined by

$$G(\mathbf{p}, \boldsymbol{\omega}) \equiv g(\mathbf{p}, \boldsymbol{\omega}, \mathbf{x}(t_f, \mathbf{p}, \boldsymbol{\omega})). \quad (4.5)$$

Specifically, we will show in §4.4 that the desired relaxations of the expected value $\mathcal{G}(\mathbf{p}) = \mathbb{E}[G(\mathbf{p}, \boldsymbol{\omega})]$ can be readily computed from convex and concave relaxations of G *jointly* with respect to \mathbf{p} and $\boldsymbol{\omega}$. Assuming that g is known in closed form, and hence amenable to standard relaxation techniques [13, 15], the only complication in computing such joint relaxations of G is the presence of the terminal time state vector $\mathbf{x}(t_f, \mathbf{p}, \boldsymbol{\omega})$ in (4.5), which we naturally assume is not known in closed form. To deal with this, we will construct joint *state relaxations* defined as follows.

Definition 44. Choose any intervals $P \in \mathbb{I}\bar{P}$ and $\Omega \in \mathbb{I}\bar{\Omega}$. Two functions $\mathbf{x}^{cv}, \mathbf{x}^{cc} : I \times P \times \Omega \rightarrow \mathbb{R}^{n_x}$ are called *state relaxations* for (4.2) on $P \times \Omega$ if $\mathbf{x}^{cv}(t, \cdot, \cdot)$ and $\mathbf{x}^{cc}(t, \cdot, \cdot)$ are, respectively, convex and concave relaxations of $\mathbf{x}(t, \cdot, \cdot)$ on $P \times \Omega$, for every $t \in I$.

Several methods have been developed for computing state relaxations in the deterministic case [32, 38, 39, 43, 44, 37]. Here, we extend the method in [38] to produce joint relaxations on $P \times \Omega$. However, because Definition 44 makes no mathematical distinction between the decisions \mathbf{p} and the RVs $\boldsymbol{\omega}$, the extension is direct (our overall relaxation procedure treats \mathbf{p} and $\boldsymbol{\omega}$ differently beginning in §4.4).

The method in [38] computes state relaxations as the solutions of an auxiliary system of ODEs. Defining this system requires particular kinds of relaxations of the functions \mathbf{x}_0 , \mathbf{f} and g , all of which may be nonconvex in all arguments. Although the following assumptions may seem restrictive, the required relaxations can be automatically constructed for nearly any functions \mathbf{x}_0 , \mathbf{f} , and g through a generalization of McCormick’s relaxation technique, as discussed in detail in [38, 14].

Assumption 45. *Assume that the following functions are available for any intervals $P \times \Omega \in \mathbb{I}P \times \mathbb{I}\bar{\Omega}$:*

1. $\mathbf{x}_{0,P \times \Omega}^{cv}, \mathbf{x}_{0,P \times \Omega}^{cc} : P \times \Omega \rightarrow \mathbb{R}^{n_x}$ are continuous convex and concave relaxations of \mathbf{x}_0 on $P \times \Omega$.
2. $\mathbf{f}_{P \times \Omega}^{cv}, \mathbf{f}_{P \times \Omega}^{cc} : I \times P \times \Omega \times \mathbb{R}^{n_x} \times \mathbb{R}^{n_x} \rightarrow \mathbb{R}^{n_x}$ are Lipschitz continuous and satisfy the following condition: For any continuous $\phi, \psi : I \times P \times \Omega \rightarrow \mathbb{R}^{n_x}$ and any fixed $t \in I$, the functions

$$(\mathbf{p}, \boldsymbol{\omega}) \mapsto \mathbf{f}_{P \times \Omega}^{cv}(t, \mathbf{p}, \boldsymbol{\omega}, \phi(t, \mathbf{p}, \boldsymbol{\omega}), \psi(t, \mathbf{p}, \boldsymbol{\omega})), \quad (4.6)$$

$$(\mathbf{p}, \boldsymbol{\omega}) \mapsto \mathbf{f}_{P \times \Omega}^{cc}(t, \mathbf{p}, \boldsymbol{\omega}, \phi(t, \mathbf{p}, \boldsymbol{\omega}), \psi(t, \mathbf{p}, \boldsymbol{\omega})), \quad (4.7)$$

are respectively convex and concave relaxations of

$$(\mathbf{p}, \boldsymbol{\omega}) \mapsto \mathbf{f}(t, \mathbf{p}, \boldsymbol{\omega}, \mathbf{x}(t, \mathbf{p}, \boldsymbol{\omega})) \quad (4.8)$$

on $P \times \Omega$, provided that $\phi(t, \cdot, \cdot)$ and $\psi(t, \cdot, \cdot)$ are respectively convex and concave

relaxations of $\mathbf{x}(t, \cdot, \cdot)$ on $P \times \Omega$.

3. $g_{P \times \Omega}^{cv}, g_{P \times \Omega}^{cc} : P \times \Omega \times \mathbb{R}^{n_x} \times \mathbb{R}^{n_x} \rightarrow \mathbb{R}^{n_x}$ are Lipschitz continuous and satisfy the following condition: For any continuous $\phi, \psi : P \times \Omega \rightarrow \mathbb{R}^{n_x}$, the functions

$$(\mathbf{p}, \boldsymbol{\omega}) \mapsto g_{P \times \Omega}^{cv}(\mathbf{p}, \boldsymbol{\omega}, \phi(\mathbf{p}, \boldsymbol{\omega}), \psi(\mathbf{p}, \boldsymbol{\omega})), \quad (4.9)$$

$$(\mathbf{p}, \boldsymbol{\omega}) \mapsto g_{P \times \Omega}^{cc}(\mathbf{p}, \boldsymbol{\omega}, \phi(\mathbf{p}, \boldsymbol{\omega}), \psi(\mathbf{p}, \boldsymbol{\omega})), \quad (4.10)$$

are respectively convex and concave relaxations of

$$(\mathbf{p}, \boldsymbol{\omega}) \mapsto g(\mathbf{p}, \boldsymbol{\omega}, \mathbf{x}(t_f, \mathbf{p}, \boldsymbol{\omega})) \quad (4.11)$$

on $P \times \Omega$, provided that ϕ and ψ are respectively convex and concave relaxations of $\mathbf{x}(t_f, \cdot, \cdot)$ on $P \times \Omega$.

Under Assumption 45, the following theorem provides state relaxations for (4.2) and the desired relaxations of G .

Theorem 46. Choose any $P \times \Omega \in \mathbb{I}\bar{P} \times \mathbb{I}\bar{\Omega}$ and define the auxiliary system of ODEs:

$$\begin{aligned} \dot{\mathbf{x}}^{cv}(t, \mathbf{p}, \boldsymbol{\omega}) &= \mathbf{f}_{P \times \Omega}^{cv}(t, \mathbf{p}, \boldsymbol{\omega}, \mathbf{x}^{cv}(t, \mathbf{p}, \boldsymbol{\omega}), \mathbf{x}^{cc}(t, \mathbf{p}, \boldsymbol{\omega})), \\ \dot{\mathbf{x}}^{cc}(t, \mathbf{p}, \boldsymbol{\omega}) &= \mathbf{f}_{P \times \Omega}^{cc}(t, \mathbf{p}, \boldsymbol{\omega}, \mathbf{x}^{cv}(t, \mathbf{p}, \boldsymbol{\omega}), \mathbf{x}^{cc}(t, \mathbf{p}, \boldsymbol{\omega})), \\ \mathbf{x}^{cv}(t_0, \mathbf{p}, \boldsymbol{\omega}) &= \mathbf{x}_{0, P \times \Omega}^{cv}(\mathbf{p}, \boldsymbol{\omega}), \\ \mathbf{x}^{cc}(t_0, \mathbf{p}, \boldsymbol{\omega}) &= \mathbf{x}_{0, P \times \Omega}^{cc}(\mathbf{p}, \boldsymbol{\omega}), \end{aligned} \quad (4.12)$$

for all $(t, \mathbf{p}, \boldsymbol{\omega}) \in I \times P \times \Omega$. This system has unique solutions $\mathbf{x}^{cv}, \mathbf{x}^{cc} : I \times P \times \Omega \rightarrow \mathbb{R}^{n_x}$, and these solutions are state relaxations for (4.2) on $P \times \Omega$. Moreover, the functions

$$\begin{aligned} G_{P \times \Omega}^{cv}(\mathbf{p}, \boldsymbol{\omega}) &\equiv g_{P \times \Omega}^{cv}(\mathbf{p}, \boldsymbol{\omega}, \mathbf{x}^{cv}(t_f, \mathbf{p}, \boldsymbol{\omega}), \mathbf{x}^{cc}(t_f, \mathbf{p}, \boldsymbol{\omega})), \\ G_{P \times \Omega}^{cc}(\mathbf{p}, \boldsymbol{\omega}) &\equiv g_{P \times \Omega}^{cc}(\mathbf{p}, \boldsymbol{\omega}, \mathbf{x}^{cv}(t_f, \mathbf{p}, \boldsymbol{\omega}), \mathbf{x}^{cc}(t_f, \mathbf{p}, \boldsymbol{\omega})), \end{aligned}$$

are convex and concave relaxations of G on $P \times \Omega$.

Proof. Under Conditions 1 and 2 of Assumption 45, a direct application of Theorem 4.1 in [38] with $P := P \times \Omega$ ensures that \mathbf{x}^{cv} and \mathbf{x}^{cc} exist, are unique, and are state relaxations for (4.2) on $P \times \Omega$. Thus, Condition 3 of Assumption 45 can be applied with $\phi = \mathbf{x}^{cv}(t_f, \cdot, \cdot)$ and $\psi = \mathbf{x}^{cc}(t_f, \cdot, \cdot)$, and it follows that $G_{P \times \Omega}^{cv}$ and $G_{P \times \Omega}^{cc}$ are convex and concave relaxations of G on $P \times \Omega$. \square

Once the relaxations in Assumption 45 have been constructed (see [38]), the initial value problem (4.12) can be solved for any $(\mathbf{p}, \boldsymbol{\omega}) \in P \times \Omega$ using any standard ODE solver, after which $G_{P \times \Omega}^{cv}$ and $G_{P \times \Omega}^{cc}$ can be directly evaluated.

4.4 Relaxing the Expected Value on P

In this section, we develop a method for computing convex and concave relaxations of the expected cost function

$$\mathcal{G}(\mathbf{p}) = \mathbb{E}[G(\mathbf{p}, \boldsymbol{\omega})] = \mathbb{E}[g(\mathbf{p}, \boldsymbol{\omega}, \mathbf{x}(t_f, \mathbf{p}, \boldsymbol{\omega}))] \quad (4.13)$$

on any given $P \in \mathbb{I}\bar{P}$. In light of Theorem 46, we assume throughout this section that relaxations $G_{P \times \Omega}^{cv}$ and $G_{P \times \Omega}^{cc}$ of G are available on any desired subinterval $P \times \Omega \in \mathbb{I}\bar{P} \times \mathbb{I}\bar{\Omega}$.

To begin, note that for any $P \in \mathbb{I}\bar{P}$ and $\mathbf{p} \in P$, $\mathcal{G}(\mathbf{p})$ is bounded from above and below by the values $\mathbb{E}[G_{P \times \bar{\Omega}}^{cc}(\mathbf{p}, \boldsymbol{\omega})]$ and $\mathbb{E}[G_{P \times \bar{\Omega}}^{cv}(\mathbf{p}, \boldsymbol{\omega})]$, respectively, as a trivial consequence of integral monotonicity. Moreover, these functions can readily be shown to be concave and convex on P , respectively. However, relaxations defined in this way are of no value for B&B global optimization since they must be evaluated by sampling in general, and so guaranteed bounds cannot be computed from such relaxations finitely. To overcome this limitation, we follow the technique recently proposed for standard stochastic programs (rather than optimal control problems) in Chapter 2. Namely, we apply Jensen's inequality to pass the expectation operator inside the relaxation functions $G_{P \times \bar{\Omega}}^{cc}$ and $G_{P \times \bar{\Omega}}^{cv}$.

Lemma 47 (Jensen's inequality). *Let $\Omega \subset \bar{\Omega}$ be convex and let $h : \Omega \rightarrow \mathbb{R}$. If h is convex and $\mathbb{E}[h(\boldsymbol{\omega})]$ exists, then $\mathbb{E}[h(\boldsymbol{\omega})] \geq h(\mathbb{E}[\boldsymbol{\omega}])$. If h is concave, then $\mathbb{E}[h(\boldsymbol{\omega})] \leq h(\mathbb{E}[\boldsymbol{\omega}])$.*

Proof. See Proposition 1.1 in [72]. □

Although we could apply Jensen's inequality directly to the relaxations $G_{P \times \bar{\Omega}}^{cv}$ and $G_{P \times \bar{\Omega}}^{cc}$ on the whole uncertainty set $\bar{\Omega}$, this introduces conservatism in the resulting relaxations that cannot be controlled. In particular, relaxations defined in this way may not converge to \mathcal{G} as the interval P tends towards a singleton $[\mathbf{p}, \mathbf{p}]$ which is required for the convergence of spatial B&B algorithms [11]. Thus, we instead apply Jensen's inequality on a partition of $\bar{\Omega}$ that can be refined as needed.

Definition 48. A collection $\Phi = \{\Omega_i\}_{i=1}^n$ of intervals $\Omega_i \in \mathbb{I}\bar{\Omega}$ is called an *interval partition* of $\bar{\Omega}$ if $\bar{\Omega} = \cup_{i=1}^n \Omega_i$ and $\text{int}(\Omega_i) \cap \text{int}(\Omega_j) = \emptyset$ for all distinct i and j .

Definition 49. For any measurable $\Omega \subset \bar{\Omega}$, let $\mathbb{P}(\Omega)$ denote the probability of the event $\boldsymbol{\omega} \in \Omega$, and let $\mathbb{E}[\cdot|\Omega]$ denote the conditional expected value conditioned on the event $\boldsymbol{\omega} \in \Omega$.

The following theorem provides the desired relaxations of \mathcal{G} .

Theorem 50. *Let $\Phi = \{\Omega_i\}_{i=1}^n$ be an interval partition of $\bar{\Omega}$. For every $P \in \mathbb{I}\bar{P}$ and every $\mathbf{p} \in P$, define*

$$\mathcal{G}_{P \times \Phi}^{cv}(\mathbf{p}) \equiv \sum_{i=1}^n \mathbb{P}(\Omega_i) G_{P \times \Omega_i}^{cv}(\mathbf{p}, \mathbb{E}[\boldsymbol{\omega}|\Omega_i]), \quad (4.14)$$

$$\mathcal{G}_{P \times \Phi}^{cc}(\mathbf{p}) \equiv \sum_{i=1}^n \mathbb{P}(\Omega_i) G_{P \times \Omega_i}^{cc}(\mathbf{p}, \mathbb{E}[\boldsymbol{\omega}|\Omega_i]). \quad (4.15)$$

Then $\mathcal{G}_{P \times \Phi}^{cv}$ and $\mathcal{G}_{P \times \Phi}^{cc}$ are convex and concave relaxations of \mathcal{G} on P , respectively.

Proof. By the law of total expectation (Proposition 5.1 in [90]), $\mathcal{G}(\mathbf{p})$ can be expressed for

any $\mathbf{p} \in \overline{P}$ as

$$\mathcal{G}(\mathbf{p}) = \mathbb{E}[G(\mathbf{p}, \boldsymbol{\omega})] = \sum_{i=1}^n \mathbb{P}(\Omega_i) \mathbb{E}[G(\mathbf{p}, \boldsymbol{\omega}) | \Omega_i]. \quad (4.16)$$

Thus, for any $P \in \mathbb{I}\overline{P}$ and any $\mathbf{p} \in P$, integral monotonicity and Jensen's inequality give,

$$\mathcal{G}(\mathbf{p}) \geq \sum_{i=1}^n \mathbb{P}(\Omega_i) \mathbb{E}[G_{P \times \Omega_i}^{cv}(\mathbf{p}, \boldsymbol{\omega}) | \Omega_i], \quad (4.17)$$

$$\geq \sum_{i=1}^n \mathbb{P}(\Omega_i) G_{P \times \Omega_i}^{cv}(\mathbf{p}, \mathbb{E}[\boldsymbol{\omega} | \Omega_i]), \quad (4.18)$$

$$= \mathcal{G}_{P \times \Phi}^{cv}(\mathbf{p}). \quad (4.19)$$

Noting that $\mathcal{G}_{P \times \Phi}^{cv}$ is a sum of convex functions on P , it must be convex itself, and is therefore a convex relaxation of \mathcal{G} on P . The proof for $\mathcal{G}_{P \times \Phi}^{cc}$ is analogous. \square

By considering an exhaustive partition of $\overline{\Omega}$, Theorem 50 provides relaxations that are valid for the true expected value \mathcal{G} , rather than a finite approximation obtained via sampling or otherwise. Moreover, in contrast to sample-based approaches, the relaxations in Theorem 50 can be evaluated finitely provided that the probabilities $\mathbb{P}[\Omega_i]$ and conditional expectations $\mathbb{E}[\boldsymbol{\omega} | \Omega_i]$ are computable. This is clearly true if $\boldsymbol{\omega}$ is uniformly distributed. On the other hand, directly evaluating these quantities for more general RVs often requires difficult multidimensional integrations. However, Chapter 2 presents an approach that avoids these computations for a variety of common distributions by using well-known change-of-variables formulas to reformulate the RVs of interest as uniform RVs (e.g., using the inverse CDF transform). Since our relaxation theory does not require linearity or convexity assumptions, using such transformations poses no additional difficulties.

Clearly, the use of an exhaustive partition of $\overline{\Omega}$ in Theorem 50 is a drawback, since in practice it limits our approach to models with a modest number of RVs. Thus, solving (4.1) by sample-average approximation is likely to be more efficient when the dimension

of ω is large. However, note that Theorem 50 provides valid relaxations on *any* partition Φ , no matter how coarse. Thus, one can use partitions appropriate for any desired level of accuracy. In particular, in the context of spatial B&B, coarse partitions may be sufficient to eliminate large regions of the search space from consideration, with fine partitions being required only in the vicinity of global optimizers. We leave the issue of effective partitioning rules for future work. We also leave for future work a formal analysis of the convergence of $\mathcal{G}_{P \times \Phi}^{cv}$ and $\mathcal{G}_{P \times \Phi}^{cc}$ to \mathcal{G} as P tends towards a singleton $[\mathbf{p}, \mathbf{p}]$. However, note that Theorem 15 in Chapter 2 shows that the expected-value relaxation strategy used in Theorem 50 inherits the convergence properties of the integrand relaxations $G_{P \times \Omega_i}^{cv}$ and $G_{P \times \Omega_i}^{cc}$, provided that $\bar{\Omega}$ is partitioned sufficiently quickly as the width of P diminishes. In turn, the convergence properties of $G_{P \times \Omega_i}^{cv}$ and $G_{P \times \Omega_i}^{cc}$ depend on those of the relaxations defined in Assumption 45, and have been studied in detail in [103, 104].

4.5 Rigorous Bounds on Stochastic Optimal Control Problems

In this section, we apply the results of Sections 4.3 and 4.4 to establish computable upper and lower bounds on the optimal objective value of the stochastic optimal control problem

$$\min_{\mathbf{p} \in \bar{P}} \mathcal{G}(\mathbf{p}) \equiv \mathbb{E}[g(\mathbf{p}, \omega, \mathbf{x}(t_f, \mathbf{p}, \omega))]. \quad (4.20)$$

Specifically, in order to solve (4.20) to guaranteed global optimality using spatial B&B, it is necessary to provide the B&B routine with upper and lower bounds for (4.20) restricted to any given interval $P \in \mathbb{I}\bar{P}$. To obtain a lower bound, the standard approach is to minimize a convex relaxation over P , which is available via Theorem 50. To obtain an upper bound, one common approach is simply to evaluate the objective at any feasible $\mathbf{p} \in P$. However, this is not possible for (4.20) because $\mathcal{G}(\mathbf{p})$ cannot be evaluated finitely. Thus, a different approach is required to obtain a valid upper bound. In the following corollary, we employ a special case of the concave relaxation defined in Theorem 50.

Corollary 51. Let $\Phi = \{\Omega_i\}_{i=1}^n$ be an interval partition of $\overline{\Omega}$ and define the shorthand $\omega_i \equiv \mathbb{E}[\omega|\Omega_i]$. For any $P \in \overline{\mathbb{P}}$, a lower bound on the optimal objective value of (4.20) restricted to P is given by the optimal objective value of the following deterministic convex optimal control problem:

$$\min_{\mathbf{p} \in P} \sum_{i=1}^n \mathbb{P}(\Omega_i) g_{P \times \Omega_i}^{cv}(\mathbf{p}, \omega_i, \mathbf{x}_i^{cv}(t_f, \mathbf{p}), \mathbf{x}_i^{cc}(t_f, \mathbf{p})), \quad (4.21)$$

where $\mathbf{x}_i^{cv}(t, \mathbf{p})$ and $\mathbf{x}_i^{cc}(t, \mathbf{p})$ are the unique solutions of the n independent systems of ODEs given for each $i \in \{1, \dots, n\}$ by

$$\begin{aligned} \dot{\mathbf{x}}_i^{cv}(t, \mathbf{p}) &= \mathbf{f}_{P \times \Omega_i}^{cv}(t, \mathbf{p}, \omega_i, \mathbf{x}_i^{cv}(t, \mathbf{p}), \mathbf{x}_i^{cc}(t, \mathbf{p})), \\ \dot{\mathbf{x}}_i^{cc}(t, \mathbf{p}) &= \mathbf{f}_{P \times \Omega_i}^{cc}(t, \mathbf{p}, \omega_i, \mathbf{x}_i^{cv}(t, \mathbf{p}), \mathbf{x}_i^{cc}(t, \mathbf{p})), \\ \mathbf{x}_i^{cv}(t_0, \mathbf{p}) &= \mathbf{x}_{0, P \times \Omega_i}^{cv}(\mathbf{p}, \omega_i), \\ \mathbf{x}_i^{cc}(t_0, \mathbf{p}) &= \mathbf{x}_{0, P \times \Omega_i}^{cc}(\mathbf{p}, \omega_i). \end{aligned} \quad (4.22)$$

Moreover, for any $\mathbf{p} \in P$, an upper bound on the optimal objective value of (4.20) restricted to P is given by the value

$$\sum_{i=1}^n \mathbb{P}(\Omega_i) g_{[\mathbf{p}, \mathbf{p}] \times \Omega_i}^{cc}(\mathbf{p}, \omega_i, \mathbf{x}_i^{cv}(t_f, \mathbf{p}), \mathbf{x}_i^{cc}(t_f, \mathbf{p})), \quad (4.23)$$

where $\mathbf{x}_i^{cv}(t, \mathbf{p})$ and $\mathbf{x}_i^{cc}(t, \mathbf{p})$ now denote the unique solutions of the n independent systems of ODEs given for each $i \in \{1, \dots, n\}$ by

$$\begin{aligned} \dot{\mathbf{x}}_i^{cv}(t, \mathbf{p}) &= \mathbf{f}_{[\mathbf{p}, \mathbf{p}] \times \Omega_i}^{cv}(t, \mathbf{p}, \omega_i, \mathbf{x}_i^{cv}(t, \mathbf{p}), \mathbf{x}_i^{cc}(t, \mathbf{p})), \\ \dot{\mathbf{x}}_i^{cc}(t, \mathbf{p}) &= \mathbf{f}_{[\mathbf{p}, \mathbf{p}] \times \Omega_i}^{cc}(t, \mathbf{p}, \omega_i, \mathbf{x}_i^{cv}(t, \mathbf{p}), \mathbf{x}_i^{cc}(t, \mathbf{p})), \\ \mathbf{x}_i^{cv}(t_0, \mathbf{p}) &= \mathbf{x}_{0, [\mathbf{p}, \mathbf{p}] \times \Omega_i}^{cv}(\mathbf{p}, \omega_i), \\ \mathbf{x}_i^{cc}(t_0, \mathbf{p}) &= \mathbf{x}_{0, [\mathbf{p}, \mathbf{p}] \times \Omega_i}^{cc}(\mathbf{p}, \omega_i). \end{aligned} \quad (4.24)$$

Proof. By Theorem 50, a lower bound on the optimal objective value of (4.20) restricted to P is given by the optimal objective value of the convex problem $\min_{\mathbf{p} \in P} \mathcal{G}_{P \times \Phi}^{cv}(\mathbf{p})$. Applying the definitions of $\mathcal{G}_{P \times \Phi}^{cv}$ and $G_{P \times \Omega_i}^{cv}$ from Theorem 46 and Theorem 50, this lower bounding problem is equivalent to (4.21).

For the upper bound, note that \mathbf{p} is feasible in (4.20), so it suffices to bound $\mathcal{G}(\mathbf{p})$. Applying Theorem 50 with the degenerate interval $P = [\mathbf{p}, \mathbf{p}]$, it follows that $\mathcal{G}(\mathbf{p})$ is bounded above by $\mathcal{G}_{[\mathbf{p}, \mathbf{p}] \times \Phi}^{cc}(\mathbf{p})$. Again applying the definitions of $\mathcal{G}_{[\mathbf{p}, \mathbf{p}] \times \Phi}^{cc}$ and $G_{[\mathbf{p}, \mathbf{p}] \times \Omega_i}^{cc}$ from Theorems 46 and 50, this upper bound is equivalent to (4.23). \square

4.6 Numerical Example

The following nonlinear ODEs describe a negative resistance circuit consisting of an inductor, a capacitor, and a resistive element in parallel, where x_1 is the current through the inductor and x_2 is the voltage across the capacitor [105]:

$$\begin{aligned} \dot{x}_1 &= p_1 x_2, \\ \dot{x}_2 &= -p_2(x_1 - x_2 + x_2^3/3), \\ x_{0,1} &= \omega_1, \\ x_{0,2} &= \omega_2. \end{aligned} \tag{4.25}$$

We take the initial conditions to be independent random variables, both following a truncated normal distribution with mean $\mu_1 = \mu_2 = 1$, standard deviation $\sigma_1 = \sigma_2 = 0.1$, and truncation range $\bar{\Omega} = [\mu_1 - 3\sigma_1, \mu_1 + 3\sigma_1] \times [\mu_2 - 3\sigma_2, \mu_2 + 3\sigma_2]$. The parameters p_1 and p_2 are the inverses of the inductance and capacitance, respectively, and are scaled so that (4.25) is dimensionless.

Consider the problem of relaxing the expected-value function $\mathcal{G}(\mathbf{p}) = \mathbb{E}[x_1(t_f, \mathbf{p}, \boldsymbol{\omega})]$ on the set $\mathbf{p} \in P = [0.1, 0.3] \times [0.1, 0.3]$ with $[t_0, t_f] = [0, 5]$. Clearly, this function cannot be evaluated analytically, so standard relaxation techniques are not applicable. To apply

Theorems 46 and 50, we considered interval partitions $\Phi = \{\Omega_i\}_{i=1}^n$ of $\bar{\Omega}$ consisting of 1, 16, and 64 uniform subintervals. We computed relaxations of the initial condition functions and right-hand side functions in (4.25) satisfying Assumption 45 using generalized McCormick relaxations [14] as described in [38]. For every interval $P \times \Omega_i$, the state relaxation system defined in Theorem 46 was solved at the point $(\mathbf{p}, \boldsymbol{\omega}_i) = (\mathbf{p}, \mathbb{E}[\boldsymbol{\omega}|\Omega_i])$ using the code `CVODE` in the Sundials Matlab Toolbox [106] with default tolerances. Finally, relaxations of \mathcal{G} were constructed by summing the resulting relaxations of x_1 at t_f weighted by the probabilities $\mathbb{P}(\Omega_i)$, as described in Theorem 50.

Figure 4.1 shows the resulting convex and concave relaxations, along with several final time solutions of (4.25) computed for random samples of $\boldsymbol{\omega} \in \bar{\Omega}$ and a sample-average approximation of \mathcal{G} computed using 200 samples. Note that the relaxations enclose the true expected value as per Theorem 50, but need not enclose all solutions of (4.25) for sampled $\boldsymbol{\omega} \in \bar{\Omega}$. Figure 4.1 shows that the relaxations become tighter as the partition Φ is refined, but the improvement from 16 to 64 subintervals is minor. This suggests that the proposed method can provide reasonably tight relaxations using fairly coarse partitions of the uncertainty space.

4.7 Conclusions

The main contribution of this chapter is a new approach for computing convex and concave relaxations of nonlinear stochastic optimal control problems with final-time expected-value cost functions. These relaxations can be used to compute rigorous upper and lower bounds on the optimal objective value of such problems restricted to any given subinterval of the decision space, as required for global optimization via spatial branch-and-bound. In this context, the key features of the presented relaxations are: (i) they provide valid bounds on the true objective function, without resorting to discrete approximations of either the expected value or the embedded dynamic model; (ii) they can be computed finitely, even when the objective function itself can only be approximated by sampling or quadrature.

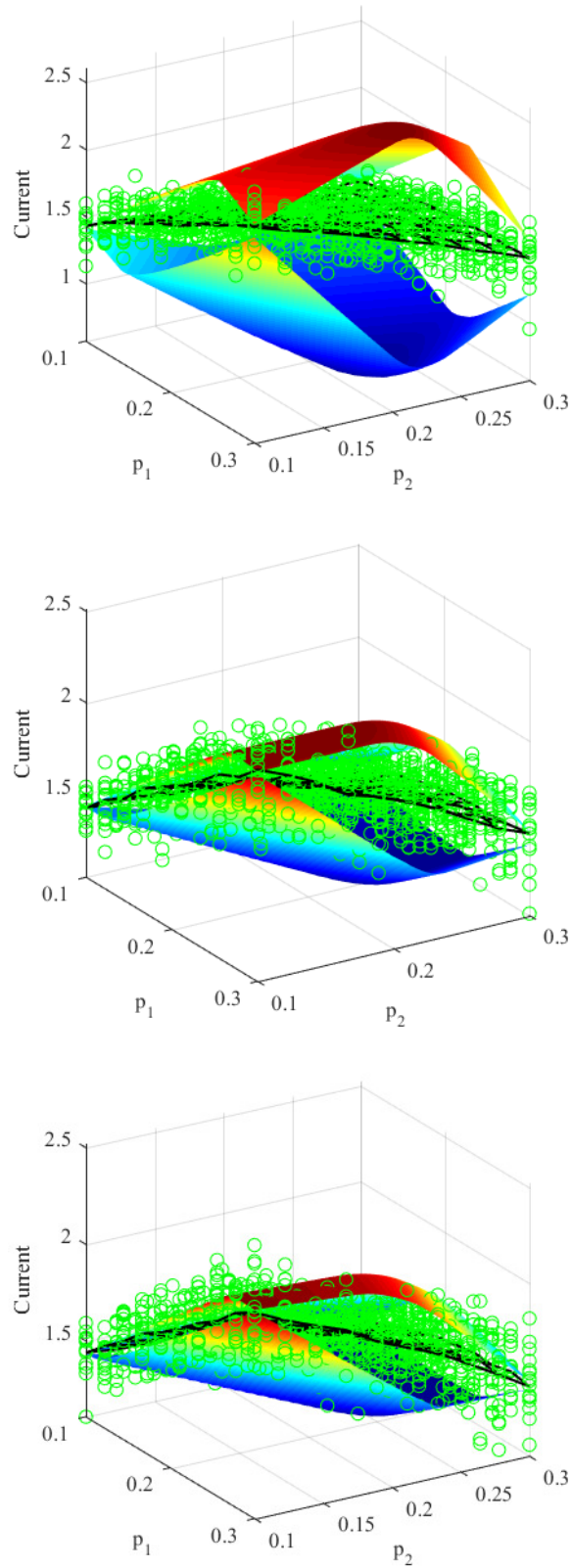


Figure 4.1: Convex and concave relaxations of $\mathcal{G}(\mathbf{p}) = \mathbb{E}[x_1(t_f, \mathbf{p}, \omega)]$ on $P = [0.1, 0.3] \times [0.1, 0.3]$ (shaded surfaces) using partitions of Ω into 1 (top), 16 (middle), and 64 (bottom) uniform subintervals, along with simulated values of $x_1(t_f, \mathbf{p}, \omega)$ at sampled ω values (\circ) and a sample-average approximation of $\mathcal{G}(\mathbf{p})$ using 200 samples (black mesh).

Yet, both of these properties result from the use of an exhaustive partition of the uncertainty space (assumed compact), which limits the applicability of these relaxations to problems with a modest number of random variables. The presented case study suggests that the proposed relaxations can be made tight with a modest partition of the uncertainty space.

CHAPTER 5
EFFICIENT BOUNDS TIGHTENING BASED ON STRENGTHENED SOCP
RELAXATIONS FOR AC OPTIMAL POWER FLOW

5.1 Introduction

This chapter presents an efficient bounds tightening scheme for solving alternating current optimal power flow (ACOPF) problems to global optimality. For a given power network, the ACOPF problem is to determine the real and reactive power outputs of all generators that minimizes cost while meeting demands, satisfying operating constraints, and satisfying the nonconvex steady-state AC power flow equations. ACOPF and its extensions are critical to power grid operations at all scales, including short-term generator dispatching, day-ahead unit commitment, and long term network design and expansion planning [1, 6]. However, due to the size and complexity of ACOPF for realistic power networks, grid operations are much more commonly based on linear approximations [7], resulting in solutions that are (after some post-processing) feasible but potentially highly suboptimal. Indeed, the Energy Information Agency estimates that the ability to globally solve practical ACOPF problems could save the US billions of dollars annually [1].

Existing ACOPF algorithms can be roughly categorized into three groups: local methods, convex relaxation methods, and global methods. Local methods aim to find a local solution or stationary point of ACOPF, with Newton-Raphson and interior point methods being the most popular [55, 6]. The primary advantage of these methods is efficiency. Surprisingly, they also locate globally optimal solutions for many test problems, and this is not well understood. However, in general, they are not guaranteed to find global or even feasible solutions.

Convex relaxation approaches aim to find a provably global or near-global solution of

ACOPF by solving a single highly accurate convex relaxation [6]. A solution of any convex relaxation provides a lower bound on the optimal objective value. Thus, assuming a local solution is available, solving a convex relaxation leads to one of the following outcomes:

- (i) The solution of the relaxation is feasible in ACOPF. Assuming that ACOPF and its relaxation have the same objective functions, which is typical, it follows that the solution of the relaxation is a global solution of ACOPF.
- (ii) The relaxation furnishes a tight lower bound that differs from the objective value of the known local solution by less than a specified tolerance ϵ . This ensures that the local solution is an ϵ -global solution of ACOPF.
- (iii) Neither (i) or (ii) occur and nothing can be concluded about either solution.

Although there is no guarantee that (i) or (ii) will occur, this approach has been popularized by the observation that semi-definite programming (SDP) relaxations of ACOPF satisfy (ii) with relative tolerances of $\sim 2\%$ or less for many standard test problems, and often satisfy (i) (e.g., see comparisons in [51]). In fact, SDP relaxations have been proven to satisfy (i) in a number of special cases including acyclic networks and cyclic networks with relaxed angle constraints [56, 107, 57]. However, these conditions are often not met in practice. Thus, a major limitation of this approach is that it can lead to outcome (iii). In principle, outcome (iii) can be eliminated using successively tighter relaxations in the Lasserre hierarchy, but this quickly becomes intractable [108]. Other strategies attempt to find a feasible point near the solution of the relaxation using projection or penalization terms [56, 109, 57]. If this point is better than the known local solution, then outcome (ii) becomes more likely, but it will still fail if the original relaxation is not tight enough. Another significant drawback is that solving SDP relaxations is computationally demanding. This can be mitigated for sparse networks using chordal decomposition techniques [110], but even these are limiting for networks of practical interest. This has led to the development of more efficiently solvable convex relaxations of ACOPF based on second-order

cone programming (SOCP) [50, 51, 52] and quadratic programming (QP) [53, 54]. However, SOCP and QP relaxations are typically weaker than SDP, making outcomes (i)–(ii) much less likely.

In contrast to convex relaxation methods, global methods solve potentially many ACOPF relaxations within an iterative procedure that is guaranteed to locate an ϵ -global solution in finite time, such as spatial branch-and-bound (sBB) or nonconvex outer-approximation with piecewise convex relaxations [58, 52, 59]. The key challenge for global methods is that practical ACOPF problems involve hundreds of thousands of variables, making exhaustive branching or piecewise relaxation impractical. However, it has been shown that optimization-based bounds tightening (OBBT) closes the optimality gap for many nontrivial test problems with little or no branching [60, 59, 61]. OBBT is a domain reduction technique typically used within sBB whereby the upper and lower bounds on each decision variable are tightened by solving a pair of min and max problems over the relaxed feasible set. This reduces the domain over which further branching or piecewise relaxation is required and also tightens the relaxation. However, OBBT requires solving two convex relaxations per tightened variable in each iteration, which is prohibitive for large problems. A fast closed-form bounds tightening scheme was developed in [62], but the bounds do not result in competitive optimality gaps even with branching. Thus, while bounds-tightening has high potential for enabling the global solution of ACOPF problems, existing OBBT methods are too costly and existing closed-form methods are too conservative.

This chapter makes three new contributions towards the global solution of ACOPF. Beginning with the formulation in [111, 112], which is the basis for all SOCP relaxations, we first prove the equivalence of replacing the nonconvex voltage angle constraints with a smaller set of nonconvex constraints based on a cycle basis for the network. A nearly identical reformulation was first proposed in [51], but was only proven to be a relaxation. Here, we impose additional linear constraints and establish equivalence. Second, we develop a new strengthened SOCP relaxation based on this reformulation. This relaxation is similar

to the strong SOCP relaxations in [51, 52]. However, we relax the cycle basis constraints differently and we add the reverse cone cuts from [52] for only a subset of buses that is adaptively generated. Third, using this relaxation, we present a new OBBT scheme that performs bounds tightening on only a select subset of variables. Among existing OBBT methods, the one that achieves the smallest optimality gaps on standard ACOPF test sets performs bounds tightening on all variables that appear in nonconvex terms [60]. Conversely, approaches that perform OBBT on only a subset of variables exhibit significantly larger gaps [52] (although there are also differences in the relaxations used). In contrast, our results for NESTA benchmarks show that performing OBBT on a small subset of the variables in our new relaxation almost always achieves a gap at least as small as the best known OBBT method while also being significantly more efficient.

5.2 AC Optimal Power Flow

Let $\mathcal{N} = (\mathcal{B}, \mathcal{A})$ be a connected, undirected graph where \mathcal{B} is the set of buses and, for any connected $b, n \in \mathcal{B}$, either $(b, n) \in \mathcal{A}$ or $(n, b) \in \mathcal{A}$, but not both. Let \mathcal{G} be the set of generators and \mathcal{G}_b the set of generators connected to bus b . For each transmission line l connecting buses $(i, j) \in \mathcal{A}$, let \mathcal{K} be the set of three-tuples containing both (l, i, j) and (l, j, i) . For every $(l, i, j) \in \mathcal{K}$, $p_{l,i,j}$ and $q_{l,i,j}$ denote the real and reactive power on line l connecting buses i and j , as measured on the i end of the line, whereas $p_{l,j,i}$ and $q_{l,j,i}$ denote the same quantities as measured at the j end. These are different because of line losses and the standard sign convention that $p_{l,i,j}$ is positive if power is leaving bus i via line l . Define $\mathcal{K}_b = \{(l, i, j) \in \mathcal{K} : i = b\}$, which indexes all quantities on lines connected to bus b as measured at the b end. We consider the following ACOPF formulation, where upper-case symbols are parameters and lower-case symbols are decision variables with the exception of the bounds in (5.8)–(5.10) and (5.14):

$$\min \sum_{g \in \mathcal{G}} [A_g^2 (p_g^G)^2 + A_g^1 p_g^G + A_g^0] \quad (5.1)$$

subject to

$$\sum_{g \in \mathcal{G}_b} p_g^G - \sum_{(l,i,j) \in \mathcal{K}_b} p_{l,i,j} = P_b^L + G_b^{Sh} w_b, \quad \forall b \in \mathcal{B} \quad (5.2)$$

$$\sum_{g \in \mathcal{G}_b} q_g^G - \sum_{(l,i,j) \in \mathcal{K}_b} q_{l,i,j} = Q_b^L - B_b^{Sh} w_b, \quad \forall b \in \mathcal{B} \quad (5.3)$$

$$p_{l,b,n} = E_{l,b,n}^{w,p} w_b + E_{l,b,n}^{c,p} c_{b,n} + E_{l,b,n}^{s,p} s_{b,n}, \quad (5.4)$$

$$q_{l,b,n} = E_{l,b,n}^{w,q} w_b + E_{l,b,n}^{c,q} c_{b,n} + E_{l,b,n}^{s,q} s_{b,n}, \quad \forall (l, b, n) \in \mathcal{K}$$

$$p_{l,b,n}^2 + q_{l,b,n}^2 \leq (S_l^{\max})^2, \quad \forall (l, b, n) \in \mathcal{K} \quad (5.5)$$

$$P_g^{G,\min} \leq p_g^G \leq P_g^{G,\max}, \quad \forall g \in \mathcal{G} \quad (5.6)$$

$$Q_g^{G,\min} \leq q_g^G \leq Q_g^{G,\max}, \quad \forall g \in \mathcal{G} \quad (5.7)$$

$$w_b^L \leq w_b \leq w_b^U, \quad \forall b \in \mathcal{B} \quad (5.8)$$

$$c_{b,n}^L \leq c_{b,n} \leq c_{b,n}^U, \quad \forall (b, n) \in \mathcal{A} \quad (5.9)$$

$$s_{b,n}^L \leq s_{b,n} \leq s_{b,n}^U, \quad \forall (b, n) \in \mathcal{A} \quad (5.10)$$

$$c_{b,n} = c_{n,b}, \quad s_{b,n} = -s_{n,b}, \quad \forall (b, n) \in \mathcal{A} \quad (5.11)$$

$$c_{b,n}^2 + s_{b,n}^2 = w_b w_n, \quad \forall (b, n) \in \mathcal{A} \quad (5.12)$$

$$\theta_n - \theta_b = \arctan \left(\frac{s_{b,n}}{c_{b,n}} \right), \quad \forall (b, n) \in \mathcal{A} \quad (5.13)$$

$$\theta_{b,n}^L \leq \theta_n - \theta_b \leq \theta_{b,n}^U, \quad \forall (b, n) \in \mathcal{A} \quad (5.14)$$

This formulation was proposed without (5.13)–(5.14) for radial networks in [113, 50] and extended to general networks in [111, 112]. The phase angle of bus b is θ_b and the real and reactive powers from generator g are p_g^G and q_g^G , respectively. The variables $c_{b,n}$,

$s_{b,n}$, and w_b are related to complex bus voltages. Specifically, for any feasible solution of (5.1)–(5.14), there exist complex voltages $v_b \in \mathbb{C}$, $\forall b \in \mathcal{B}$, that are feasible in the standard rectangular ACOPF model [60] and satisfy $c_{b,n} + js_{b,n} = v_b^* v_n$, $w_b = |v_b|^2$, and $\theta_n - \theta_b = \angle(v_b^* v_n)$, $\forall (b, n) \in \mathcal{B} \times \mathcal{B}$. It follows that $c_{b,n} = \sqrt{w_b w_n} \cos(\theta_n - \theta_b)$ and $s_{b,n} = \sqrt{w_b w_n} \sin(\theta_n - \theta_b)$. We assume that the angle difference bounds $[\theta_{b,n}^L, \theta_{b,n}^U]$ are strictly contained in $[-\pi/2, \pi/2]$ and the voltage magnitude bounds satisfy $V_b^{\min} > 0$. The bounds in (5.8)–(5.10) are then calculated as:

$$\begin{aligned}
w_b^L &= (V_b^{\min})^2, & w_b^U &= (V_b^{\max})^2, \\
c_{b,n}^L &= V_b^{\min} V_n^{\min} \cos(\max(|\theta_{b,n}^L|, |\theta_{b,n}^U|)), \\
c_{b,n}^U &= V_b^{\max} V_n^{\max} \cos(\text{mid}(0, \theta_{b,n}^L, \theta_{b,n}^U)), \\
s_{b,n}^L &= \begin{cases} V_b^{\min} V_n^{\min} \sin(\theta_{b,n}^L), & \text{if } \theta_{b,n}^L \geq 0, \\ V_b^{\max} V_n^{\max} \sin(\theta_{b,n}^L), & \text{otherwise,} \end{cases} \\
s_{b,n}^U &= \begin{cases} V_b^{\max} V_n^{\max} \sin(\theta_{b,n}^U), & \text{if } \theta_{b,n}^U \geq 0, \\ V_b^{\min} V_n^{\min} \sin(\theta_{b,n}^U), & \text{otherwise.} \end{cases}
\end{aligned} \tag{5.15}$$

The assumptions on $[\theta_{b,n}^L, \theta_{b,n}^U]$ and V_b^{\min} imply that $c_{b,n}^L > 0$, so (5.13) is well-defined at all feasible points.

Although $c_{b,n}$ and $s_{b,n}$ are indexed by $\mathcal{B} \times \mathcal{B}$ above, constraint (5.11) can be used to eliminate half of these variables, keeping only those with $(b, n) \in \mathcal{A}$. This is done in our numerical implementation. By arbitrarily ordering the elements of \mathcal{B} and \mathcal{A} , sets of variables indexed by \mathcal{B} and \mathcal{A} can be viewed as vectors; i.e., $\boldsymbol{\theta} = \{\theta_b\}_{b \in \mathcal{B}} \in \mathbb{R}^{|\mathcal{B}|}$ and $\mathbf{s} = \{s_{b,n}\}_{(b,n) \in \mathcal{A}} \in \mathbb{R}^{|\mathcal{A}|}$. We assume a fixed ordering and use this shorthand henceforth.

The objective of this chapter is to develop effective bounds tightening algorithms for (5.1)–(5.14). These are based on a new strengthened SOCP relaxation developed next.

5.3 Strengthened SOCP Relaxation

The basic SOCP relaxation of (5.1)–(5.14) is obtained by removing nonconvex constraints (5.13), constraints (5.14) and relaxing the nonconvex equality (5.12) to the inequality

$$c_{b,n}^2 + s_{b,n}^2 \leq w_b w_n, \quad \forall (b, n) \in \mathcal{A}. \quad (5.16)$$

Although SOCPs can be solved very efficiently, using the standard SOCP relaxation for OBBT results in large optimality gaps (e.g., significantly worse than SDP [52]). This section presents a new strengthened SOCP relaxation that is significantly tighter but still efficiently solvable. Strengthened SOCP relaxations have previously been proposed in [51, 52, 60]. In [60], the SOCP relaxation is strengthened by adding a large number of additional variables and cuts derived from the rectangular ACOPF formulation, which leads to much tighter optimality gaps but also makes OBBT much more expensive. In [51], the basic SOCP relaxation is strengthened by reformulating (5.13) in terms of a cycle basis and using several new methods for relaxing this reformulation. Additional cuts derived from the solutions of auxiliary SDPs were also added. However, OBBT was not performed. In [52], the relaxation from [51] was further strengthened using so-called reverse cone cuts and matrix minor cuts. These relaxations were then used in a spatial branch-and-bound algorithm with OBBT in each node. However, OBBT was only performed on a subset of the problem variables, and OBBT results in the root node (i.e., without branching) were not competitive with state-of-the-art OBBT methods [61, 60].

The strengthened SOCP relaxation presented here is similar to those in [51, 52]. First, we reformulate (5.13) in terms of a cycle basis as in [51]. In [51], this is only shown to be a relaxation of the original problem. In contrast, we add further linear cuts and prove that these make the reformulation equivalent. Next, we relax the reformulated constraints in a way that is different and simpler than in [51]. We also add the reverse cone cuts from [52], but omit the matrix minor and SDP cuts. Finally, we implement the reverse cone cuts on

only a subset of buses that is determined adaptively within the proposed bounds tightening algorithms. These modifications result in a smaller optimization problem that can be solved more efficiently.

5.3.1 Equivalent Reformulation of ACOPF

This section presents a reformulation of the angle constraints (5.13) in terms of a cycle basis for $\mathcal{N} = (\mathcal{B}, \mathcal{A})$ following the original ideas in [51]. Although \mathcal{N} is undirected, the notion of a *directed cycle* of \mathcal{N} is useful for writing the reformulation with correct signs. A nonzero vector $\mathbf{v} \equiv \{v_{b,n}\}_{(b,n) \in \mathcal{A}} \in \mathbb{R}^{|\mathcal{A}|}$ is a *directed cycle* of \mathcal{N} if

$$\sum_{b:(b,n) \in \mathcal{A}} v_{b,n} - \sum_{b:(n,b) \in \mathcal{A}} v_{n,b} = 0, \quad \forall n \in \mathcal{B}. \quad (5.17)$$

The *support* of \mathbf{v} , denoted $\mathcal{A}_{\mathbf{v}} \equiv \text{supp}(\mathbf{v})$, is the set of edges $(b, n) \in \mathcal{A}$ such that $v_{b,n} \neq 0$. A directed cycle \mathbf{v} is called a *directed circuit* if $v_{b,n} \in \{-1, 0, 1\}, \forall (b, n) \in \mathcal{A}$. The *directed cycle space* of \mathcal{N} , which is a linear subspace of $\mathbb{R}^{|\mathcal{A}|}$, is

$$\mathcal{S} \equiv \{\mathbf{v} \in \mathbb{R}^{|\mathcal{A}|} : \mathbf{v} \text{ is a directed cycle of } \mathcal{N}\}. \quad (5.18)$$

Finally, $\mathcal{C} \equiv \{\mathbf{v}_1, \dots, \mathbf{v}_v\}$ is a *directed cycle basis* for \mathcal{N} if each \mathbf{v}_i is a directed circuit and $\mathbf{v}_1, \dots, \mathbf{v}_v$ is a basis for \mathcal{S} .

Lemma 52. *There exists a directed cycle basis \mathcal{C} for $\mathcal{N} = (\mathcal{B}, \mathcal{A})$ and the number of directed cycles in \mathcal{C} is*

$$|\mathcal{C}| = |\mathcal{A}| - |\mathcal{B}| + 1. \quad (5.19)$$

Proof. Existence is shown on p. 202 of [114]. Theorem 2.3 in [114] with $\kappa = \mathbb{R}$ shows that $|\mathcal{C}| = |\mathcal{A}| - |\mathcal{B}| + cc$, where cc is the number of connected components of \mathcal{N} . Since \mathcal{N} is connected by assumption, $cc = 1$. \square

Next, we formalize the observation in [51] that the angle differences in (5.13) sum to zero over cycles.

Lemma 53. *For any directed cycle \mathbf{v} of \mathcal{N} and any vector $\boldsymbol{\theta} = \{\theta_b\}_{b \in \mathcal{B}} \in \mathbb{R}^{|\mathcal{B}|}$,*

$$\sum_{(b,n) \in \mathcal{A}} v_{b,n}(\theta_n - \theta_b) = \sum_{(b,n) \in \mathcal{A}_{\mathbf{v}}} v_{b,n}(\theta_n - \theta_b) = 0. \quad (5.20)$$

Proof. The first equality holds because $v_{b,n} = 0$ for all $(b, n) \notin \mathcal{A}_{\mathbf{v}}$. To prove the second, we first multiply (5.17) by θ_n and sum over $n \in \mathcal{B}$ to obtain

$$\sum_{n \in \mathcal{B}} \left(\sum_{b: (b,n) \in \mathcal{A}} v_{b,n} - \sum_{b: (n,b) \in \mathcal{A}} v_{n,b} \right) \theta_n = 0. \quad (5.21)$$

Choose any fixed $(l, k) \in \mathcal{A}$ and note that $(l, k) \in \mathcal{A}$ implies $(k, l) \notin \mathcal{A}$. Therefore, the sum above has exactly two terms corresponding to (l, k) . The first occurs when $n = l$ and $b = k$ and evaluates to $-v_{l,k}\theta_l$. The second occurs when $n = k$ and $b = l$ and evaluates to $v_{l,k}\theta_k$. Therefore, (5.21) can be rewritten as $\sum_{(l,k) \in \mathcal{A}} v_{l,k}(\theta_k - \theta_l) = 0$, which is the desired result. \square

Given a directed cycle basis \mathcal{C} , our proposed reformulation of (5.1)–(5.14) is to remove the decision variables $\{\theta_b\}_{b \in \mathcal{B}}$, add new decision variables $\{\theta_{b,n}\}_{(b,n) \in \mathcal{A}_{\mathbf{v}}, \mathbf{v} \in \mathcal{C}}$, and replace the constraints (5.13)–(5.14) with

$$\theta_{b,n} = \arctan\left(\frac{s_{b,n}}{c_{b,n}}\right), \quad \forall (b, n) \in \mathcal{A}_{\mathbf{v}}, \forall \mathbf{v} \in \mathcal{C}, \quad (5.22)$$

$$\sum_{(b,n) \in \mathcal{A}_{\mathbf{v}}} v_{b,n} \theta_{b,n} = 0, \quad \forall \mathbf{v} \in \mathcal{C}, \quad (5.23)$$

$$c_{b,n} \tan(\theta_{b,n}^L) \leq s_{b,n} \leq c_{b,n} \tan(\theta_{b,n}^U), \quad \forall (b, n) \in \mathcal{A}. \quad (5.24)$$

Compared to (5.1)–(5.14), this has the distinct advantage of only requiring the nonconvex term $\arctan(s_{b,n}/c_{b,n})$ for edges that appear in the cycle basis, which is often a small

fraction of the total edges. It was argued in [51] that replacing (5.13)–(5.14) with only (5.22)–(5.23) is a (nonconvex) relaxation of (5.1)–(5.14). We now prove that adding (5.24) leads to an equivalent reformulation.

Theorem 54. *For any feasible solution of the reformulation (5.1)–(5.12), (5.22)–(5.24) with components $\{\theta_{b,n}\}_{(b,n) \in \mathcal{A}_v, v \in \mathcal{C}}$, $\mathbf{c} = \{c_{b,n}\}_{(b,n) \in \mathcal{A}}$, and $\mathbf{s} = \{s_{b,n}\}_{(b,n) \in \mathcal{A}}$, and any choice of reference bus $r \in \mathcal{B}$, there exists exactly one complete set of bus angles $\boldsymbol{\theta} = \{\theta_b\}_{b \in \mathcal{B}}$ such that:*

1. $\theta_{b,n} = \theta_n - \theta_b, \forall (b, n) \in \mathcal{A}_v, \forall v \in \mathcal{C}$,
2. $\theta_r = 0$,
3. (5.13)–(5.14) holds for all $(b, n) \in \mathcal{A}$.

Proof. Let $\mathbf{A}\boldsymbol{\theta} = \mathbf{b}$ denote the following linear system, where $\mathbf{A} \in \mathbb{R}^{(|\mathcal{A}|+1) \times |\mathcal{B}|}$, $\mathbf{b} \in \mathbb{R}^{|\mathcal{A}|+1}$, the equations in (5.25) are ordered according to the fixed ordering of \mathcal{A} assumed in Section 5.2, and (5.26) is the last equation:

$$\theta_n - \theta_b = \arctan\left(\frac{s_{b,n}}{c_{b,n}}\right), \forall (b, n) \in \mathcal{A}, \quad (5.25)$$

$$\theta_r = 0. \quad (5.26)$$

We will prove that this system has a unique solution. For each $v_i \in \mathcal{C}$, let $\mathbf{u}_i = (v_i, 0) \in \mathbb{R}^{|\mathcal{A}|+1}$. We first prove that:

- (i.) \mathbf{b} is orthogonal to $\mathbf{u}_i, \forall i \in \{1, \dots, v\}$.
- (ii.) \mathbf{u}_i is in the left nullspace of $\mathbf{A}, \mathcal{N}_L(\mathbf{A}), \forall i \in \{1, \dots, v\}$.
- (iii.) The nullspace of $\mathbf{A}, \mathcal{N}(\mathbf{A})$, has dimension zero.

By the definitions \mathbf{u}_i and \mathbf{b} ,

$$\mathbf{u}_i^T \mathbf{b} = \sum_{(b,n) \in \mathcal{A}_{\mathbf{v}_i}} v_{i,(b,n)} \arctan \left(\frac{s_{b,n}}{c_{b,n}} \right). \quad (5.27)$$

But this is zero by (5.22)–(5.23), so \mathbf{u}_i is orthogonal to \mathbf{b} .

To see that $\mathbf{u}_i \in \mathcal{N}_L(\mathbf{A})$, note that, for any $\boldsymbol{\theta} \in \mathbb{R}^{|\mathcal{B}|}$,

$$\mathbf{u}_i^T \mathbf{A} \boldsymbol{\theta} = \sum_{(b,n) \in \mathcal{A}} v_{i,(b,n)} (\theta_n - \theta_b). \quad (5.28)$$

But this is zero by Lemma 53, and since it holds for any $\boldsymbol{\theta}$, it follows that $\mathbf{u}_i^T \mathbf{A} = \mathbf{0}$.

To show that $\mathcal{N}(\mathbf{A}) = \{\mathbf{0}\}$, let $\boldsymbol{\lambda} \in \mathbb{R}^{|\mathcal{B}|}$ be any vector such that $\mathbf{A} \boldsymbol{\lambda} = \mathbf{0}$. From (5.26), the last row of \mathbf{A} has only a single nonzero element in column r . Therefore, $\mathbf{A} \boldsymbol{\lambda} = \mathbf{0}$ implies that $\lambda_r = 0$. Let $r' \in \mathcal{B}$ be any neighbor of r , so that either $(r, r') \in \mathcal{A}$ or $(r', r) \in \mathcal{A}$. Then, the row of $\mathbf{A} \boldsymbol{\lambda} = \mathbf{0}$ corresponding to the pair (r, r') (or (r', r)) gives $\lambda_{r'} - \lambda_r = 0$ (or $\lambda_r - \lambda_{r'} = 0$), which implies that $\lambda_{r'} = 0$. By the same argument, we also have $\lambda_{r''} = 0$ for any neighbor of r' . Because \mathcal{N} is a connected graph, it follows by induction that $\boldsymbol{\lambda} = \mathbf{0}$. Since $\boldsymbol{\lambda}$ was chosen arbitrarily, $\mathcal{N}(\mathbf{A}) = \{\mathbf{0}\}$.

We now prove that $\mathbf{A} \boldsymbol{\theta} = \mathbf{b}$ has a unique solution. Since $\mathcal{N}(\mathbf{A})$ is the orthogonal complement of the row space of \mathbf{A} in $\mathbb{R}^{|\mathcal{B}|}$ and $\dim(\mathcal{N}(\mathbf{A})) = 0$, \mathbf{A} has $|\mathcal{B}|$ linearly independent rows. It follows that \mathbf{A} also has $|\mathcal{B}|$ linearly independent columns, and hence $\dim(\mathcal{R}(\mathbf{A})) = |\mathcal{B}|$. Since $\mathcal{N}_L(\mathbf{A})$ is the orthogonal complement of $\mathcal{R}(\mathbf{A})$ in $\mathbb{R}^{|\mathcal{A}|+1}$, $\dim(\mathcal{N}_L(\mathbf{A})) = |\mathcal{A}| + 1 - |\mathcal{B}|$. Thus, by Lemma 52, $\dim(\mathcal{N}_L(\mathbf{A})) = |\mathcal{C}| = v$. Since $\{\mathbf{v}_1, \dots, \mathbf{v}_v\}$ is linearly independent, so is $\{\mathbf{u}_1, \dots, \mathbf{u}_v\}$. Since each \mathbf{u}_i is in $\mathcal{N}_L(\mathbf{A})$, $\{\mathbf{u}_1, \dots, \mathbf{u}_v\}$ must be a basis for $\mathcal{N}_L(\mathbf{A})$. Then, since \mathbf{b} is orthogonal to each \mathbf{u}_i , $\mathbf{b} \in \mathcal{R}(\mathbf{A})$. It follows that $\mathbf{A} \boldsymbol{\theta} = \mathbf{b}$ has at least one solution. Uniqueness follows from $\mathcal{N}(\mathbf{A}) = \{\mathbf{0}\}$.

We now show that the solution of $\mathbf{A} \boldsymbol{\theta} = \mathbf{b}$ satisfies Conclusions 1–3. Conclusions 1–2

follow readily from (5.22), (5.25), and (5.26). By (5.25), (5.13) holds for all $(b, n) \in \mathcal{A}$. Finally, by (5.24) and the fact that $c_{b,n} \geq c_{b,n}^L > 0$,

$$\begin{aligned}
c_{b,n} \tan(\theta_{b,n}^L) &\leq s_{b,n} \leq c_{b,n} \tan(\theta_{b,n}^U), & (5.29) \\
\iff \tan(\theta_{b,n}^L) &\leq \frac{s_{b,n}}{c_{b,n}} \leq \tan(\theta_{b,n}^U), \\
\iff \theta_{b,n}^L &\leq \arctan\left(\frac{s_{b,n}}{c_{b,n}}\right) \leq \theta_{b,n}^U, \\
\iff \theta_{b,n}^L &\leq \theta_n - \theta_b \leq \theta_{b,n}^U \text{ (by (5.25))}.
\end{aligned}$$

Thus, (5.14) holds for all $(b, n) \in \mathcal{A}$, so Conclusion 3 holds. \square

Theorem 55. *The ACOPF reformulation (5.1)–(5.12), (5.22)–(5.24) is equivalent to the original ACOPF formulation (5.1)–(5.14).*

Proof. Given any feasible point of (5.1)–(5.12), (5.22)–(5.24), replacing $\{\theta_{b,n}\}_{(b,n) \in \mathcal{A}_v, v \in \mathcal{C}}$ with any $\{\theta_b\}_{b \in \mathcal{B}}$ satisfying Theorem 54 (i.e., with any choice of r) gives a feasible point of the original formulation (5.1)–(5.14) with the same objective value. Conversely, choose any feasible point of the original formulation and define $\theta_{b,n} = \theta_n - \theta_b, \forall (b, n) \in \mathcal{A}_v, v \in \mathcal{C}$. Then, (5.13) implies that $\theta_{b,n}$ satisfies (5.22) and Lemma 53 implies that $\theta_{b,n}$ satisfies (5.23). Finally, by the chain of implications in (5.29), (5.13)–(5.14) imply (5.24). Therefore, this defines a feasible point of (5.1)–(5.12), (5.22)–(5.24) with the same objective value. Thus, the two formulations are equivalent. \square

Remark 56. Some codes for computing cycle bases return an *undirected* cycle basis $\mathcal{N}_1, \dots, \mathcal{N}_v$ composed of undirected cycles $\mathcal{N}_v = (\mathcal{B}_v, \mathcal{A}_v)$ (see [114] for formal definitions). Since each \mathcal{N}_v is an Eulerian subgraph, there is a closed traversal of \mathcal{N}_v of the form $((b_1, b_2), (b_2, b_3), \dots, (b_k, b_1))$. In fact, the software used here describes each \mathcal{N}_v by the corresponding list of vertices (b_1, b_2, \dots, b_k) [115]. From this traversal, a corresponding

directed cycle \mathbf{v} can be obtained by

$$v_{b,n} = \begin{cases} 1 & \text{if } (b, n) \text{ is in the traversal of } \mathcal{N}_{\mathbf{v}}, \\ -1 & \text{if } (n, b) \text{ is in the traversal of } \mathcal{N}_{\mathbf{v}}, \\ 0 & \text{otherwise.} \end{cases}$$

$\forall (b, n) \in \mathcal{A}$. By Lemma 2.4 in [114], if $\{\mathcal{N}_1, \dots, \mathcal{N}_v\}$ is an undirected cycle basis for \mathcal{N} and \mathbf{v}_i is obtained from each \mathcal{N}_i in this way, then $\{\mathbf{v}_1, \dots, \mathbf{v}_v\}$ is a directed cycle basis for \mathcal{N} .

5.3.2 Cycle-Based Relaxation

We now formulate a convex piecewise linear relaxation of the constraints (5.22). To do so, we introduce a new auxiliary variable $sc.inv_{b,n}$ for all $(b, n) \in \mathcal{A}_{\mathbf{v}}$, $\forall \mathbf{v} \in \mathcal{C}$, and rewrite (5.22) as the pair of constraints $\theta_{b,n} = \arctan(sc.inv_{b,n})$ and $s_{b,n} = c_{b,n} \times sc.inv_{b,n}$. Next, these constraints are relaxed by

$$(s_{b,n}, c_{b,n}, sc.inv_{b,n}) \in \mathbf{MC}[s_{b,n} = c_{b,n} \times sc.inv_{b,n}], \quad (5.30)$$

$$(sc.inv_{b,n}, \theta_{b,n}) \in \mathbf{Rel}[\theta_{b,n} = \arctan(sc.inv_{b,n})], \quad (5.31)$$

where $\mathbf{MC}[w = xy]$ denotes the standard linear McCormick envelop of the set $\{(x, y, w) : w = xy, x \in [x^L, x^U], y \in [y^L, y^U]\}$ [13] and $\mathbf{Rel}[w = \arctan(x)]$ denotes a convex enclosure of the set $\{(x, w) : w = \arctan(x), x \in [x^L, x^U]\}$. The latter enclosure takes the form $\{w : u(x) \leq w \leq o(x), x \in [x^L, x^U]\}$ where u and o are convex and concave relaxations of \arctan on $[x^L, x^U]$, respectively.

To define u and o , first consider the case where $x^L \geq 0$, which implies that \arctan is concave on $[x^L, x^U]$ (see Figure 5.1 left). In this case, the convex envelope u is the secant between x^L and x^U , and we create a concave overestimator o using two linear cuts derived by linearizing \arctan at x^L and x^U . Recall that the derivative of $\arctan(x)$ is $\frac{1}{1+x^2}$. These

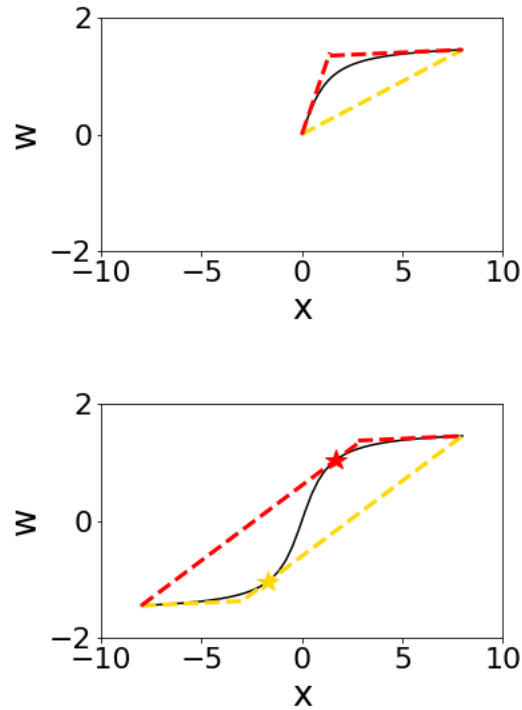


Figure 5.1: Convex (gold dashed) and concave (red dashed) relaxations of $\arctan(x)$ (black solid) for $x \in [0, 8]$ (left) and $x \in [-8, 8]$ (right). The gold star indicates x_*^L and the red star indicates x_*^U .

relaxations are given below and shown in Figure 5.1:

$$u(x) = \frac{\arctan(x^U) - \arctan(x^L)}{x^U - x^L}(x - x^L) + \arctan(x^L),$$

$$o(x) = \min \left\{ \frac{1}{1 + (x^L)^2}(x - x^L) + \arctan(x^L), \right. \\ \left. \frac{1}{1 + (x^U)^2}(x - x^U) + \arctan(x^U) \right\}.$$

Next consider $x^U \leq 0$, in which case \arctan is concave on $[x^L, x^U]$. By analogy to the first case, we define o as the secant between x^L and x^U and u as the max of two linear cuts derived by linearizing \arctan at x^L and x^U .

Finally, consider the case $0 \in (x^L, x^U)$. To define u , we first locate the point $x_*^L \in (-\infty, 0]$ such that the secant between x^U and x_*^L has the same slope as \arctan at x_*^L (gold

star in Figure 5.1). This point is the unique solution in $(-\infty, 0]$ of

$$\frac{\arctan(x^U) - \arctan(x)}{x^U - x} - \frac{1}{1 + x^2} = 0. \quad (5.32)$$

If $x^L \leq x_*^L$, then we define u as the maximum of two linear cuts. The first is the secant between x_*^L and x^U . It can be shown that this is the tightest linear underestimator on $[x^L, x^U]$ that agrees with \arctan at x^U . However, it is potentially weak near x^L , so we strengthen it by adding the linearization of \arctan at x^L (see Figure 5.1). Since \arctan is convex on $(-\infty, 0]$, this linearization is an underestimator on $[x^L, 0]$. Moreover, since both \arctan and its slope are monotonically increasing on $[x^L, 0]$ and $x < x_*^L$, it can be shown that the linearization is dominated by the secant between x_*^L and x^U on $[x_*^L, x^U]$, and hence on $[0, x^U]$. Therefore, this linearization is an underestimator on all of $[x^L, x^U]$ and we set

$$u(x) = \max \left\{ \frac{1}{1 + (x^L)^2} (x - x^L) + \arctan(x^L), \frac{\arctan(x^U) - \arctan(x_*^L)}{x^U - x_*^L} (x - x_*^L) + \arctan(x_*^L) \right\}.$$

If instead $x^L > x_*^L$, then we define u as the secant between x^L and x^U . Although \arctan is not concave on $[x^L, x^U]$, this secant can be proven to underestimate \arctan on $[x^L, x^U]$ using the fact the slope of \arctan is monotonically increasing and decreasing on the positive and negative domains, respectively.

Similarly, to define u when $0 \in (x^L, x^U)$, we first locate the unique point $x_*^U \in [0, +\infty)$ such that the secant between x^L and x_*^U has the same slope as \arctan at x_*^U (red star in Figure 5.1). If $x^U \geq x_*^U$, then we define o as the minimum of two linear cuts. The first is the secant between x^L and x_*^U , and the second is the linearization of \arctan at x^U (see Figure 5.1). Otherwise, we define o as the secant between x^L and x^U . In all cases, the min and max functions in u and o are implemented using two linear cuts.

5.3.3 Reverse Cone Cuts

The standard SOCP relaxation replaces the nonconvex equality constraint (5.12) by the inequality (5.16). Although this enables the use of efficient SOCP solvers, it loses the information contained in the nonconvex *reverse cone constraint*,

$$c_{b,n}^2 + s_{b,n}^2 \geq w_b w_n, \quad \forall (b, n) \in \mathcal{A}. \quad (5.33)$$

To address this, we further enhance our relaxation by adding the so-called *reverse cone cuts* from [52], which we denote by $\text{LP}[c_{b,n}^2 + s_{b,n}^2 \geq w_b w_n]$. The reader is referred to Proposition 3.5 in [52] for the derivation of these cuts.

Our numerical experiments show that reverse cone cuts are very important for OBBT. This is because the inequality (5.16) implies nothing about the lower bounds for $c_{b,n}$ and $s_{b,n}$, which makes these bounds difficult to tighten. At the same time, tight bounds on $c_{b,n}$ and $s_{b,n}$ are crucial for the overall relaxation because they affect the McCormick envelopes (5.30) and the error introduced by relaxing (5.12) to (5.16). However, adding reverse cone cuts for every $(b, n) \in \mathcal{A}$ leads to a very large and inefficient relaxation. Therefore, we add them only for a subset $\mathcal{V} \subset \mathcal{A}$ of bus pairs for which (5.12) was violated in a previous OBBT iteration, as described in the next section:

$$(c_{b,n}, s_{b,n}, w_b, w_n) \in \text{LP}[c_{b,n}^2 + s_{b,n}^2 \geq w_b w_n], \quad (5.34)$$

for all $(b, n) \in \mathcal{V}$. Our results in Section 5.5 show that $|\mathcal{V}|$ is typically much less than $|\mathcal{A}|$ in practice.

Our final strengthened SOCP relaxation is given by Equations (5.1–5.11, 5.16, 5.23–5.24, 5.30–5.31, 5.34).

5.4 Bounds Tightening

This section briefly reviews optimization-based bounds tightening (OBBT) generally and then presents our bounds tightening algorithm for ACOPT.

5.4.1 Optimization-Based Bounds Tightening

Consider the following optimization problem, where $X \subset \mathbb{R}^n$ is a compact interval and both the feasible set $F \subset X$ and the objective $f : X \rightarrow \mathbb{R}$ are potentially nonconvex:

$$\min_{\mathbf{x} \in X} f(\mathbf{x}) \quad \text{s.t. } \mathbf{x} \in F. \quad (5.35)$$

Let $f_X^{cv} : X_k \rightarrow \mathbb{R}$ be a convex relaxation of f on X and let $\mathcal{R}(X) \supset F$ be a relaxation of F . We write f_X^{cv} and $\mathcal{R}(X)$ with dependence on X to emphasize the fact that many relaxation techniques produce relaxations that depend explicitly on interval bounds on the decision variables (e.g., the McCormick envelope and arctan relaxations in Section 5.3). A convex relaxation of (5.35) is given by

$$\min_{\mathbf{x}} f_X^{cv}(\mathbf{x}) \quad \text{s.t. } \mathbf{x} \in \mathcal{R}(X). \quad (5.36)$$

Let \mathbf{x}^* be the best known feasible point of (5.35), and let $\text{UB} \equiv f(\mathbf{x}^*)$. OBBT computes an updated set of bounds for \mathbf{x} , hopefully tighter than X , that are guaranteed to contain all \mathbf{x} that are feasible and potentially optimal in (5.36). This is done by maximizing and minimizing each variable x_i subject to the convex constraints in (5.36) and the *optimality cut* $f_X^{cv}(\mathbf{x}) \leq \text{UB}$. This procedure can be applied iteratively as follows, where $X_k \equiv [x_{1,k}^L, x_{1,k}^U] \times \cdots \times [x_{n,k}^L, x_{n,k}^U]$ denotes the bounds obtained in the k^{th} iteration:

$$x_{i,k+1}^{L/U} \leftarrow \min_{\mathbf{x} \in X_k} / \max_{\mathbf{x} \in X_k} x_i \quad (5.37)$$

$$\text{s.t. } \mathbf{x} \in \mathcal{R}(X_k), f_{X_k}^{cv}(\mathbf{x}) \leq \text{UB}.$$

The final bounds X^* can be used to compute an improved lower bound by solving (5.36) with updated relaxations $f_{X^*}^{cv}$ and $\mathcal{R}(X^*)$, which in turn provides an improved optimality gap $(\text{UB} - \text{LB})/\text{UB}$.

OBBT is a key enabling technology in branch-and-bound global optimization codes. By reducing the search space, it can dramatically reduce the need for branching, which is especially important in high dimensions. Indeed, OBBT has been shown to globally solve many ACOPF benchmarks to reasonably tight tolerances in the root node (i.e., with no branching at all) [61, 60]. However, existing OBBT algorithms for ACOPF are computationally demanding due to the number of subproblems (5.37) that must be solved. In the following subsections, we present several strategies for reducing this burden, leading to our final OBBT algorithms.

5.4.2 Selecting a Subset of Variables for OBBT

Clearly, the cost of OBBT can be reduced by only solving the subproblems (5.37) for a subset of the decision variables. In general, this will lead to weaker bounds but greater efficiency. A general approach is to only solve (5.37) for variables that appear in nonlinear terms in the original problem, or auxiliary variables introduced by relaxing these nonlinear terms. However, for ACOPF this still leaves very many variables. For our strengthened SOCP relaxation, this includes $\{c_{b,n}, s_{b,n}\}_{(b,n) \in \mathcal{A}}$, $\{w_b\}_{b \in \mathcal{B}}$, and $\{sc.in v_{b,n}, \theta_{b,n}\}_{(b,n) \in \mathcal{A}_v, v \in \mathcal{C}}$. This is relatively few variables relative to other relaxations, which is a significant advantage, but it is still inefficient. To further reduce the number of variables, note that there are only two ways for improved bounds to improve our relaxation:

- (i) Improved bounds can lead to tighter McCormick envelopes and arctan relaxations in (5.30)–(5.31). These are specifically affected by the bounds on the cycle basis variables $\{c_{b,n}, sc.in v_{b,n}\}_{(b,n) \in \mathcal{A}_v, v \in \mathcal{C}}$.
- (ii) Improved bounds can also reduce the conservatism associated with relaxing (5.12) by (5.16) and (5.34). Specifically, improved bounds on $s_{b,n}$, $c_{b,n}$, w_b , and w_n directly

affect the reverse cone cuts (5.34), and although they do not directly affect the cone constraint (5.16), they do affect how different the feasible sets of (5.16) and (5.12) can be when restricted to these bounds.

To address (i), we perform OBBT on all $c_{b,n}$ and $sc.inv_{b,n}$ with (b, n) in the cycle basis. This a relatively small number of variables because the cycle basis is often much smaller than the total number of bus pairs. Addressing (ii) strictly requires doing OBBT on $\{c_{b,n}, s_{b,n}, w_b, w_n\}$ for all $(b, n) \in \mathcal{A}$, which is a large set of variables. However, we find that (5.12) is typically only violated for a small number of bus pairs (b, n) at the solution of the lower bounding problem in each OBBT iteration. Therefore, we accumulate these violating (b, n) in a subset $\mathcal{V} \subset \mathcal{A}$ and only do OBBT on $\{c_{b,n}, s_{b,n}, w_b, w_n\}$ with $(b, n) \in \mathcal{V}$ (see Algorithm 2). This is the same subset used for adding reverse cone cuts in §5.3.3. Finally, we skip the OBBT subproblems for any variable whose bounds are within 10^{-4} .

5.4.3 OBBT Scheme

Algorithm 2 below describes our proposed OBBT scheme based on the strengthened SOCP relaxation (5.1–5.11, 5.16, 5.23–5.24, 5.30–5.31, 5.34). We denote the initial bounds on all decision variables by X_0 and assume that an upper bound $UB = f(\mathbf{x}^*)$ has previously been computed using a local solver. In each iteration, OBBT is performed on variables described in Section 5.4.2. At the end of each iteration, a tighter relaxation is constructed by using the updated bounds to rebuild the constraints (5.8–5.10, 5.24, 5.30–5.31, and 5.34). The updated relaxation is then solved to obtain a new LB. The procedure is repeated until the optimality gap improves by less than ϵ_1 or becomes less than ϵ_2 .

5.5 Numerical Results

Table 5.1 compares Algorithms 2 with existing OBBT methods on all NESTA benchmark problems up to 300 buses. All methods were applied in the root node only (i.e., with no branching). Columns 2–4 show the tightest root node optimality gaps (%) achieved by

Algorithm 2 OBBT Scheme

```
1: function PURE OBBT SCHEME( $X_0, \epsilon_1, \epsilon_2, \text{UB}$ )
2:    $k \leftarrow 0, \mathcal{V} \leftarrow \emptyset, \delta_{gap} \leftarrow \text{inf}, \text{gap} \leftarrow \text{inf}$ 
3:   while  $\delta_{gap} > \epsilon_1$  and  $\text{gap} > \epsilon_2$  do
4:     Do OBBT on  $\{c_{b,n}, s_{b,n}, w_b, w_n\}_{(b,n) \in \mathcal{V}}$  subject to constraints (5.2–5.11, 5.16, 5.23–
5.24, 5.30–5.31, 5.34) and an optimality cut w.r.t  $X_k$ 
5:     Do OBBT on  $\{c_{b,n}, sc.invb_{b,n}\}_{(b,n) \in \mathcal{A}_v, v \in \mathcal{C}}$  subject to (5.2–5.11, 5.16, 5.23–5.24, 5.30–
5.31, 5.34) and an optimality cut w.r.t  $X_k$ 
6:     Set updated bounds  $X_{k+1}$  based on the results of lines 4–5
7:     Build a strengthened SOCP relaxation (5.1–5.11, 5.16, 5.23–5.24, 5.30–5.31, 5.34)
      based on the bounds  $X_{k+1}$ 
8:     Solve the relaxation to obtain LB, set  $\delta_{gap} \leftarrow \text{gap} - (\text{UB} - \text{LB})/\text{UB}$ ,  $\text{gap} \leftarrow (\text{UB} -$ 
       $\text{LB})/\text{UB}$ , and  $k \leftarrow k + 1$ 
9:     Update the cumulative violated cone set:  $\mathcal{V} \leftarrow \mathcal{V} \cup \{(b, n) \in \mathcal{A} : (5.12)$ 
      is violated at the relaxation solution}
10:  end while
11: end function
```

existing OBBT methods using SDP, QP, and SOCP relaxations. The best SDP gaps are from [61], while the best QP and SOCP gaps are from [60]. Notably, the SOCP relaxation that achieves these gaps in [60] also includes rectangular voltage variables and constraints, making it much more accurate but also much larger than the standard SOCP. The results of Algorithms 2 are given in Columns 5–8, which show the optimality gap, number of OBBT iterations, number of violated cones $|\mathcal{V}|$, and wall-clock time (s). The last two columns show the speed up of Algorithm 2 relative to the SOCP and QC methods from Columns 3–4 [60]. To compare wall-clock times, all methods except the SDP method in Column 2 were implemented in Pyomo [116]. Upper bounding problems were solved using IPOPT 3.12.10 [117] with MA27 [118]. Relaxations were solved with IPOPT 3.12.10 for instances with fewer than 100 buses and with Gurobi 7.0.2 [119] for larger cases. For all methods, OBBT was performed in parallel on the Clemson University Palmetto Cluster with 8 64-GB-RAM nodes (28 2.6 GHz Intel Xeon cores per node). For Algorithms 2, we set $\epsilon_1 = \epsilon_2 = 0.04\%$. Furthermore, constraints (5.24) were omitted because they did not significantly improve the results.

Table 5.1 shows that OBBT can close the optimality gap for almost every test case to

within 0.1%. Algorithm 2 matches the best gap previously achieved by any method for all problems except 5_pjm and 118_api, where it is worse, and 29_edin_sad and 89_pegase_api, where it is significantly better. Overall, Algorithm 2 achieves the best gap for 96.2% of the test cases, whereas the best SDP, SOCP, and QC methods achieve the best gap in only 64.0%, 39.6%, and 71.7% of cases, respectively. At the same time, Algorithm 2 terminates about $5.2\times$ faster than the SOCP method and $21.2\times$ faster than the QC method on average when achieving the same optimality gap (excluding three empty entries in the SpeedUp columns in Table 5.1 due to numerical issues). Since some fraction of the wall-clock time for all methods is required to build the original Pyomo model, the speed ups in terms of pure solver time may be higher. We attribute these results to the fact that Algorithm 2 solves OBBT subproblems for at most $4N_l^c + 2|\mathcal{V}|$ variables per iteration, where N_l^c is the number of distinct bus pairs in the cycle basis. Importantly, Table 5.1 shows that $|\mathcal{V}|$ is often less than 5, even for cases with thousands of bus pairs. Moreover, large networks usually have $N_l^c \ll |\mathcal{A}|$. For comparison, if OBBT is done for all variables that appear in nonlinear terms in the formulations used by the best SOCP and QC relaxations in [60], then the numbers of OBBT variables per iteration are $2|\mathcal{B}|$ and $4|\mathcal{A}| + |\mathcal{B}|$, respectively. Another important effect is that each SOCP relaxation solved in Algorithm 2 is significantly smaller than the SOCPs solved in [60]. Thus, our proposed OBBT method achieves state-of-the-art results in both speed and accuracy for the NESTA benchmarks.

5.6 Conclusion

A new bounds tightening algorithm for the global solution of ACOPF have been developed. The algorithm achieves 96.2% of the best optimality gaps achieved by all existing OBBT methods for NESTA benchmarks, where SDP, SOCP, and QC methods achieve the best gap in only 64.0%, 39.6%, and 71.7% of cases. We also do so significantly more efficiently, and about $5.2\times$ and $21.2\times$ faster than the SOCP and the QC methods on average. The

key ideas enabling this speed-up are the use of an exact cycle-based ACOPF reformulation with relatively few nonconvex terms, the observation that the set of violated cones \mathcal{V} is very small in practice and can be used to effectively manage both the size of the relaxations and the number of OBBT subproblems.

Table 5.1: Root node bounds tightening results for NESTA up to 300 buses. Columns 2–4 are the tightest optimality gaps achieved by existing OBBT methods using SDP, SOCP, and QC relaxations. Columns 5–8 show optimality gaps (%), number iterations, number of violated cones $|\mathcal{V}|$, and wall-clock time (s) for our proposed OBBT scheme. Columns 9–10 show speed-up of our scheme relative to the methods in Columns 3–4.

Case	Best Gap [60]			Proposed OBBT				SpeedUp	
	SDP	SOCP	QP	Gap	Iter	$ \mathcal{V} $	Time	SOCP	QC
3_lmbd	0.1	0.0	0.0	0.0	4	1	0.6	2.0	3.8
5_pjm	5.2	0.1	5.7	5.7	17	0	3.4	0.3	7.1
6_c	0.0	0.0	0.1	0.0	2	0	0.6	3.5	9.0
6_ww	0.0	0.1	0.0	0.0	1	0	0.5	7.0	10.6
14_ieee	0.0	0.1	0.0	0.0	1	0	1.0	4.3	10.9
29_edin	0.0	0.1	0.1	0.0	2	0	13.8	1.7	12.5
30_as	0.0	0.0	0.0	0.0	1	0	2.0	4.2	21.9
30_fsr	0.0	0.1	0.1	0.0	3	2	4.7	4.2	18.1
30_ieee	0.0	0.0	0.0	0.0	3	0	4.8	2.8	13.8
39_epri	0.0	0.0	0.0	0.0	1	0	2.1	8.2	23.2
57_ieee	0.0	0.0	0.0	0.0	1	0	5.4	7.0	17.6
118_ieee	0.1	0.7	0.1	0.0	6	6	59.8	8.3	10.6
162_ieee	1.0	4.0	0.1	0.0	11	280	252.8	1.1	18.2
189_edin	0.1	0.2	0.1	0.1	2	3	19.3	3.0	33.5
300_ieee	0.1	1.2	0.0	0.0	5	16	242.1	1.3	19.3
3_lmbd_api	0.0	0.1	0.0	0.0	4	1	0.7	2.3	3.3
4_gs_api	0.0	0.0	0.0	0.0	3	0	0.6	2.7	5.7
5_pjm_api	0.0	0.0	0.0	0.0	2	0	0.5	3.0	8.6
6_c_api	0.0	0.0	0.0	0.0	3	0	0.7	2.1	6.3
14_ieee_api	0.0	0.0	0.1	0.0	6	0	7.8	1.3	5.1
24_rts_ieee_api	0.0	0.6	0.1	0.0	7	3	19.6	2.4	16.1
29_edin_api	-	0.4	0.1	0.0	4	0	11.1	2.5	54.5
30_as_api	0.0	0.1	0.0	0.0	4	1	6.2	4.0	12.6
30_fsr_api	3.6	41.2	0.1	0.0	14	7	19.9	13.9	16.8
30_ieee_api	0.0	0.1	0.0	0.0	4	1	8.8	2.4	10.3
39_epri_api	0.0	0.1	0.0	0.0	3	1	5.0	8.5	11.1
57_ieee_api	0.0	0.1	0.0	0.0	2	2	4.9	5.2	54.6
73_ieee_rts_api	0.9	14.4	0.0	0.0	6	14	341.5	2.5	1.4
89_pegase_api	-	20.2	9.1	4.5	150	206	117.8	1.6	4.3
118_ieee_api	16.7	26.4	8.7	9.7	14	179	212.7	19.0	3.5
162_ieee_dtc_api	0.6	0.9	0.1	0.0	10	280	283.7	4.7	26.7
189_edin_api	0.1	2.9	0.1	0.1	3	2	10.7	-	6.3
300_ieee_api	0.0	0.7	0.0	0.0	4	89	117.7	1.4	1.9
3_lmbd_sad	0.1	0.0	0.0	0.0	3	1	0.5	2.4	3.8
4_gs_sad	0.0	0.0	0.0	0.0	1	0	0.3	3.0	7.0
5_pjm_sad	0.0	0.0	0.0	0.0	2	0	0.5	3.2	10.4
6_c_sad	0.0	0.0	0.0	0.0	2	0	0.5	4.6	9.2
6_ww_sad	0.0	0.0	0.0	0.0	1	0	0.5	6.6	9.4
9_wscs_sad	0.0	0.0	0.0	0.0	1	0	0.4	9.3	9.5
14_ieee_sad	0.0	0.0	0.0	0.0	1	0	1.0	3.5	12.7
24_ieee_rts_sad	1.4	0.0	0.0	0.0	3	1	8.9	1.4	10.5
29_edin_sad	5.8	0.5	0.5	0.0	9	4	29.7	13.6	51.9
30_as_sad	0.1	0.1	0.0	0.0	3	3	5.0	3.8	13.7
30_fsr_sad	0.1	0.0	0.0	0.0	4	5	6.9	2.1	12.0
30_ieee_sad	0.0	0.1	0.0	0.0	2	0	3.4	3.6	16.6
39_epri_sad	0.0	0.0	0.0	0.0	2	2	3.7	7.2	69.7
57_ieee_sad	0.0	0.1	0.1	0.0	2	1	4.2	7.3	141.3
73_ieee_rts_sad	2.4	2.0	0.0	0.0	3	3	34.6	18.2	38.2
89_pegase_sad	-	0.1	0.1	0.0	4	8	303.3	29.3	110.6
118_ieee_sad	4.0	1.5	0.1	0.1	11	179	149.3	-	38.0
162_ieee_dtc_sad	1.7	7.1	0.0	0.0	11	280	253.6	1.2	24.7
189_edin_sad	1.2	1.8	0.8	0.8	2	3	12.4	-	-
300_ieee_sad	0.1	1.3	0.0	0.0	4	13	107.6	1.3	35.3

CHAPTER 6

CONCLUSION

6.1 Summary of Contributions

In Chapter 2, we developed the first method for computing rigorous convex and concave relaxations of nonconvex expected-value functions. Specifically, we established the Jensen-McCormick relaxation technique. This technique combines Jensen’s inequality, which is widely used to relax convex stochastic programs, and McCormick relaxation technique, which can relax factorable nonconvex functions. This new relaxation method can be used to compute both upper and lower bounds for use in branch-and-bound procedures for finding a global solution. In addition, we proved a second-order pointwise convergence property for the convex relaxation scheme, which is sufficient for finite termination of branch-and-bound under standard assumptions. Moreover, we compiled a library of *primitive* continuous random variables that the Jensen-McCormick relaxation technique can directly support. Table 2.1 lists formulas for the cumulative probability distributions (CDFs) and conditional expectations that are needed for computing the relaxation. Next, we extended our relaxation theory to problems with *factorable* random variables, which are those random variables that can be transformed into primitive random variables by a factorable function. We provide general strategies for finding such transformations that avoid the need to compute any difficult multidimensional integrals. Our numerical examples illustrate a second-order pointwise convergence rate for the relaxation scheme, and show that tight relaxations can be obtained with fairly coarse partitions.

In Chapter 3, we developed a complete spatial branch-and-bound (B&B) algorithm for solving expected-value minimization problems with continuous random variables to guaranteed global optimality. Based on the Jensen-McCormick relaxation technique developed

in Chapter 2, we formalized a general lower bounding approach, a general upper bounding approach, and an efficient implementation of the overall B&B algorithm. The accuracy of both bounding procedures depends on the partition of the decision variable space and the random variable space. Thus, to ensure convergence, the random variable space must be refined as the algorithm proceeds. To address this, we designed an efficient adaptive uncertainty set partitioning rule that maintains tractability of the lower bounding problem. A critical feature of our approach is that all computed bounds are rigorous at all stages of the algorithm, regardless of how coarse or fine the uncertainty set partition is. This implies that fathoming and termination decisions can be made with certainty at any time, which enables the uncertainty set to be adaptively refined as B&B proceeds without loss of rigor. This is in contrast to the existing stochastic B&B algorithm proposed in [3], which applies spatial-B&B using probabilistic upper and lower bounds and therefore has a nonzero probability of inadvertently fathoming global solutions. With our proposed partitioning rule, large regions of the search space can often be fathomed using only coarse partitions, while very fine partitions are only required in few nodes very near a global solution. This is in contrast to state-of-the-art sample-average approximation (SAA) approaches, where the expected-value objective is approximated using a fixed (typically large) number of samples that remains constant throughout the B&B search. Moreover, the number of scenarios required to achieve a high-quality solution in practice is unknown [25, 26, 27], so solution quality must be tested by solving the optimization problem multiple times with independent sample sets, despite the fact that solving a single instance globally is already computationally demanding. Therefore, a significant advantage of our method is that we only need a single run to solve the problem to guaranteed global optimality without sampling errors. Our numerical results showed this approach is more than one order of magnitude faster than SAA for the considered test problems.

In Chapter 4, the Jensen-McCormick relaxation technique from Chapter 2 was extended to develop the first ever method for computing guaranteed convex and concave re-

laxations of nonlinear stochastic optimal control problems with final-time expected-value cost functions. This method is motivated by similar methods for deterministic optimal control problems, which have been successfully applied within B&B techniques to obtain guaranteed global optima. Specifically, the method relies on an existing method for computing time-varying convex and concave relaxations for the solutions of nonlinear ODEs with no uncertainty. That method was first modified to obtain convex and concave relaxations with respect to both decision variables and uncertain parameters, and then combined Jensen's inequality as in Chapter 2 to obtain convex and concave relaxations of the final-time expected-value cost function. Compared to the state-of-the-art sample-based approaches, which only provide probabilistic bounds, our dynamic Jensen-McCormick relaxation technique can be used to compute rigorous upper and lower bounds on the optimal objective value of such problems restricted to any given subinterval of the decision space. Therefore, this technique enables deterministic global optimization for this class of problems. Our numerical example showed that this method can provide reasonably tight relaxations using fairly coarse partitions of the uncertainty space.

In Chapter 5, we developed a new bounds-tightening algorithm for globally solving AC optimal power flow (ACOPF) problems. Practical ACOPF instances are too large to be solved by conventional global optimization algorithms. However, tailored optimization-based bounds tightening (OBBT) algorithms using advanced relaxation techniques have been shown to achieve tight optimality gaps for many test cases with no partitioning at all. Unfortunately, OBBT is still costly because it requires solving two convex subproblems per decision variable in each iteration. To address this, we established a new OBBT algorithm, based on a new strengthened SOCP relaxation, that achieves tight optimality gaps while only solving subproblems for a small subset of variables. First, we proved the equivalence of an ACOPF reformulation that is beneficial for constructing tight and concise convex relaxations. Second, we developed a new strengthened SOCP relaxation based on this reformulation. Third, using this relaxation, we established a new OBBT scheme that

performs bounds tightening on only a selected subset of variables. Our numerical results for NESTA benchmarks showed that performing OBBT on a small subset of the variables in our new relaxation outperformed existing OBBT algorithms in terms of both optimality gap and efficiency up to 300 buses. We achieved the best optimality gap among all existing OBBT methods for 96.2% of the benchmarks, whereas existing SDP, SOCP, and QC methods achieved the best gap in only 64.0%, 39.6%, and 71.7% of cases, respectively. At the same time, our algorithm is about $5.1\times$ (resp. $21.2\times$) faster than the existing SOCP (resp. QC) methods on average.

6.2 Future Work

It is generally agreed that guaranteed global optimization is extremely challenging in terms of constructing rigorous and tight convex relaxations, designing efficient domain reduction techniques that reduce the search space, and facing the exponential run-time complexity caused by exhaustively partitioning the search space. The advances in global optimization methods for nonconvex stochastic programs and AC optimal power flow problems in this thesis open up new avenues for future research in both fundamental theory and applications. Actually, we are still in early stages of solving such problems and many paths are open to possibly push the current state forward.

For nonconvex stochastic optimization, one important future path is to tackle the global optimization of nonconvex chance-constrained problems. Chance constraints refer to constraints that are required to hold with a specified (typically high) probability, but not with certainty. Such constraints are often essential for obtaining sensible optimization results, specifically in cases where it would be impossible or inordinately costly to ensure that a constraint could be satisfied in every possible realization of uncertainty, no matter how unlikely (e.g., committing enough power generation units to satisfy demand under every possible realization of random demands, renewable power outputs, contingency scenarios, etc.). However, effective methods for rigorously solving chance constrained programs are

currently limited to special cases where equivalent deterministic constraints can be derived, such as problems with independent linear chance constraints affected by random variables with simple (e.g., Gaussian) distributions. A number of existing approaches are available for deriving and solving deterministic restrictions of the original problem by replacing the chance constraints with more conservative deterministic constraints, often derived from probabilistic inequalities such as the Cantelli-Chebyshev inequality. However, such constraints are often significantly more restrictive than the original chance constraints, and no general-purpose approaches are available for refining these approximations. Nowadays chance constraints are commonly approximated using sample-based methods, but this often requires many samples to achieve high accuracy. Moreover, without further approximations, sample-based approximations of chance constraints are discontinuous with respect to the optimization variables, which can greatly hinder efficient optimization. To conquer those issues, extensions of the Jensen-McCormick relaxation technique for expected-values in Chapter 2 should be pursued to tractable convex and concave relaxations of nonconvex chance constraints. Such relaxations could be made to converge to the original chance constraints by partitioning the uncertainty space, which would enable finite convergence of the overall B&B algorithm. Moreover, a rigorous theoretical analysis of the convergence rate could be established.

Another important future research direction is extending the novel B&B method for single-stage stochastic programs developed in Chapter 3 to address the efficient global solution of two-stage nonconvex stochastic programs. Two-stage models capture the important case where some decisions must be made ‘here-and-now’ under uncertainty, while other ‘recourse’ decisions can be made in the future after the uncertain quantities become known. A variety of applications in energy planning, manufacturing, etc. can be formulated as two-stage stochastic programs. Currently, there are no general techniques capable of furnishing rigorous convex and concave relaxations for two-stage problems with continuous random variables. At the same time, discretizing the uncertainties in advance as

in SAA methods leads to a prohibitive number of recourse variables. This problem could possibly be addressed by extending our Jensen-McCormick relaxation theory in Chapter 2 to two-stage problems because this would enable the uncertainty set to be partitioned adaptively as needed during the B&B search. Beyond this, designing decomposition strategies that can solve the problem more efficiently is another potentially rich research area. Moreover, following our work in Chapter 4, all of the above methods can be further extended to continuous-time and discrete-time dynamical systems. Besides enriching the theory of nonconvex stochastic optimization, software development for this class of problems is also a wide open field to grow. Last but not least, many efforts are needed to formulate practical problems into our problem of interest, including picking suitable continuous random variables distributions, choosing reasonable truncated range for the uncertainty set, and so on.

There are also several fruitful areas for future work related to the AC optimal power flow (ACOPF) problems considered in this thesis. Our work in Chapter 5 demonstrates that iteratively running optimization-based bounds tightening (OBBT) based on advanced convex relaxations can achieve the global solution for the majority of the NESTA benchmark test cases without branching at all. However, this empirical result is not well understood. In theory, OBBT without branching is neither guaranteed or even expected to achieve an arbitrarily accurate ϵ -global solution, even when run for an infinite number of iterations. Moreover, for nonconvex optimization problems arising in other applications, such OBBT procedures are not typically effective without branching. Therefore, a detailed investigation of why these procedures are uniquely effective for ACOPF is likely to yield insights with very significant implications for power systems and beyond. Another unique feature of ACOPF problems is that good local solvers find global solutions surprisingly often, even without multi-start or initialization, despite these problems being highly nonconvex and very high-dimensional. This unexpected behavior should also be investigated further.

Another future direction is to designing a fast interval arithmetic bounds tightening

(IABT) methods to replace optimization-based bounds tightening calculations used in this thesis for some or all of the decision variables. IABT infers updated bounds on given variables by applying interval arithmetic (IA) [120] to one or more constraints involving those variables. This is very efficient but often results in weaker bounds than solving a full OBBT problem. However, IABT can be highly effective at propagating bounds through simple constraints and can even yield tighter bounds than OBBT since IA can be applied directly to nonconvex expressions, whereas OBBT updates are always based on the relaxed feasible set. Furthermore, by combining a selected set of IABT calculations with OBBT on other variables, a hybrid bounds tightening method might be developed that inherits the merits of both approaches. Finally, the OBBT method developed in this thesis should be extended to develop a complete branch-and-bound algorithm, possibly with specialized branching rules, that can guarantee an ϵ -global solution in all cases.

However, our developed global optimization methods for nonconvex stochastic programs in this thesis have not been tested for complex practical problems yet. Formulating problems into the form of our interest might be nontrivial, including picking suitable continuous random variables distributions, choosing reasonable truncated range for the uncertainty set, constructing a reduced-space model, and designing custom convex relaxations for specific structures.

REFERENCES

- [1] M. Cain, R. O'Neill, and A. Castillo, "History of optimal power flow and formulations", Dec. 2012.
- [2] S. Liu, S. S. Farid, and L. G. Papageorgiou, "Integrated optimization of upstream and downstream processing in biopharmaceutical manufacturing under uncertainty: A chance constrained programming approach", *Industrial & Engineering Chemistry Research*, vol. 55, no. 16, pp. 4599–4612, 2016. eprint: <http://dx.doi.org/10.1021/acs.iecr.5b04403>.
- [3] V. I. Norikin, G. C. Pflug, and A. Ruszczyński, "A branch and bound method for stochastic global optimization", *Mathematical Programming*, vol. 83, no. 1, pp. 425–450, 1998.
- [4] J. A. Momoh, R. Adapa, and M. E. El-Hawary, "A review of selected optimal power flow literature to 1993. i. nonlinear and quadratic programming approaches", *IEEE Transactions on Power Systems*, vol. 14, no. 1, pp. 96–104, 1999.
- [5] J. A. Momoh, M. E. El-Hawary, and R. Adapa, "A review of selected optimal power flow literature to 1993. ii. newton, linear programming and interior point methods", *IEEE Transactions on Power Systems*, vol. 14, no. 1, pp. 105–111, 1999.
- [6] Z. Yang, H. Zhong, Q. Xia, and C. Kang, "Fundamental review of the opf problem: Challenges, solutions, and state-of-the-art algorithms", *Journal of Energy Engineering*, vol. 144, no. 1, p. 04 017 075, 2018.
- [7] Z. Yang, H. Zhong, Q. Xia, and C. Kang, "Solving opf using linear approximations: Fundamental analysis and numerical demonstration", *IET Generation, Transmission Distribution*, vol. 11, no. 17, pp. 4115–4125, 2017.
- [8] C. G. Moles, P. Mendes, and J. R. Banga, "Parameter estimation in biochemical pathways: A comparison of global optimization methods", *Genome Research*, vol. 13, no. 11, pp. 2467–2474, 2003.
- [9] A. B. Singer, J. W. Taylor, P. I. Barton, and W. H. Green, "Global dynamic optimization for parameter estimation in chemical kinetics", *Journal of Physical Chemistry A*, vol. 110, no. 3, pp. 971–976, 2006.
- [10] J. W. Taylor, G. Ehlker, H.-H. Carstensen, L. Ruslen, R. W. Field, and W. H. Green, "Direct measurement of the fast, reversible addition of oxygen to cyclohexadienyl radicals in nonpolar solvents", *J. Phys. Chem. A*, vol. 108, pp. 7193–7203, 2004.

- [11] R. Horst and H. Tuy, *Global Optimization: Deterministic Approaches*, third. New York: Springer, 1996.
- [12] R. Moore, *Methods and Applications of Interval Analysis*. Philadelphia, PA: SIAM, 1979.
- [13] G. McCormick, “Computability of global solutions to factorable nonconvex programs: Part I - convex underestimating problems”, *Mathematical Programming*, vol. 10, pp. 147–175, 1976.
- [14] J. Scott, M. Stuber, and P. Barton, “Generalized McCormick relaxations”, *Journal of Global Optimization*, vol. 51, pp. 569–606, 2011.
- [15] M. Tawarmalani and N. V. Sahinidis, *Convexification and Global Optimization in Continuous and Mixed-Integer Nonlinear Programming*. Kluwer Academic Publishers, 2002.
- [16] H. D. Sherali, R. Krishnamurthy, and F. Al-Khayyal, “Enumeration approach for linear complementarity problems based on a reformulation-linearization technique”, *Journal of Optimization Theory and Applications*, vol. 99, no. 2, pp. 481–507, 1998.
- [17] C. S. Adjiman, I. P. Androulakis, and C. A. Floudas, “A global optimization method, alpha BB, for general twice-differentiable constrained NLPs - II. Implementation and computational results”, *Computers & Chemical Engineering*, vol. 22, no. 9, pp. 1159–1179, 1998.
- [18] C. S. Khor, B. Chachuat, and N. Shah, “Fixed-flowrate total water network synthesis under uncertainty with risk management”, *Journal of Cleaner Production*, vol. 77, pp. 79–93, 2014.
- [19] X. Li, E. Armagan, A. Tomagard, and P. I. Barton, “Stochastic pooling problem for natural gas production network design and operation under uncertainty”, *AIChE Journal*, vol. 57, no. 8, pp. 2120–2135, 2011.
- [20] X. Li, A. Tomagard, and P. I. Barton, “Decomposition strategy for the stochastic pooling problem”, *Journal of Global Optimization*, vol. 54, no. 4, pp. 765–790, 2012.
- [21] X. Li and P. I. Barton, “Optimal design and operation of energy systems under uncertainty”, *Journal of Process Control*, vol. 30, pp. 1–9, 2015.
- [22] N. V. Sahinidis, “BARON: A general purpose global optimization software package”, *J. Glob. Optim.*, vol. 8, no. 2, pp. 201–205, 1996.

- [23] R. Misener and C. A. Floudas, “ANTIGONE: Algorithms for coNTinuous/Integer Global Optimization of Nonlinear Equations”, *Journal of Global Optimization*, vol. 59, no. 2-3, pp. 503–526, 2014.
- [24] A. Shapiro, “Stochastic programming approach to optimization under uncertainty”, *Mathematical Programming*, vol. 112, no. 1, pp. 183–220, 2008.
- [25] B. Verweij, S. Ahmed, A. J. Kleywegt, G. Nemhauser, and A. Shapiro, “The sample average approximation method applied to stochastic routing problems: A computational study”, *Computational Optimization and Applications*, vol. 24, no. 2, pp. 289–333, 2003.
- [26] J. Linderoth, A. Shapiro, and S. Wright, “The empirical behavior of sampling methods for stochastic programming”, *Annals of Operations Research*, vol. 142, no. 1, pp. 215–241, 2006.
- [27] N. Lohndorf, “An empirical analysis of scenario generation methods for stochastic optimization”, *European Journal of Operational Research*, vol. 255, no. 1, pp. 121–132, 2016.
- [28] L. Blackmore, M. Ono, and B. Williams, “Chance-constrained optimal path planning with obstacles”, *IEEE Trans. Robotics*, vol. 27, no. 6, pp. 1080–1094, 2011.
- [29] F. HERZOG, G. DONDI, and H. P. GEERING, “Stochastic model predictive control and portfolio optimization”, *International Journal of Theoretical and Applied Finance*, vol. 10, no. 02, pp. 203–233, 2007. eprint: <https://doi.org/10.1142/S0219024907004196>.
- [30] A. Hakizimana and J. Scott, “Differentiability conditions for stochastic hybrid systems arising in the optimal design of microgrids”, *J. Optim. Theor. Appl.*, vol. 173, no. 2, pp. 658–682, 2017.
- [31] H. Ahmadian Behrooz, “Robust design and control of extractive distillation processes under feed disturbances”, *Industrial & Engineering Chemistry Research*, vol. 56, no. 15, pp. 4446–4462, 2017. eprint: <http://dx.doi.org/10.1021/acs.iecr.7b00004>.
- [32] A. Singer and P. Barton, “Global optimization with nonlinear ordinary differential equations”, *J. Glob. Optim.*, vol. 34, pp. 159–190, 2006.
- [33] J. Scott and P. Barton, “Reachability analysis and deterministic global optimization of DAE models”, in *Surveys in Differential Algebraic Equations III*, A. Ilchman and T. Reis, Eds., vol. 3, Springer International Publishing, 2015, pp. 61–116.

- [34] B. Houska and B. Chachuat, “Branch-and-lift algorithm for deterministic global optimization in nonlinear optimal control”, *J. Optim. Theor. Appl.*, vol. 162, no. 1, pp. 208–248, 2014.
- [35] Y. Lin and M. Stadtherr, “Deterministic global optimization of nonlinear dynamic systems”, *AIChE Journal*, vol. 53, no. 4, pp. 866–875, 2007.
- [36] Y. Zhao and M. A. Stadtherr, “Rigorous global optimization for dynamic systems subject to inequality path constraints”, *Industrial & Engineering Chemistry Research*, vol. 50, no. 22, pp. 12 678–12 693, 2011. eprint: <http://dx.doi.org/10.1021/ie200996f>.
- [37] I. Papamichail and C. Adjiman, “A rigorous global optimization algorithm for problems with ordinary differential equations”, *J. Glob. Optim.*, vol. 24, no. 1, pp. 1–33, 2002.
- [38] J. Scott, B. Chachuat, and P. Barton, “Nonlinear convex and concave relaxations for the solutions of parametric ODEs”, *Optimal Control Applications and Methods*, vol. 34, no. 2, pp. 145–163, 2013.
- [39] J. Scott and P. Barton, “Improved relaxations for the parametric solutions of ODEs using differential inequalities”, *J. Glob. Optim.*, vol. 57, no. 1, pp. 143–176, 2013.
- [40] J. Scott and P. Barton, “Convex and concave relaxations for the parametric solutions of semi-explicit index-one differential-algebraic equations”, *Journal of Optimization Theory and Applications*, vol. 156, Mar. 2013.
- [41] S. M. Harwood and P. I. Barton, “Affine relaxations for the solutions of constrained parametric ordinary differential equations”, *Optimal Control Applications and Methods*, pp. 1–22, 2017.
- [42] J. K. Scott and P. I. Barton, “Convex relaxations for nonconvex optimal control problems”, *Proc. 50th IEEE Conference on Decision and Control*, pp. 1042–1047, 2011.
- [43] A. Sahlodin and B. Chachuat, “Convex/concave relaxations of parametric ODEs using Taylor models”, *Computers and Chemical Engineering*, vol. 35, pp. 844–857, 2011.
- [44] A. Sahlodin and B. Chachuat, “Discretize-then-relax approach for convex/concave relaxations of the solutions of parametric odes”, *Applied Numerical Mathematics - APPL NUMER MATH*, vol. 61, pp. 803–820, Jul. 2011.
- [45] A. Shapiro, “On complexity of multistage stochastic programs”, *Operations Research Letters*, vol. 34, no. 1, pp. 1–8, 2006.

- [46] Y. Wu, A. S. Debs, and R. E. Marsten, “A direct nonlinear predictor-corrector primal-dual interior point algorithm for optimal power flows”, *IEEE Transactions on Power Systems*, vol. 9, no. 2, pp. 876–883, 1994.
- [47] G. L. Torres and V. H. Quintana, “An interior-point method for nonlinear optimal power flow using voltage rectangular coordinates”, *IEEE Transactions on Power Systems*, vol. 13, no. 4, pp. 1211–1218, 1998.
- [48] R. A. Jabr, “Exploiting sparsity in sdp relaxations of the opf problem”, *IEEE Transactions on Power Systems*, vol. 27, no. 2, pp. 1138–1139, 2012.
- [49] T. Liu, B. Sun, and D. H. K. Tsang, “Rank-one solutions for sdp relaxation of qcqp in power systems”, *IEEE Transactions on Smart Grid*, vol. 10, no. 1, pp. 5–15, 2019.
- [50] R. A. Jabr, “Radial distribution load flow using conic programming”, *IEEE Transactions on Power Systems*, vol. 21, no. 3, pp. 1458–1459, 2006.
- [51] B. Kocuk, S. S. Dey, and X. A. Sun, “Strong socp relaxations for the optimal power flow problem”, *Operations Research*, vol. 64, no. 6, pp. 1177–1196, 2016.
- [52] B. Kocuk, S. Dey, and X. Sun, “Matrix minor reformulation and socp-based spatial branch-and-cut method for the ac optimal power flow problem”, *Mathematical Programming Computation*, vol. 10, 557–596, Dec. 2018.
- [53] C. Coffrin, H. L. Hijazi, and P. V. Hentenryck, “The qc relaxation: A theoretical and computational study on optimal power flow”, *IEEE Transactions on Power Systems*, vol. 31, no. 4, pp. 3008–3018, 2016.
- [54] H. Hijazi, C. Coffrin, and P. V. Hentenryck, “Convex quadratic relaxations for mixed-integer nonlinear programs in power systems”, *Mathematical Programming Computation*, vol. 9, no. 3, pp. 321–367, 2017.
- [55] A Castillo and R. O’Neill, “Survey of approaches to solving the acopf”, Mar. 2013.
- [56] S. Sojoudi and J. Lavaei, “Physics of power networks makes hard optimization problems easy to solve”, in *2012 IEEE Power and Energy Society General Meeting*, 2012, pp. 1–8.
- [57] R. Madani, S. Sojoudi, and J. Lavaei, “Convex relaxation for optimal power flow problem: Mesh networks”, *IEEE Transactions on Power Systems*, vol. 30, no. 1, pp. 199–211, 2015.
- [58] A. Gopalakrishnan, A. U. Raghunathan, D. Nikovski, and L. T. Biegler, “Global optimization of optimal power flow using a branch and bound algorithm”, in

2012 50th Annual Allerton Conference on Communication, Control, and Computing (Allerton), 2012, pp. 609–616.

- [59] M. Lu, H. Nagarajan, R. Bent, S. D. Eksioglu, and S. J. Mason, “Tight piecewise convex relaxations for global optimization of optimal power flow”, in *2018 Power Systems Computation Conference (PSCC)*, 2018, pp. 1–7.
- [60] M. Bynum, A. Castillo, J. Watson, and C. D. Laird, “Tightening mccormick relaxations toward global solution of the acopf problem”, *IEEE Transactions on Power Systems*, pp. 1–1, 2018.
- [61] C. Coffrin, H. L. Hijazi, and P. Van Hentenryck, “Strengthening convex relaxations with bound tightening for power network optimization”, in *Principles and Practice of Constraint Programming*, G. Pesant, Ed., Cham: Springer International Publishing, 2015, pp. 39–57, ISBN: 978-3-319-23219-5.
- [62] C. Chen, A. Atamtürk, and S. S. Oren, “Bound tightening for the alternating current optimal power flow problem”, *IEEE Transactions on Power Systems*, vol. 31, no. 5, pp. 3729–3736, 2016.
- [63] C. S. Adjiman, S. Dallwig, C. A. Floudas, and A. Neumaier, “A global optimization method, alpha BB, for general twice-differentiable constrained NLPs - I. Theoretical advances”, *Computers & Chemical Engineering*, vol. 22, no. 9, pp. 1137–1158, 1998.
- [64] R. P. Liem, J. R. Martins, and G. K. Kenway, “Expected drag minimization for aerodynamic design optimization based on aircraft operational data”, *Aerospace Science and Technology*, vol. 63, pp. 344–362, 2017.
- [65] A. I. Papadopoulos, G. Giannakoudis, and S. Voutetakis, “Efficient design under uncertainty of renewable power generation systems using partitioning and regression in the course of optimization”, *Ind. Eng. Chem. Res.*, vol. 51, no. 39, pp. 12 862–12 876, 2012. eprint: <http://pubs.acs.org/doi/pdf/10.1021/ie3005918>.
- [66] L.-P. Pang, S. Chen, and J.-H. Wang, “Risk management in portfolio applications of non-convex stochastic programming”, *Applied Mathematics and Computation*, vol. 258, pp. 565–575, 2015.
- [67] M. Farina, L. Giulioni, L. Magni, and R. Scattolini, “An approach to output-feedback mpc of stochastic linear discrete-time systems”, *Automatica*, vol. 55, pp. 140–149, 2015.
- [68] A. Mesbah, “Stochastic model predictive control: An overview and perspectives for future research”, *IEEE Control Systems*, vol. 36, no. 6, pp. 30–44, 2016.

- [69] Y. M. E. and V. I. Norikin, “On nonsmooth and discontinuous problems of stochastic systems optimization”, *European Journal of Operational Research*, vol. 101, no. 2, pp. 230–244, 1997.
- [70] A. Georghiou, W. Wiesemann, and D. Kuhn, “Generalized decision rule approximations for stochastic programming via liftings”, *Mathematical Programming*, vol. 152, no. 1, pp. 301–338, 2015.
- [71] J. Wei and M. J. Realff, “Sample average approximation methods for stochastic minlps”, *Computers & Chemical Engineering*, vol. 28, no. 3, pp. 333–346, 2004.
- [72] M. D. Perlman, “Jensen’s inequality for a convex vector-valued function on an infinite-dimensional space”, *Journal of Multivariate Analysis*, vol. 4, no. 1, pp. 52–65, 1974.
- [73] J. R. Birge and R. J.-B. Wets, “Designing approximation schemes for stochastic optimization problems, in particular for stochastic programs with recourse”, in *Stochastic Programming 84 Part I*, A. Prékopa and R. J.-B. Wets, Eds. Berlin, Heidelberg: Springer Berlin Heidelberg, 1986, pp. 54–102, ISBN: 978-3-642-00925-9.
- [74] A. Madansky, “Bounds on the expectation of a convex function of a multivariate random variable”, *Annals of Mathematical Statistics*, vol. 30, no. 3, pp. 743–746, 1959.
- [75] K. Frauendorfer, D. Kuhn, and M. Schurle, “Barycentric bounds in stochastic programming: Theory and application”, in *Stochastic Programming: the State of the Art in Honor of George B. Dantzig*, G. Infanger, Ed., ser. International Series in Operations Research & Management Science. New York: Springer, 2011, vol. 150, pp. 67–96, ISBN: 978-1-4419-1641-9.
- [76] S. P. Dokov and D. P. Morton, *Higher-Order Upper Bounds on the Expectation of a Convex Function*, J. L. Higle, W. Römisch, and S. Sen, Eds. Humboldt-Universität zu Berlin, Mathematisch-Naturwissenschaftliche Fakultät II, Institut für Mathematik, 2002.
- [77] N. C. P. Edirisinghe, “New second-order bounds on the expectation of saddle functions with applications to stochastic linear programming”, *Operations Research*, vol. 44, no. 6, pp. 909–922, 1996.
- [78] A. Bompadre and A. Mitsos, “Convergence rate of McCormick relaxations”, *J. Glob. Optim.*, vol. 52, no. 1, pp. 1–28, 2012.
- [79] R. Kannan and P. I. Barton, “The cluster problem in constrained global optimization”, *J. Glob. Optim.*, vol. 69, pp. 629–676, 2017.

- [80] A. Skjal, T. Westerlund, R. Misener, and C. A. Floudas, “A generalization of the classical alpha-bb convex underestimation via diagonal and nondiagonal quadratic terms”, *Journal of Optimization Theory and Applications*, vol. 154, no. 2, pp. 462–490, 2012.
- [81] C. A. Meyer and C. A. Floudas, “Convex envelopes for edge-concave functions”, *Mathematical Programming*, vol. 103, no. 2, pp. 207–224, 2005, Meyer, CA Floudas, CA.
- [82] C. E. Gounaris and C. A. Floudas, “Tight convex underestimators for c2-continuous problems: Ii. multivariate functions”, *Journal of Global Optimization*, vol. 42, no. 1, pp. 69–89, 2008.
- [83] X. Bao, A. Khajavirad, N. Sahinidis, and M. Tawarmalani, “Global optimization of nonconvex problems with multilinear intermediates”, *Mathematical Programming Computation*, vol. 7, no. 1, pp. 1–37, 2015.
- [84] A. Tsoukalas and A. Mitsos, “Multivariate mccormick relaxations”, *Journal of Global Optimization*, vol. 59, no. 2, pp. 633–662, 2014.
- [85] K. A. Khan, H. A. J. Watson, and P. I. Barton, “Differentiable mccormick relaxations”, *Journal of Global Optimization*, vol. 67, no. 4, pp. 687–729, 2017.
- [86] A. Wechsung, J. Scott, H. Watson, and P. Barton, “Reverse propagation of McCormick relaxations”, *J. Glob. Optim.*, vol. 63, no. 1, pp. 1–36, 2015.
- [87] M. Stuber, J. Scott, and P. Barton, “Convex and concave relaxations of implicit functions”, *Optimization Methods and Software*, vol. 30, no. 3, pp. 424–460, 2015.
- [88] W. R. Esposito and C. A. Floudas, “Deterministic global optimization in nonlinear optimal control problems”, *J. Glob. Optim.*, vol. 17, pp. 97–126, 2000.
- [89] A. Karr, *Probability*, ser. Springer texts in statistics. Springer-Verlag, 1993, ISBN: 9783540940715.
- [90] S. Ross, *A First Course in Probability*. Prentice Hall, 2002, ISBN: 9780130338518.
- [91] N. L. Johnson, S. Kotz, and N. Balakrishnan, *Continuous Univariate Distributions*. Wiley-Interscience, 1994, vol. 1, ISBN: 0471584959.
- [92] M. K. Okasha and I. M. Alqanoo, “Inference on the doubly truncated gamma distribution for lifetime data”, *Int. J. Math. Stat. Invent* 2, pp. 1–17, 2014.
- [93] J. R. Munkres, *Analysis on Manifolds*. Cambridge, MA: Westview Press, 1991.

- [94] B. D. Ripley, *Stochastic Simulation*. John Wiley & Sons, 2006.
- [95] L. Martino, D. Luengo, and J. Miguez, “Efficient sampling from truncated bivariate Gaussians via Box-Muller transformation”, *Electronics Letters*, vol. 48, no. 24, pp. 1533–1534, 2012.
- [96] H. S. Ryoo and N. V. Sahinidis, “Global optimization of nonconvex nlp and minlp with applications in-process design”, *Computers & Chemical Engineering*, vol. 19, no. 5, pp. 551–566, 1995.
- [97] Y. Shao and J. K. Scott, “Convex relaxations for global optimization under uncertainty described by continuous random variables”, *AIChE Journal. In Press*, 2017.
- [98] J. K. Scott, “Reachability analysis and deterministic global optimization of differential algebraic systems”, Ph.D. dissertation, Massachusetts Institute of Technology, 2012.
- [99] I. I. Cplex, “V12. 1: User’s manual for cplex”, *International Business Machines Corporation*, vol. 46, no. 53, p. 157, 2009.
- [100] A. J. Kleywegt, A. Shapiro, and T. Homem-de Mello, “The sample average approximation method for stochastic discrete optimization”, *SIAM Journal on Optimization*, vol. 12, no. 2, pp. 479–502, 2002. eprint: <https://doi.org/10.1137/S1052623499363220>.
- [101] J. Enszer, Y. Lin, S. Ferson, G. Corliss, and M. Stadtherr, “Probability bounds analysis for nonlinear dynamic process models”, *AIChE Journal*, vol. 57, no. 2, pp. 404–422, 2011.
- [102] J. A. Enszer, D. A. Maces, and M. A. Stadtherr, “Probability bounds analysis for nonlinear population ecology models”, *Mathematical Biosciences*, vol. 267, pp. 97–108, 2015.
- [103] S. Schaber, J. Scott, and P. Barton, “Convergence-order analysis for differential-inequalities-based bounds and relaxations of the solutions of ODEs”, *Submitted*, pp. 1–39, 2017.
- [104] S. D. Schaber, “Tools for dynamic model development”, Ph.D. dissertation, Massachusetts Institute of Technology, 2014.
- [105] K. H. Khalil, *Nonlinear Systems*, Third. Upper Saddle River, NJ: Prentice Hall, 2002.
- [106] A. C. Hindmarsh, P. N. Brown, K. E. Grant, S. L. Lee, R. Serban, D. E. Shumaker, and C. S. Woodward, “SUNDIALS, suite of nonlinear and differential/algebraic

- equation solvers”, *ACM Transactions on Mathematical Software*, vol. 31, pp. 363–396, 2005.
- [107] S. H. Low, “Convex relaxation of optimal power flow—Part II: Exactness”, *IEEE Transactions on Control of Network Systems*, vol. 1, no. 2, pp. 177–189, 2014.
- [108] J. B. Lasserre, “Global optimization with polynomials and the problem of moments”, *SIAM J. on Optimization*, vol. 11, no. 3, pp. 796–817, Mar. 2000.
- [109] J. Liu, C. D. Laird, J. K. Scott, J. Watson, and A. Castillo, “Global solution strategies for the network-constrained unit commitment problem with ac transmission constraints”, *IEEE Transactions on Power Systems*, vol. 34, no. 2, pp. 1139–1150, 2019.
- [110] Y. Liu, J. Li, L. Wu, and T. Ortmeier, “Chordal relaxation based acopf for unbalanced distribution systems with ders and voltage regulation devices”, *IEEE Transactions on Power Systems*, vol. 33, no. 1, pp. 970–984, 2018.
- [111] R. A. Jabr, “A conic quadratic format for the load flow equations of meshed networks”, *IEEE Transactions on Power Systems*, vol. 22, no. 4, pp. 2285–2286, 2007.
- [112] R. A. Jabr, “Optimal power flow using an extended conic quadratic formulation”, *IEEE Transactions on Power Systems*, vol. 23, no. 3, pp. 1000–1008, 2008.
- [113] A. Gómez Expósito and E. Romero Ramos, “Reliable load flow technique for radial distribution networks”, *IEEE Transactions on Power Systems*, vol. 14, no. 3, pp. 1063–1069, 1999.
- [114] T. Kavitha, C. Liebchen, K. Mehlhorn, D. Michail, R. Rizzi, T. Ueckerdt, and K. A. Zweig, “Survey: Cycle bases in graphs characterization, algorithms, complexity, and applications”, *Comput. Sci. Rev.*, vol. 3, no. 4, pp. 199–243, Nov. 2009.
- [115] A. A. Hagberg, D. A. Schult, and P. J. Swart, “Exploring network structure, dynamics, and function using networkx”, in *Proceedings of the 7th Python in Science Conference*, G. Varoquaux, T. Vaught, and J. Millman, Eds., Pasadena, CA USA, 2008, pp. 11–15.
- [116] W. E. Hart, C. D. Laird, J.-P. Watson, D. L. Woodruff, G. A. Hackebeil, B. L. Nicholson, and J. D. Siirola, *Pyomo—optimization modeling in python*, Second. Springer Science & Business Media, 2017, vol. 67.
- [117] A. Wächter and L. Biegler, “On the implementation of an interior-point filter line-search algorithm for large-scale nonlinear programming”, *Mathematical programming*, vol. 106, pp. 25–57, Mar. 2006.

- [118] HSL, “A collection of fortran codes for large scale scientific computation”,
- [119] L. Gurobi Optimization, *Gurobi optimizer reference manual*, 2020.
- [120] E. Hansen, “A generalized interval arithmetic”, in *Lecture Notes in Computer Science*, Vol. 29, New York: Springer Verlag, 1975, pp. 7–18.